Title
Microstructure of deciduous dentin

Author
Sumikawa, David A.

Publication Date
1996

Peer reviewed|Thesis/dissertation

Microstructure of Deciduous Dentin

by

David A. Sumikawa, D.D.S.

THESIS

Submitted in partial satisfaction of the requirements for the degree of

MASTER OF SCIENCE

in

Oral Biology

in the

GRADUATE DIVISION

of the

UNIVERSITY OF CALIFORNIA

San Francisco

. . . . . .

Date University Librarian

Degree Conferred: . . . . . .

Table of Contents

ACKNOWLEDGMENTS

The completion of this project was the result of the efforts of many people, to whom I owe my deepest gratitude.

Beginning with my committee members, I would like to thank Dr. Raymond Braham for serving on my thesis committee and for providing invaluable guidance and support during my educational endeavors here. Very special thanks go to my advisors and mentors, Dr. Grayson Marshall and Dr. Sally Marshall (Committee Chair) for their inspiration and expertise, and their generous and undying patience and guidance. They have taught me far more than they will ever realize, and I am eternally grateful.

I am indebted to Larry Watanabe for his expert technical assistance and comic relief in times of stress. Additional thanks is owed to I-Chien Wu-Magidi and Eric Fuji for assistance with sample preparation and Sue Strawn for image analysis assistance. I would also like to thank Lauren Gee and Dr. John Hutton for statistical analysis assistance and Vickie Leow for graphical assistance. Special thanks to Colin Yoshiyama for his excellent artistic contributions during a very busy time period.

Lastly, I would like to thank my parents and family, for without whom none of this would have been possible.

This work was supported in part by NIH/NIDR Grant P01 DE09859.

List of Figures

List of Tables

ABSTRACT

Although permanent tooth dentin has been studied extensively, the microstructure of dentin in deciduous (primary) teeth has received only very limited attention. A better understanding of dentin in deciduous teeth will lead to improved bonding methods that will make dental restorations more efficient and effective, and may have major implications in the areas of prevention, remineralization, permeability, and sensitivity. The purpose of this study was to measure the numerical tubule density, tubule diameter, and peritubular width in deciduous maxillary anterior teeth. Freshly extracted teeth sterilized by gamma radiation were sectioned to produce 1 mm square sticks of dentin, roughly parallel to the long axis of the tubules, from the distal side of the tooth and from the center. The dentin sticks were invested in epoxy, serially sectioned at 0.5 mm intervals from the DEJ and polished through 0.05 μm alumina. The samples were examined by scanning electron microscopy in the wet mode (ISI SX-40A modified with a CFAS system, Topcon Instruments, Pleasanton, CA) at 2000x. Images were collected from 9 areas on each square at each depth, and analyses of the microstructural characteristics were done using image analysis software (Features II, Kevex Corp., San Carlos, CA).

In 4 of 20 teeth examined, the dentin structure included a series of microcanals in a mesio-distal line at the midpoint facio-lingually. These features resembled giant dentin tubules approximately 5-10 times larger than normal tubules, and had a less well-defined peritubular zone. Linear regression analysis of the tubule density versus distance from the DEJ for the lateral incisors demonstrated an increase of 5,500 tubules/mm^2/mm, while the central and distal sticks of the canines demonstrated increases of 4,400 and 11,700 tubules/mm^2/mm respectively. The tubule diameters for the canines and lateral incisors were found to increase 0.28 and 0.39 μm/mm, respectively, while the peritubular widths decreased 0.13 and 0.05 μm/mm, respectively.

The results of this study suggest that microstructural characteristics of deciduous dentin have some unique features and show higher tubule densities and larger tubule diameters near the DEJ, as well as peritubular widths as great or greater than that found in permanent dentin. This may result in less solid dentin available for bonding after resin bonding procedures such as acid etching. Numerical tubule density and tubule diameter increased toward the pulp while peritubular width decreased, and changes in the features as a function of depth were dependent on tooth type and in some cases on specific directions within a tooth.

1. BACKGROUND AND LITERATURE REVIEW

1.1 REVIEW OF DENTIN

Human dental hard tissue is composed of three types of calcified material. The inner layer, circumferentially surrounding the pulpal tissue, is composed of dentin. The outer layers exposed to the oral cavity are composed of enamel and cementum and cover the coronal and root portions of the tooth, respectively.

1.1.1 Structure and composition of dentin

Dentin is a mineralized, collagenous matrix secreted by odontoblasts as they migrate from the dentino-enamel junction (DEJ) towards the pulp chamber, and is considered the living and vital part of the hard tooth structure (Pashley, 1991). Dentin has a high degree of elasticity (elastic modulus of 1.23×10^4 MPa), and both piezo- and pyro-electric properties (Berkovitz, et.al., 1989). It can be described as a "complex hydrated composite" containing four principle elements (Marshall, 1993). The first is the dentin tubules, the long, narrow channels that penetrate the collagenous matrix and are basically oriented somewhat parallel to each other and perpendicular to the DEJ and dentin-pulp junction. These tubules are surrounded by a peritubular zone of hypermineralized matrix containing apatite and very little collagen (Pashley, 1989). The tubules and their accompanying peritubular zones are surrounded by and embedded within an intertubular matrix that is composed mostly of type I collagen (90%) embedded with apatite crystals as well as dentinal fluid and/or odontoblastic processes (Allred, 1968). Other non-collagenous proteins with specific functions are also present in smaller amounts.

Information regarding the overall composition is varied, ranging from 50-70 vol % mineral, 18-30 vol % organic matter, and 12-20 vol % fluid (Carrigan, et.al., 1984; Marshall, 1993). Driessens and Verbeeck (1990) compared the mineral, organic, and fluid content of bone, dentin, and enamel. In terms of volume % mineral,

enamel had the highest at 90%, followed by dentin at 50%, and bone at 40%. Bone contained the most organic matter at 48%, followed by dentin at 30%, and enamel at 2%. Finally, dentin had the highest fluid content at 20%, followed by bone at 12%, and enamel at 8%. The major inorganic constituents of dentin are (in mean dry wt. %) : calcium (26.9), phosphorus (13.2), carbonate (4.6), magnesium (0.8), sodium (0.6), chlorine (0.06), and potassium (0.02) (Driessens and Verbeeck, 1990).

The mineral content of dentin has been compared to hydroxyapatite, but a couple of differences exist. Apatite crystals in dentin are small relative to those found in hydroxyapatite or enamel and the crystals contain 4-5% carbonate, thus leading to a higher carbonate content and lower calcium content (Marshall, 1993; Mjor and Fejerskov, 1979; Driessens and Verbeeck, 1990). Marshall (1993), discussed this small, Ca-deficient crystal as having a higher solubility and the potential for ionic substitutions such as fluoride.

Dentinogenesis begins during the 8^{th} week *in utero*. During the process, dentin is the first of the calcified tissues to be deposited (Berkovitz, et.al., 1989). Undifferentiated mesenchymal cells derived from the dental papilla position themselves adjacent to the inner enamel epithelium, on the basement membrane. As these cells mature to become odontoblasts, their morphology takes on a more polar nature. The organelles in the odontoblast responsible for the manufacture, packaging, and secretion of the organic dentin matrix are the rough endoplasmic reticulum and the Golgi apparatus (Carrigan, et.al., 1984).

During dentinogenesis, each dentin tubule is produced by an odontoblast. As the cell lays down its collagen matrix and moves from the DEJ towards the pulp, an odontoblast process trails the cell body. While some authors claim the odontoblast process extends to the enamel, many maintain that it only extends about 25-30% of the length of the tubule as the tooth ages (Pashley, 1989; Berkovitz, et.al., 1989). Dentin tubules have irregular walls with many lateral

branches and microchannels connecting neighboring tubules. Scanning electron microscope studies of longitudinal sections have shown that the inner walls of the dentin tubules are fully lined with peritubular dentin, and that most lateral branches are approximately 0.2 to 0.3 μm in diameter (Kubota, et.al., 1969). It's thought that these lateral branches are the result of cell junctions between odontoblasts or small cell processes that become entrapped during dentinogenesis (Moss-Salentijn and Hendricks-Klyvert, 1985). Under normal conditions, the tubules are filled or partially filled with fluid. These fluid-laden channels are sensitive to external stimuli, which in turn causes fluid movement in either direction. The ability of the tubules to permit rapid movement of fluid is thought to be related to pain and sensitivity transmission (Marshall, 1993; Pashley, 1991). While the tubules permit the free flow of intratubular fluid, they have been found to have a functional diameter of only 5-10% of the anatomic diameter. Thus, the tubules serve as an excellent pulpal protective barrier that is effective at trapping bacteria from saliva (Pashley, 1989).

Viewed in longitudinal section, the dentin tubules are not straight but gently curved in an S-shape. This strange course results from the fact that as the odontoblasts move towards the center of the dental papilla, the cells start out on a larger surface and end up on a much smaller surface. If the original surface and the later surface were spherical, the cells would all move centrally in a straight line, becoming more densely packed. A tooth however, is fairly cylindrical, forcing the odontoblasts to move obliquely in an apical direction, producing an S-shaped curve making accommodations for the more occlusally/incisally located odontoblasts. The resultant odontoblasts become evenly distributed, despite being densely packed (Moss-Salentijn and Hendricks-Klyvert, 1985). The formative cells leave behind a structural arrangement with variation in tubule size and number and quantity of intertubular and peritubular dentin. It is generally accepted that the tubule diameters and numerical density increase from the DEJ towards the pulp, with peritubular

dentin displaying the inverse trend (Marshall, 1993). This aspect will be covered in greater detail later.

The collagen matrix becomes mineralized as the tooth matures, except for a very thin layer of immature dentin in the pulp known as predentin (Pashley, 1991). Mineralization of dentin involves the progressive growth of apatite crystals on the organic matrix (Carrigan, et.al., 1984; Berkovitz, et.al., 1989). During the course of initial mineralization, no peritubular dentin is present. The formation and calcification of the intertubular matrix and the peritubular zones appear to be distinct stages in dentin development. The development of peritubular dentin takes place at the expense of the periodontoblastic space and occurs through centripetal mineral deposition (Berkovitz, et.al., 1989). The peritubular dentin collar is approximately 40% more mineralized than the intertubular dentin (Ten Cate, 1994). The formation of peritubular dentin is not fully understood. Three possibilities exist. The first, is that peritubular dentin forms as the result of intertubular dentin derived mineral passively redistributing around preexisting components of the dentin tubule. Second, that an active response by the odontoblast process produces an organic matrix that is actively mineralized as the result of odontoblast activity. Third, that the odontoblast produces an organic matrix that becomes mineralized by redistribution of mineral from intertubular dentin (Ten Cate, 1994). The third theory differs from the first, in the sense that the third theory implies that the odontoblast plays an active part in secreting a target matrix for mineralization while the first theory assumes the mineralization occurs around the tubule without regard to a specifically secreted target.

Ultrastructurally, dentin can be classified into several other categories that are visible centripetally on longitudinal sections. Mantle dentin, is the first thin layer of dentin formed during dentinogenesis. Primary dentin, formed prior to eruption is the normal and regular dentin. Secondary dentin is a continuation of primary dentin formation and is produced circumpulpally during the

later periods of the life of the tooth in response to the irritating effects of normal biological function. Very often, a line of demarcation and a change in tubule curvature is apparent at the primary/secondary dentin junction. Tertiary dentin is a more or less irregular dentin produced as a reaction to noxious stimuli such as abrasive, mechanical, chemical or thermal stresses. Tertiary dentin is only produced in the area directly affected by the stimulus and often occurs with irregular or even absent tubules (Berkovitz, et.al., 1989).

There are several other ultrastructural features of normal dentin. Interglobular dentin is a normal histological feature that consists of a region of unmineralized dentin matrix found in the outer third of the coronal dentin, running parallel to the DEJ. The granular layer of Tomes is found in the peripheral regions of the root dentin running parallel to the cemento-dentinal junction (CDJ). This granular layer is separated from the CDJ by the mantle dentin and is thought to be caused by odontoblast development and matrix production being out of synchrony, resulting in an increase in the odontoblast process space (Berkovitz, et.al., 1989). Incremental lines are indicative of the normal rhythmical process of dentin formation which proceeds with alternating periods of activity and inactivity. Neonatal lines are particularly accentuated incremental lines found in deciduous teeth and first permanent molars indicating the dentin formed before and after birth. It has been reported that the period of arrested dentin development in the perinatal period is on the order of 15 days (Berkovitz, et.al., 1989). Finally, translucent dentin or sclerotic dentin is formed by the obliteration of the dentin tubule lumens. This process occurs by the deposition of calcified material with a refractive index similar to that of normal dentin. Translucent dentin represents a special type of tissue metamorphosis that occurs under normal physiological or pathologic conditions such as aging, caries, attrition or dental erosion. This process generally affects coronal or cervical root dentin. Sclerotic dentin is reportedly harder than normal opaque root dentin and the amount of root sclerosis increases linearly with age (Berkovitz, et.al., 1989).

1.1.2 Dentin smear layer

As dentin and enamel are cut or shaped, a layer of cutting debris is created on the dentin surface, known as the smear layer. The dentin smear layer is made up of apatite crystals and partially denatured collagen that have come mostly from the underlying dentin (Heyman and Bayne, 1993). It is likely that the composition of the smear layer may change accordingly as deeper dentin is cut since the composition of the underlying dentin matrix may change as the pulp is approached (Pashley, 1989). The thickness of the smear layer has been reported as thin as 1 μm (Pashley, 1989) to as thick as 5 μm (Heyman and Bayne, 1993). While the smear layer is partly porous, studies have shown that it does form a physiologic barrier to hydrodynamic fluid shifts and to the diffusion of exogenous toxins toward the pulp. Pashley (1991), reports that the smear layer/smear plug accounts for 86% of the resistance to fluid movement across dentin. It has been found that removing the smear layer results in an increase of the dentin permeability by diffusion *in vitro* by 5-6 times and an increase by convection (filtration) by 25-36 times (Pashley, 1984). Thus, the smear layer helps to exclude bacteria from dentinal tubules as well as restricting the surface area available for diffusion of both large and small molecules. In this manner, the smear layer has been described as a "biological Band-Aid", reducing postoperative tooth sensitivity and creating a drier surface for adhesion (Heyman and Bayne, 1993; Pashley, 1991; Pashley, et.al., 1981).

Most of the early dentin adhesives were designed to bond directly onto the smear layer (Heyman and Bayne, 1993). However, smear layers are intrinsically quite weak. When present, the adhesive bond is made to the smear layer instead of the underlying dentin, thus limiting the strength of adhesive bonds (Pashley, 1991). The theoretical bond strength is increased if the smear layer is removed. However, because the smear layer cannot be washed or rinsed off, treatment to remove the smear layers (EDTA or acidic conditioners) depletes the surface of mineral. Recently developed

bonding systems have attempted to modify the smear layer and retain the smear plugs prior to adhesion. By doing so, the dentin permeability is much lower and the dentin can be dried more easily (Pashley, 1991).

1.2 Deciduous versus permanent tooth dentin

In this study, primary teeth and its dentin will be referred to as deciduous teeth and dentin to avoid confusion with primary dentin. The dentin found in permanent and deciduous teeth has basically the same morphological and compositional elements. It has been generally assumed that both kinds of teeth are similar in histologic structure and thus the accepted practice has been to apply the findings obtained from studies of permanent teeth to deciduous teeth. However, there is evidence suggesting significant chemical and morphological differences between the dentin found in the two dentitions (Bordin-Aykroyd, et.al., 1992; Agematsu, et.al., 1990). These differences were detected as the result of morphologic studies as well as studies related to dentin bonding.

1.2.1 Mineral content

Hirayama, et.al. (1986) and Shellis (1981) found, via electron microscopy, that the peritubular dentin of deciduous teeth was 2 to 5 times thicker compared to that of permanent teeth. In a later study, Hirayama (1994) used an energy dispersive X-ray spectrometer and a software system developed for the quantitative analysis of elemental concentrations in biological specimens to report that: deciduous intertubular dentin contained 24.9%(w/w) calcium and 12.1%(w/w) phosphorus; and deciduous peritubular dentin contained 30.7%(w/w) calcium and 15.3%(w/w) phosphorus. This was compared to the findings in permanent intertubular dentin containing 25.5%(w/w) calcium and 12.5%(w/w) phosphorus; with permanent peritubular dentin containing 34.5%(w/w) calcium and 16.9%(w/w) phosphorus. These findings suggested that in both deciduous and permanent teeth, the concentrations of Ca and P may be higher in peritubular dentin than in intertubular dentin and that

the concentrations of both Ca and P might be lower for peritubular dentin in deciduous teeth. However, it is possible that the apparent differences could all be within experimental variability, therefore the results must be interpreted with caution.

1.2.2 Morphology

1.2.2.1 *Dentinal tubules*

Investigations of dentin morphology have concentrated primarily on dentin tubules of permanent teeth and overall results are summarized in Table 1-1.

An early electron microscopy study by Kubota, et.al. (1969), of teeth (unspecified as to deciduous or permanent) revealed that the diameter of a dentin tubule was 2.0 to 3.0 μm. This varied somewhat from the results of Ketterl (1961), Bradford (1955), and Meyer (1951) , who reported tubule diameters ranging from 1.0 μm near the enamel to 4 or 5 μm near the pulp. In the same study, Ketterl (1961) observed (Table 1-1) that near the enamel, the tubule numbers ranged from 9,000 to 24,000 per mm^2. At a distance of 1.0 mm away from the pulp, the numerical tubule density was 64,000 and close to the pulp he found 70,000 tubules per mm^2.

One of the first studies concentrating on the microstructure of dentin tubules was performed by Brannstrom and Garberoglio (1972). In an SEM study of young permanent premolars, they reported that: at a distance of 0.4 to 0.6 mm from the pulp the diameter of the tubules varied from 1.8 to 2.0 μm, at 1.0 mm from the pulp the diameter was about 1.5 μm, and near the enamel border the diameter was around 1.0 μm.

A study by Tronstad (1973), revealed (Table 1-1) that under the SEM and TEM, without a systematic investigation, peripheral dentin displayed a numerical tubule density of 7,000 per mm^2, compared to a density of 60,000 near the pulp. He also found that the tubule diameter was between 2 and 3 μm near the pulp, and less

than 0.5 μm near the enamel. There was no mention of whether or not the findings were statistically significant.

In a subsequent study to their 1972 investigation, Garberoglio and Brannstrom (1976), studied 24 premolars and 1 permanent incisor under the SEM and reported (Table 1-1) that at 1.0 mm from the pulp, the tubule density ranged from 30,000 to 40,000 per mm^2. Their study measured the tubule densities at 0.5 mm increments from the pulpal wall and found that at 2.0 mm from the pulp the numerical tubule density ranged from 23,000 to 30,000 per mm^2, and that at 3.0 mm from the pulp the density ranged from 19,000 to 20,000 per mm^2. Regarding tubule diameters, at 1.0 mm from the pulp the mean diameter was 1.6 μm, at 2.0 mm from the pulp wall the mean was 1.1 μm, and at 3.0 mm away it was 0.8 μm. The investigators also noted a large variation among teeth in numerical tubule density. They attributed this finding to true variations among individual teeth and to inaccurate measurements of distances from the pulp. The authors also discussed the significance of the effects of demineralization on dentin. They cited evidence that as demineralization removes peritubular dentin, the diameter of the tubules increases, and that demineralizing dentin followed by drying results in an 18% shrinkage linearly. These effects are likely to result in inaccurate measurements of the numerical tubule densities and tubule diameters. The effects of shrinkage following demineralization thus probably affected the results of many earlier studies.

Mjor and Fejerskov (1979), reported the diameter of dentin tubules in "young" teeth to be between 4-5 μm, and that the average numerical tubule densities (Table 1-1) in the periphery, middle, near the pulp were: 15,000 per mm^2, 35,000 per mm^2, and 65,000 per mm^2, respectively. There was no mention as to whether or not their findings were statistically significant.

•Table 1-1

Numerical tubule density (#/mm^2) of permanent teeth as reported by various authors.

INVESTIGATORS	NEAR THE DEJ	MIDDLE	NEAR THE PULP
Ketterl, 1961	9,000-24,000	64,000	70,000
Tronstad, 1973	7,000		60,000
Brannstrom & Garberoglio, 1976	19,000-20,000 (3.0 mm from pulp)	23,000-30,000 (2.0 mm from pulp)	30,000-40,000 (1.0 mm from pulp)
Mjor & Fejerskov, 1979	15,000	35,000	65,000
Pashley, 1984	19,000-23,000	35,000	43,000
Pashley et.al., 1985			82,900 (projected)
Tidmarsh & Arrowsmith, 1989	13,000	24,000	28,000
Fosse et.al., 1992	13,458-22,244	33,819-43,177	40,297-61,586
Olsson et.al., 1993 (occlusal sites)	24,500	40,400	51,100
Olsson et.al., 1993 (buccal sites)	18,200	30,900	43,400
Amory & Yvon, 1994	20,000		42,000-70,000
Ten Cate, 1994	30,000-37,500		59,000-76,000

Carrigan, et.al. (1984), studied permanent incisors in young and old teeth via the SEM to determine if a correlation existed between numerical tubule density and dentin location and/or age of the

specimen. Their results (Table 1-2) revealed that the mean number of dentin tubules for all teeth in each of four locations were as follows: apical root dentin (8,190 per mm^2), mid-root dentin (39,010 per mm^2), cervical root dentin (42,360 per mm^2) and coronal dentin (44,243 per mm^2). The results were statistically significant ($p < 0.01$). In regards to numerical tubule density in relation to age, they found a significant difference ($p < 0.01$) between the mean number of dentin tubules for the 20 to 34 years age group (242,775 = mean number of tubules in combined apical, mid-root, cervical, and coronal dentin) compared to the 80 years and above age group (149,025 = mean number of tubules in combined apical, mid-root, cervical, and coronal dentin). The authors did not report what unit area was utilized for the final two findings.

•Table 1-2
Numerical tubule density (#/mm^2) by locations as reported by Carrigan et.al., (1984).

INVESTIGATOR	APICAL ROOT	MID-ROOT	CERVICAL	CORONAL
Carrigan, et.al., 1984	8,190	39,010	42,360	44,243

Pashley and co-workers have studied dentin extensively, including tubule density, permeability and microhardness. Pashley (1984) adapted Garberoglio and Brannstrom's (1976) findings and reported (Table 1-1) the mean number of dentin tubules at 0.5 mm from the pulp to be 43,000 per mm^2, 35,000 per mm^2 at 1.5 mm from the pulp, 23,000 per mm^2 at 2.5 mm from the pulp, and 19,000 per mm^2 at 3.5 mm from the pulp. Pashley, et.al.'s (1985) investigation of unerupted third molars under serial SEM study revealed a projected tubule density (in regards to a linear regression against dentin hardness) of 82,000 per mm^2 close to the pulp. A later study reported a general approximation of 20,000 to 30,000 tubules per mm^2 (Pashley, 1990).

Koutsi, et.al. (1994), investigated deciduous molar dentin and found that the numerical tubule densities for deciduous teeth were somewhat lower than in permanent teeth. They reported (Table 1-3) superficial dentin with a density of 17,433 per mm^2, outer dentin at 18,075 per mm^2, intermediate dentin at 20,433 per mm^2, and deep dentin at 26,391 per mm^2. The tubule diameters also were smaller than those of permanent teeth: 0.96 μm, 1.08 μm, 1.10 μm, and 1.29 μm, for the above mentioned locations, respectively. While no statistical comparison was made between the deciduous and permanent teeth, comparisons were made within the deciduous teeth. The tubule densities for the intermediate and deep layers were significantly different from each other ($p < 0.05$) as well as from the superficial and outer layers, which were not statistically different from each other. While the tubule diameters between the outer and intermediate layers were not significantly different, the tubule diameters of the superficial and deep layers were significantly different ($p < 0.05$) from the outer and intermediate layers.

•Table 1-3

Numerical tubule density (#/mm^2) of deciduous teeth as reported by Koutsi, et.al. (1994).

INVESTIG.	SUPERFICIAL	OUTER	INTERMEDIATE	DEEP
Koutsi, et.al., 1994	17,433	18,075	20,433	26,391

Tidmarsh and Arrowsmith (1989), studied root dentin of permanent incisors via the SEM and reported (Table 1-1) that just inside the dentin-cementum junction (CDJ), the mean numerical tubule density was 13,000 per mm^2; halfway between the CDJ and the pulp canal the mean was 24,000 per mm^2; and close to the root canal the mean numerical tubule density was 28,000 per mm^2. There was no mention as to whether or not their findings were statistically significant.

Hojo (1990), studied permanent mandibular incisors under the SEM and reported (Table 1-4) the number of tubule openings in the dentin of teeth in three different age groups. In the 20 to 39 year old group the mean numerical tubule density was 34,146 per mm^2, in the 40 to 59 year old group it was 32,317 per mm^2, and in the over 60 year old group it was 23,537 per mm^2. The difference between the 20-39 year old group and the > 40 year old group was significant ($p < 0.01$). The author attributed the decreased numerical tubule density with age to the occlusion of dentin tubules from masticatory wear ("hard diets") and the consumption of food items with high levels of calcium.

•Table 1-4

Numerical tubule density (#/mm^2) by age as reported by Hojo (1990).

INVESTIGATOR	20-39 years	40-59 years	> 60 years
Hojo, 1990	34,146	32,317	23,537

Schellenberg, et.al. (1992), studied premolars and third molars under the SEM and reported (Table 1-5) a substantial variation among locations within and between teeth of the same individual and between teeth of different individuals. For the maxillary first premolars, the average numerical tubule density (per mm^2) at the pulpal wall of the mesial and distal segments was 44,000 at the CEJ and 31,000 at the mid-root level. On the facial segment, it was 72,000 at the CEJ and 44,000 at mid-root. On the lingual segment, it was 69,000 at the CEJ and 40,000 at mid-root. On the occlusal segment (at the pulpal roof), it was 67,000. For the mandibular second premolars, the values on the mesial and distal segments were 55,000 at the CEJ and 28,000 at mid-root. On the facial segment, it was 77,000 at the CEJ and 48,000 at mid-root. On the lingual segment, it was 68,000 at the CEJ and 43,000 at mid-root. On the occlusal segment, it was 67,000. For the maxillary third molars, the values were taken at the CEJ only. The values were: 61,000 on the mesial, 56,000 on the distal, 66,000 on the facial, 65,000 on the

lingual, and 63,000 on the occlusal. Only the values at the CEJ were given for the mandibular third molars and were: 65,000 on the mesial, 72,000 on the distal, 71,000 on the facial, 68,000 on the lingual, and 59,000 on the occlusal. The numerical tubule density of the pulpal aspect of the coronal dentin wall was significantly greater than that of the radicular wall in all the other sites in the study ($p < 0.01$). The numerical tubule densities of the facial/lingual walls were significantly greater ($p < 0.01$) than that of the mesial/distal walls. There was also a significant difference ($p < 0.05$) between the mesial, distal and occlusal segments for the maxillary and mandibular third molars.

•Table 1-5

Numerical tubule density (#/mm^2) by location as reported by Schellenberg, et.al., (1992).

SEGMENT	REGION	Max. 1st premolars	Mand. 2nd premolars	Max. third molars	Mand. third molars
Mesial	CEJ	44,000	55,000	61,000	65,000
	Mid-root	31,000	28,000		
Distal	CEJ	44,000	55,000	56,000	72,000
	Mid-root	31,000	28,000		
Facial	CEJ	72,000	77,000	66,000	71,000
	Mid-root	44,000	48,000		
Lingual	CEJ	69,000	68,000	65,000	68,000
	Mid-root	40,000	43,000		
Occlusal		67,000	76,000	63,000	59,000

Fosse, et.al. (1992), attempted to track a given bundle of dentin tubules from the DEJ to the pulp wall and measure the changes in numerical density (Table 1-1) and peritubular diameters within a single tooth. Maxillary premolars were studied under light microscopy and they found that at three levels from the DEJ to the pulp, the numerical tubule densities increased more than 3 times and the peritubular diameters decreased by one-tenth. Tubule densities near the DEJ ranged from 13,458 to 22,244 per mm^2, at midway

between the pulp and DEJ from 33,819 to 43,177 per mm^2, and near the pulp wall from 40,297 to 61,586 per mm^2. The differences between each group were statistically significant ($p < 0.01$). Raw data regarding peritubular diameter was confusing as presented.

Olsson, et.al.(1993), studied the coronal dentin of third molars at different locations and different depths under the SEM. Attempts were made to measure the dentin in the same areas at 3 different levels and average numerical tubule densities for occlusal and buccal sites were reported (Table 1-1). For the occlusal site, the average tubule density varied from 24,500 to 40,400 to 51,100 per mm^2 as the depth changed by 1.25 mm increments from DEJ to the pulp. For the buccal sites under the same conditions, they reported tubule densities of 18,200 to 30,900 to 43,400 per mm^2. Levels 1 and 2 showed a significant difference between the buccal and occlusal sites ($p < 0.05$).

Amory and Yvon (1994), studied the dentin of third molars near the pulp and peripherally (Table 1-1). Near the periphery the numerical tubule density averaged 20,000 per mm^2 and near the pulp it ranged from 42,000 to 70,000 per mm^2. They reported an average tubule diameter of 2.1 μm, and that the tubule diameters increased as the pulp was approached. There was no mention as to whether or not their findings were statistically significant.

Ten Cate (1994), presented the diameters of the dentin tubules as approximately 900 nm near the DEJ, 1.2 μm in the midportion of the dentin, and 2.5 μm near the pulp. The numerical tubule density of the coronal dentin from young premolar and molar teeth (Table 1-1) ranged from 59,000 to 76,000 per mm^2 at the pulp and approximately 30,000 to 37,500 per mm^2 near the DEJ. There was no mention as to whether or not the findings were statistically significant.

Arends, et.al. (1995), studied the effects of air drying and/or demineralization on tubule diameter in premolars. At a depth of

approximately 1.5 mm from the DEJ, wet, sound dentin was found to have an average tubule diameter of 1.3 μm. The tubule diameters of the mineralized samples did not change significantly after being subjected to periods of drying. Samples that had been demineralized for one week showed diameters of: 2.5 μm (wet) to 3.3 μm (dry). After two weeks, the diameters were: 2.2 μm (wet) to 2.8 μm (dry). After three weeks: 1.7 μm (wet) to 2.1 μm (dry). The differences between the sound and demineralized samples were found to be significant ($p < 0.05$) and the differences between the three week demineralized group and the one and two week demineralized groups were significant ($p < 0.05$).

1.2.2.2 *Peritubular dentin*

Studies quantifying peritubular dentin have not been as extensive as those for the dentin tubules, and the results have been quite varied.

In a study describing a method of differentially staining peritubular and intertubular dentin matrices using Pollak trichrome connective tissue stain, Allred (1968) reported that the peritubular matrix in molar and premolar teeth ranged from 1.0 to 2.5 μm in width. Moss-Salentijn and Hendricks-Klyvert (1985) described peritubular dentin as a heavily calcified sheath consisting of a delicate collagenous matrix and a relatively abundant ground substance with a width of 1 μm.

Ten Cate (1994) referred to peritubular dentin as intratubular dentin and reported that it is approximately 0.044 μm (sic) thick near the pulpal end and approximately 0.75 μm thick near the DEJ.

1.2.2.3 *Microcanals*

In the literature, unusual structures known as microcanals (Agematsu, et.al., 1990) or giant tubules (Hals, 1984) have been described in both incisors and cusped teeth (Agematsu, et.al., 1990).

Recognized in the dentin of canine teeth in the red deer (Hals, 1984), human deciduous and permanent teeth (Hals, 1983), and bovine teeth (Dyngeland, et.al., 1984; Dyngeland and Fosse, 1986 b), microcanals are in fact best described as giant dentin tubules. In lower magnification studies, an opaque zone in the incisal dentin of worn teeth has been described (Dyngeland and Fosse, 1986 a). It had been generally assumed that this was a "dead tract" caused by exposure of the dentin. Later studies described a "chain of holes" or occasionally a slit observed in the mesio-distal axis and situated in a mesio-distal opaque band (Agematsu, et.al., 1990) of the dentin, visible in transverse section (Hals, 1983). Further investigations under the SEM enabled microcanals to be described in detail. These tubules with enlarged lumina, arranged in a chain of holes axially oriented (Dyngeland, 1988), running mesio-distally in transverse section, followed the course of the dentin tubules from the border of the pulpal cavity almost to the incisal DEJ. Their lumina were 5 to 40 μm in diameter and usually accompanied by a hypermineralized rim of dentin. Polarized light microscopy has shown that the lumen of each microcanal was limited by a 5 to 15 μm thick collagenous mantle in which the fibers were oriented parallel to its long axis (Hals, 1983; Hals, 1984). While microcanals were described as a normally occurring feature in incisors, studies have shown that the incidence of microcanals occurring in a single tooth can range from 0 to 30 (Hals, 1983).

Agematsu, et.al. (1990), performed a detailed SEM study investigating the ultrastructure of microcanals in deciduous anterior teeth. Their findings described microcanals as: "commingled" and arranged linearly in the mesio-distal direction almost entirely within the labio-lingual central portion of the dentin. Microcanals were observed to run continuously from the incisal edge to the direction of the pulp cavity running parallel to the dentin tubules in longitudinally fractured dentin. Diameters of the microcanals were found to range from 6.0 to 7.5 μm (clearly thicker than dentin tubules) and on the peripheral wall of these microcanals, the wall structure resembled a thin peritubular matrix. Further investigation

of the microcanals under higher magnification showed longitudinally oriented fibers inside the microcanal to be bundles of collagen fibers with typical striation structures and spherical bodies (2.0 to 2.5 μm in size) attached to them to be composed of "regular parallelepipedal crystals." While the findings of this study agreed with the observations made by previous authors describing giant tubules, Agematsu's group dubbed the structures as microcanals. Earlier work by Miller (1981), had described similar structures in a deciduous incisor.

In the literature describing the microstructure of dentin in anterior teeth, microcanals/giant tubules are not often mentioned. Perhaps this is because while they are a normally occurring phenomenon, they are not found in all anterior teeth all the time, and when they do occur, they are quite variable in number. Various theories regarding their origin, genesis, and function have been discussed.

Dyngeland (1988), hypothesized that the cause of giant tubule formation was the passive accumulation and subsequent necrosis of odontoblasts. However, he later found that within the giant tubules, cells of the pulpal vascularized portion demonstrated an intact organellar apparatus. Other salient points include: very few dentinal tubules enter the giant tubules; a blood vessel loop is situated within the pulpal giant tubule portion; and that cellular components within the giant tubules show vital staining reactions and vital enzymatic reactions. From this he concluded that the giant tubules are canals containing unmineralized collagen and the organic components of the pulpal vascularized portions are responsible for their formation. Regarding their function, he suggested that two possible functions are: 1) to encourage diffusion processes to the most distal part of the incisal dentin, facilitating secondary mineralization and 2) to increase the sensitivity of the tooth.

Agematsu, et.al. (1990), found that the microcanals manifested themselves mainly in the labio-lingual central portion of the dentin

and hypothesized that this region of dentin in particular had some traits conducive to formation of these distinctive structures. They suggested that at the initiation of dentin formation, odontoblasts differentiated at the location of the DEJ shift inward (towards the dental papilla) to a region with a small surface area. As a result, dentin formed on the labial side collides with dentin formed on the lingual side, causing a disruption and imperfection in the dentinogenesis functions of odontoblasts directly below the incisal center. They concluded that the microcanals are the result of these phenomena generating defects in the ultrastructure of the dentin below the incisal edge. Further support for this theory of imperfect formation may be derived from studies by Wright and Gantt (1985), who demonstrated the presence of giant tubules appearing more frequently in teeth with dentinogenesis imperfecta.

Further information is needed concerning the development of microcanals in order to determine whether they should be considered as anomalous dentinal tubules or as a different type of structure (Hals, 1984). While current studies cite the existence of microcanals in both deciduous and permanent teeth, several papers appear to suggest a sense of uniqueness to deciduous teeth (Agematsu, et.al., 1990; Agematsu, 1988). Hals (1983) noted the existence of microcanals in both deciduous and permanent teeth but did not discuss differences in their prevalence. Miller (1981) reported on these features in deciduous teeth only. A definitive conclusion regarding whether or not microcanals are features that are more unique to either dentition type cannot be drawn from the available literature. However, the literature that does exist regarding microcanals is focused largely on deciduous teeth, suggesting that they may be more common in deciduous teeth. Future studies should focus also on comparisons/contrasts between the existence of microcanals in deciduous and permanent teeth.

1.3 Dentin bonding properties of deciduous vs. permanent teeth

Any discussion involving deciduous and permanent dentin will invariably lead to comparisons regarding dentin bonding/adhesion. Dentin bonding systems typically consist of an acidic conditioner, a hydrophilic resin monomer or primer, and an intermediate unfilled resin adhesive. In some recently developed systems, the primer is composed partially of an acidic resin monomer that acts as the dentin conditioner as well (Mazzeo, et.al., 1995). Currently, there are products that advocate complete smear layer removal and there are those that advocate smear layer modification prior to bonding (Gwinnett and Kanca, 1992).

The role of the dentin conditioner is to remove, penetrate or solubilize the smear layer and demineralize the exposed dentin surfaces. The primer infiltrates into the demineralized dentin, allowing the monomer component to polymerize and interlock with the dentin. The alteration modifies the collagen fiber arrangement, elasticity, and wettability, allowing for improved adhesive resin penetration (Mazzeo, et.al., 1995). Penetration of the primer and adhesive into the demineralized dentin subsurface and its subsequent polymerization generates the adhesive bonds. These adhesive bonds are a function of how penetrable the dentin is and how well the primer diffuses into it (Nakabayashi, et.al., 1992). A hybrid layer is created as a result of the monomer impregnating the demineralized dentin surface. This hybrid zone, or transitional zone of resin-reinforced dentin, sandwiched between cured resin and unaltered dentin appears to be the primary site for dentin adhesion (Heyman and Bayne, 1993; Gwinnett and Kanca, 1992). Ultimately, the dentin adhesive bond is thought to be derived from micromechanical retention of the dentin adhesive to intertubular dentin. A chemical interaction of the bonding system to the inorganic/organic components could also play a role in adhesion (Asmussen and Ino, 1992). It is believed that two-thirds of the adhesive bond strength results from an interaction between the bonding system and intertubular dentin, and only one-third from the penetration of resin into the dentinal tubules (Retief, et.al., 1992). It

has also been determined that the bond strength to deep dentin is only 30 to 40% that of the bond strength to superficial dentin. This has been attributed to the percentage area of solid dentin available for bonding, or in other words, the total area of dentin minus the percent area of exposed dentinal tubules (Suzuki and Finger, 1988).

It has been documented that the restoration of deciduous teeth, particularly anterior teeth, is often a difficult task. Reasons cited for this include the small size of the teeth, thinness of enamel and enamel morphology, pulpal anatomy, and rapid spread and extent of decay (Olsson, et.al., 1993; Atkins, et.al., 1986). Most reports on bond strengths relate to permanent teeth and little literature exists on the bond strength of dentin bonding agents to deciduous teeth (Elkins and McCourt, 1993). Recent investigations have produced mixed reviews regarding differences between bonding to dentin of deciduous and permanent teeth.

Walls et.al. (1988), studied the bond strength of Ketac-Fil (glass ionomer) to deciduous dentin and compared it to that of permanent dentin. Tensile bond strengths to 10 non-carious deciduous molars were compared to those to 30 non-carious permanent molars. The bond strength of Ketac-Fil to deciduous dentin was significantly less than that to permanent dentin ($p < 0.001$). The authors attributed the discrepancy to difficulties in preparing a flat deciduous dentin specimen capable of receiving the desired bond diameter, and to the possibility that the mineralization levels of deciduous dentin are markedly less than those for permanent dentin. While glass ionomer compounds interact to dentin via a different mechanism than do adhesive resins, the study was still able to demonstrate a difference between deciduous and permanent dentin.

Salama and Tao (1991), studied the shear bond strength of Gluma/Lumifor to the occlusal dentin of non-carious deciduous first and second molars and compared that to the bond strength of non-carious permanent first and second molars and premolars. Analysis of variance and Duncan's Multiple Range test indicated that the bond

strength of Gluma/Lumifor to deciduous molar dentin was significantly lower than to permanent first and second molars and premolars ($p = .05$). In this study, the smear layers were removed according to manufacturers' specifications. The authors postulated the discrepancies between deciduous and permanent dentin possibly were due to differences in prepared dentin depths.

Bordin-Aykroyd, et.al. (1992), investigated three chemically different dentin adhesive systems by measuring the *in vitro* shear bond strengths between dentin and anterior composite restorative materials on both deciduous and permanent teeth. Scotchbond 2, Gluma, and Tenure were used according to the manufacturers' specifications on non-carious specimens. For all the materials tested, permanent teeth showed a higher mean bond strength than the deciduous teeth and these differences were found to be statistically significant ($p< 0.001$). It has been previously shown that the bond strengths of some dentin adhesives decrease as the dentin approaches the pulp. This was interpreted as the bond being dependent on the calcium level or the total area of solid dentin available, both of which decrease towards the pulp. Hirayama (1990) and Shellis (1981) reported that peritubular dentin was 2 to 5 times thicker for deciduous teeth compared to permanent teeth. A layer with few crystals was found in the inner part of the peritubular dentin surrounding the lumen in deciduous teeth. These differences may affect bonding ability because of the effects on chemical bonding of the adhesive or because of differing effects of the pre-treatment regimens on the dentin (Bordin-Aykroyd, et.al., 1992). The dentin pre-treatment of the 3 systems in this study tended to remove the peritubular dentin, which resulted in wider, less retentive tubules and also decreased the area of solid, available dentin in the deciduous teeth.

Elkins and McCourt (1993), focused specifically on bond strength to deciduous dentin. They determined the *in vitro* bond strength of three dentin bonding agents to deciduous molars and incisors. Scotchbond 2, All-Bond, and Amalgambond were applied to

deciduous teeth according to manufacturers' specifications. All the materials tested showed higher bond strengths to anterior deciduous teeth than to posterior teeth. The anterior teeth resulted in a shear strength nearly twice that of the posterior teeth. Unfortunately, the authors were not able to speculate as to any reasons for this difference.

Contrasting the findings that bond strength to deciduous dentin is less than that to permanent dentin, Fagan, et.al.(1986), investigated the shear bond strengths of 2 dentin bonding techniques on deciduous and permanent teeth. The authors reported no statistically significant difference between dentin bond strengths in deciduous teeth and permanent teeth using their techniques, although the authors admitted that some of the methods used did not lend themselves to practical clinical use. An example of this is the technique described by Bowen, et.al., (1982 a, 1982 b) for manipulating dental adhesives that the authors utilized as part of their study. This method involves the preparation and application of ferric oxalate, NTG-GMA (the adduct of N(p-tolyl)glycine and glycidyl methacrylate) and PMDM (the addition reaction product of pyromellitic dianhydride and 2-hydroxyethylmethacrylate). NTG-GMA has a short shelf life (must be prepared every several weeks) and must be stored under anaerobic conditions. The preparation and application of ferric oxalate, NTG-GMA and PMDM solutions onto the tooth structure is also very time consuming in comparison to the application of Scotchbond adhesive, for example (Fagan, et.al., 1986).

Donly, et.al. (1991), studied the *in vitro* bond strengths of four dentin bonding agents on deciduous molars and compared their findings to previous studies on permanent teeth. Their findings for the mean shear values were similar to mean values reported by other investigators for the shear strengths of dentin bonding agents to permanent dentin (Reinhardt, et.al., 1987). Such findings however, need to be evaluated in a direct comparison study in order to conclude that no difference exists between the bond strengths to deciduous and permanent teeth.

Recently, Mazzeo, et.al. (1995), studied the *in vitro* bond strengths of three resin adhesive systems to deciduous teeth. They concluded that "resin adhesive systems may achieve bond strengths to primary dentin comparable to those of primary enamel and that these bonds may be as strong as bonds to permanent enamel and dentin." While such claims would seem encouraging, their study offered no direct comparisons to the bond strengths of permanent teeth.

In summary, while most adhesive resins are developed with the principle intention of bonding to permanent dentin, comparisons of the ability of these materials to bond to deciduous and permanent dentin have been investigated to a limited degree. A few authors have reported no difference between the bonding ability of deciduous and permanent dentin. However, the majority of investigators have shown that with present materials and techniques, the bonding ability of deciduous dentin is significantly less than that of permanent dentin. This difference, in conjunction with the frustration of many clinicians who routinely place adhesive resin restorations in deciduous teeth, establishes the need for a better understanding of deciduous dentin.

1.4 Previous methods of dentin microstructure study

There are several factors to consider when reviewing literature regarding different methods of dentin microstructure study. Previous methods involved fracturing the tooth with a chisel and hammer or liquid nitrogen in order to visualize the desired dentin surface under conventional (secondary or backscattered) SEM study (Garberoglio and Brannstrom, 1976; Kubota, et.al., 1969). Fracturing the tooth structure was advocated because it is generally thought that fractured surfaces represented undisturbed dentin. The advantage of this is that the dentin surface is exposed without contamination or introduction of artifact through surface preparation

or instrumentation, all of which would contribute to a smear layer which subsequently covers the normal structural components of the dentin surface (Marshall, 1993). The major disadvantage of fracturing is that there is very little control over the exact location at which the dentin surface will be exposed.

Improved accuracy of sample preparation was accomplished via sectioning the teeth with various cutting surfaces such as diamond saws (Toda, et.al., 1981) and disks (Kubota, et.al., 1978). Methods utilizing saws or disks to expose the desired dentin surfaces allowed for more accurate location determination and for serial section studies as well (Asmussen and Ino, 1992; Arends, et.al., 1989; Foreman and Soames, 1989; Pashley, et.al., 1987). A consequence of mechanical cutting was the production of a smear layer on the exposed dentin surface. This was addressed by subjecting the tooth specimen to an acid or other chemical treatment (e.g., citric acid, sodium hypochlorite, EDTA, phosphoric acid, etc.). Such treatment removed the smear layer from the surface, and exposed the surface structure of the dentin tissue, giving access to the intrinsic microstructural features (Panighi and G'Sell, 1993). The major disadvantage of acid treating the dentin samples is that such methods for smear layer removal also cause demineralization of the dentin. Acid treatment preferentially removes the peritubular dentin, which will widen the tubule openings and possibly lead to an overestimation of tubule size (Marshall, 1993; Olsson, et.al., 1993). Under conditions of severe demineralization (such as a caries attack), the tubule diameter may increase by as much as 30% (Arends, et.al., 1995; Arends, et.al., 1989). It has been found that demineralization of dentin results in substantial shrinkage, estimated at about 18% (Garberoglio and Brannstrom, 1976). Also, it has been noted that water losses caused by drying contribute to an increased tubule size in demineralized dentin (Arends, et.al., 1995). It has been suggested that the macroscopic dimensional changes observed with elastic strain necessitated that microscopic measurements of tubule dimensions and packing density be corrected by 1.4 to 2% to account for strain upon drying (Van der Graaf and Ten Bosch, 1993).

However, Kinney, et.al. (1993), studied dimensional changes in human dentin during drying utilizing an atomic force microscope and found that drying lead to contraction that caused microstrains, which were dependent upon the degree of mineralization in the dentin. For fully mineralized dentin, these strains were small (<0.1%) and well within the elastic limits of dentin, leading them to conclude that drying-induced strain is too small to require corrections for tubule size and tubule density.

Instruments routinely used to study the features of dentin include light and scanning electron microscopy (Arends, et.al., 1995). Advantages of using an SEM are the ease at which magnification can be changed as well as its ability to transmit images of a sample over a wide magnification range of approximately 5x to 150,000x. Other features of the SEM are its ability to study chemical elements, magnetic and electrical fields, voltage distributions, resistivity, light emission, and crystallography of the sample (Marshall, 1989). The primary requirements for a sample to be studied under conventional SEM conditions are that the specimen: exhibit electrical conductivity, be rigid enough to withstand deformation under extreme vacuum conditions, and be dry and clean. Biological tissues such as teeth are non-conducting specimens and need to be coated with a thin conducting layer (approximately 10 to 20 nm thick) that will provide the necessary conductivity without obscuring the surface detail. This is accomplished for specimens such as teeth by sputter coating the sample with metals (gold/palladium) or carbon (Marshall, 1989). Such preparative treatments and consequent subjection to extreme vacuum conditions of conventional SEM however, can cause significant alterations and deterioration of the microstructural appearance of the dentin surface (Kodaka, et.al., 1992).

As a remedy for this dilemma, SEM's have been developed that use a differential vacuum system, so that biological samples in an unfixed or wet state, can be studied under near environmental conditions. Marshall (1989) described the direct observation of non-conducting and wet samples that allows for studying samples in a

more natural state, using a Robinson scintillator backscattered detector and independent pumping of the electron column and specimen chamber. Kodaka, et.al. (1992, 1993), have also recently described the use of an SEM equipped with a low vacuum specimen chamber and a Robinson backscattered electron detector to study dental hard tissues nearer their natural state. When non-conducting samples are being used, backscattered electrons do not become affected by the phenomenon of charge build-up. This property of backscattered electrons is the result of their high energy. This allows for efficient backscattered collection that can be used when observing poorly conducting or "chargeable" samples (Marshall, 1989).

Because electrons interact strongly with each other and become scattered by the atmosphere, the SEM must operate at a high vacuum. A solution to by-pass this dilemma is to have a specimen chamber operating at a relatively poor vacuum and the filament, lenses, and scanning coils operating at a high vacuum. An example of this is the charge free anti-contamination system (CFAS). The principle behind this system is that charging can be almost completely eliminated and not affect the backscattered signal. This process involves the charge that accumulates on the specimen being balanced by gas ionization, and oxygen present within the chamber (poor vacuum) reducing contamination as such carbon based contaminates are oxidized and removed via pumps (Marshall, 1989).

Achieving a good result is dependent directly on maintaining a "delicate balance" between the pressure within the chamber, the operating voltage, the beam current, and the specimen conductivity. The ultimate resolution of conventional backscattered or secondary electron microscopy is much greater than that resulting from a system such as the CFAS, but the trade off is that a non-conducting specimen may be observed in a "wet" state without metal coating (Marshall, 1989). While the specimen is not observed in a truly wet state and is still subject to drying within the chamber, this is not of

great concern since Kinney, et.al. (1995) found that unless the dentin is demineralized, it does not shrink significantly.

1.5 Description of various experimental methods

Brannstrom and Garberoglio's early study (1972) examined the dentin tubules via the SEM (summary of experimental methods, Table 1-6). Young permanent premolars that had been fixed in formalin or glutaraldehyde for a few hours had their roots sectioned off with a diamond wheel. A groove was cut in the buccolingual or mesiodistal direction leaving either the buccal or one of the proximal surfaces intact. Liquid nitrogen was used to induce spontaneous fracture of the teeth. The teeth were then freeze-dried, mounted for examination, and gold coated for study under SEM at 20 kV and 1000, 2000, 5000, or 10,000x magnification. Observations were made before and after demineralization with 5% nitric acid over a period of 5 days. Photomicrographs were taken in series (with slight overlap) from the pulp tissue outwards. Tubule diameters at varying distances from the pulp (approximately 0.4-0.6 mm increments) were measured, however no description of their method for quantification was given. In a subsequent study, the same authors looked at 30 permanent teeth that were prepared in the same manner except that some of the teeth were sectioned to view the dentin tubules transversely and grooved so that the distance from the pulp to the area studied could be measured (Garberoglio and Brannstrom, 1976). Photomicrographs were taken from 3 to 5 areas at various distances from the pulp to the DEJ at 5,000 to 12,000x magnification. The number of tubules was counted physically from each photograph and the tubule density (number per mm^2) calculated. The mean tubule density and diameter at measured distances from the pulp were presented. To correct for their previously mentioned 18% shrinkage factor, the values collected for the tubule diameters of the demineralized dentin were multiplied by 1.22. The values they found for numerical tubule density and tubule

diameter were: between 30,000-40,000 per mm^2 and 1.6 μm at 1.0 mm from the pulp, between 23,000-30,000 per mm^2 and 1.1 μm at 2.0 mm from the pulp, and between 19,000-20,000 per mm^2 and 0.8 μm at 1.0 mm from the pulp. A linear regression analysis can be applied to their findings. The adapted slope or rate of change of the numerical tubule density was an increase of 8,571 tubules per mm^2/mm as distance to pulp decreased. The adapted slope or rate of change of the tubule diameters was an increase of 0.37 $\mu m/mm$ as distance to the pulp decreased.

Carrigan, et.al. (1984), studied the relationship between the number of tubules and dentin location and age. 30 maxillary central incisors were stored in saline and arranged into 5 age categories. The teeth were prepared for SEM study by splitting them into buccal and lingual halves with a mallet and chisel. The buccal specimens were placed in sodium hypochlorite and fixed in formalin, sonicated, and then dehydrated and gold sputtered. Each sample was examined via SEM at 20 kV and 3000x magnification. Photomicrographs were taken at three areas of the root and the central area of the crown. The number of tubules per mm^2 was calculated via the photomicrographs. The numerical tubule densities were presented according to age of the tooth and location on the tooth. They found that the mean number of tubules was for apical root dentin 8,190 per mm^2, for mid-root dentin 39,010 per mm^2, for cervical root dentin 42,360 per mm^2, and for coronal dentin 44,243 per mm^2.

•Table 1-6
Previous experimental methods for studying dentin tubules as reported by various authors.

Investigators	Tooth type	Fractured or blade-sectioned	Deminer.	Microscopy	Precise control of depth, location	Method of quantif.
Brannstrom & Garberoglio, 1972	perm.	fracture	Yes	conven. SEM (1000, 2000, 5000, 10,000x)	No, No	manual
Brannstrom & Garberoglio, 1976	perm.	fracture	Yes	conven. SEM (5,000 to 12,000x)	Approx., No	manual
Carrigan, 1984	perm.	fracture	Yes	conven. SEM (3000x)	No, No	manual
Pashley, et.al., 1985	perm.	blade	No	light (240x)	Approx., Approx.	manual
Hojo, 1990	perm.	neither	No	conven. SEM, (3000x)	No, No	digitizer
Schellenberg, et.al., 1992	perm.	blade	Yes	conven. SEM (1030x)	No, No	manual
Fosse, et.al., 1992	perm.	blade	No	light	Approx., Approx.	manual
Olsson, et.al., 1993	perm.	blade	No	conven. SEM	Approx., Approx,	image analysis
Koutsi, et.al., 1994	deciduous	blade	No	conven. SEM (6,000x)	Approx., No	image analysis
Amory & Yvon, 1994	perm.	blade	No	light	No, Approx.	image analysis
Arends, et.al., 1995	perm.	blade	Yes	light & conven. SEM (200x)	Approx., Approx.	image analysis

Pashley, et.al. (1985), correlated dentin microhardness and dentin tubule density. Unerupted third molars were stored in phosphate buffered saline. The roots were sectioned from the crown using a diamond saw at the level of the CEJ and the occlusal enamel

was removed by a second section parallel to the first. The specimens were sliced several times, approximately 0.5 to 1.0 mm apart, thus allowing for observation of the tubules in direct cross-section. Tangentially-cut tubules were excluded from the study. Microhardness indentations were made across each dentin surface. The samples were polished with an alumina slurry and photographs were taken at a 240x magnification with a metallograph. By drawing a 5 mm x 50 mm rectangle on the print alongside the long axis of the indentation, corresponding to a known area of 4340 μm^2, the tubules were counted and expressed as number per mm^2. Attempts were made to count the tubules at the same location for each photograph, however this was not always accomplished. Numerical tubule density was plotted against dentin hardness to show in a linear regression the relationship of microhardness versus numerical tubule density. Their results showed that as numerical tubule density increases near the pulp, the area occupied by open tubules can increase to as much as 22%, that the tubule diameters increase, and that peritubular dentin decreases. The microhardness in KHN (Knoop hardness numbers) of dentin at the DEJ was found to be about 57, falling to near 20 as the pulp chamber was approached. Their linear regression projected 82,000 tubules per mm^2 at zero KHN.

A few innovations in dentin study were made by Hojo (1990), who studied the changes in closing pattern of openings of dentinal tubules on worn occlusal surfaces of incisors. Permanent mandibular incisors of different age groups were observed *in vivo*. Attempting to study only the dentin on worn incisal surfaces of the non-extracted teeth, he made high resolution casts of the teeth using a polysiloxane impression material and a low-viscosity epoxy resin for the positive cast. The casts were sputter coated with platinum and observed via SEM at 20 or 25 kV and magnifications ranging from 50 to 3,000x. Tubule diameters and densities (number of open tubules only) were quantified by the use of a digitizer and presented according to varying age groups. He found that in the 20 to 39 year old group the mean numerical tubule density was 34,146 per mm^2,

in the 40 to 59 year old group the mean numerical tubule density was 32,317 per mm^2, and in the over 60 year old group the mean was 23,537 per mm^2.

Schellenberg, et.al. (1992), obtained site-specific data of tubule density of specified human teeth by systematic survey. They investigated a total of 125 maxillary first premolars, mandibular second premolars, and maxillary/mandibular third molars to assess the tubule density at the pulpal wall. The teeth were fixed in formalin and stored in sodium cacodylate buffer solution. Each tooth was divided into two segments with a diamond saw, some at the level of the CEJ to contain the roof of the pulp chamber, and some to produce either mesial/distal halves or vestibulo/oral halves. The prepared segments were stored in sodium hypochlorite, rinsed, ultrasonically cleaned, and critical point dried. The samples were gold coated and observed in the SEM. A graticle (sic) was fitted before the micrographs were taken; each grid square of the graticle represented an area of 100 μm^2. Photomicrographs were taken from the CEJ and the mid-root level, at 10 to 16 kV and at 1030x magnification. An area representing 4000 μm^2 was marked on each micrograph and the dentin tubules found within that area were counted and the number of tubules per mm^2 was calculated. Numerical tubule densities per mm^2 for the 2 sites per segment were presented for the mesial, distal, vestibular, oral, and occlusal segments and arranged according to the type of tooth. For the maxillary first premolars, the average numerical tubule density (per mm^2) at the pulpal wall of the mesial and distal segments were 44,000 at the CEJ and 31,000 at the mid-root level. On the facial segment, it was 72,000 at the CEJ and 44,000 at mid-root. On the lingual segment, it was 69,000 at the CEJ and 40,000 at mid-root. On the occlusal segment (at the pulpal roof), it was 67,000. For the mandibular second premolars, the values on the mesial and distal segments were 55,000 at the CEJ and 28,000 at mid-root. On the facial segment, it was 77,000 at the CEJ and 48,000 at mid-root. On the lingual segment, it was 68,000 at the CEJ and 43,000 at mid-root. On the occlusal segment, it was 67,000. For the maxillary third

molars, the values were taken at the CEJ only. The values were: 61,000 on the mesial, 56,000 on the distal, 66,000 on the facial, 65,000 on the lingual, and 63,000 on the occlusal. For the mandibular third molars the values were also only given for the CEJ and were: 65,000 on the mesial, 72,000 on the distal, 71,000 on the facial, 68,000 on the lingual, and 59,000 on the occlusal.

Fosse, et.al. (1992), remarked that except for Ketterl's (1961) study, no strong attempts to quantify numerical tubule density and tubule diameter of a given bundle of dentin tubules within a single tooth had been made. Their study aimed to determine the numerical tubule density, distributional pattern of a bundle of dentin tubules, mean area and diameter of peritubular dentin and the mean proportion of peritubular dentin within single teeth. The bundles of dentin tubules were to be cut transversely, to observe the dentin tubules near the DEJ, midway to the pulp, and near the pulp wall. 8 maxillary premolars were collected and stored in formalin. The central buccolingual plane of each tooth was exposed by slicing just lateral to the long axis in an axio-bucco-lingual direction. On this plane, in the coronal part, a guideline was engraved buccally, following the main course of a bundle of dentin tubules and crossing the DEJ approximately 3.5 mm from the CEJ. Perpendicular to this line, 2 new sectioning lines were engraved, one about 300 μm pulpal to the DEJ and one about 300 μm peripheral to the pulp wall. Attempts were made to create 3 sections from each sample, peripheral, middle and pulpal to observe the tubules transversely. However the blade thickness prohibited this so the pulpal and peripheral sections were taken from some teeth, and the middle section was taken from others. The specimens were observed under light microscopy as the authors felt that the exact magnification in SEM micrographs is not easily determined and a distortion in one direction may occur. Tubule density and peritubular areas were calculated by a method involving triangulation, as the tubules appear in a closest packing pattern in cross-section. Numerical tubule densities and peritubular diameters were presented according to the three depth levels. Tubule densities near the DEJ ranged from

13,458 to 22,244 per mm^2, at midway between the pulp and DEJ from 33,819 to 43,177 per mm^2, and near the pulp wall from 40,297 to 61,586 per mm^2.

Olsson, et.al. (1993), investigated the variation of tubule numbers in various parts of teeth. Third molars were stored in saline mixed with chloramin (sic). 5 teeth were cut with a diamond blade to expose a dentin surface at 3 different levels, near enamel, central and near the pulp from both the buccal and occlusal parts of the teeth. Each section was 1.25 mm deeper than the preceding section. The disks were examined under an SEM. In order to observe the dentin surfaces in their natural state, no attempts were made to remove the smear layer, thus observations were made on areas with minimal smear. The disks were measured at 5 different areas in each of 5 different sites, approximately 1 mm apart along a 5 mm straight line across the central part of the disk. The 5 areas in each site were chosen from sites that were relatively free from smear layer and were spotted as close as possible to the center of each measuring site. The field area at each reading site was 0.0033 mm^2. A computer-assisted image analyzer was used to quantify the number of tubule openings per unit area and to calculate the area percentage covered by the tubule openings. Tubule openings smaller than 0.5 μm in diameter were not recorded. Irregularities, such as cracks caused by the vacuum drying, were excluded. Numerical tubule densities were presented according to the three depth levels for each (buccal, occlusal) area. For the occlusal site, the average tubule density varied from 24,500 to 40,400 to 51,100 per mm^2 as the depth varied in 1.25 mm increments from the DEJ to the pulp. For the buccal sites under the same conditions, they reported tubule densities of 18,200 to 30,900 to 43,400 per mm^2. A linear regression analysis can be applied to their findings. The adapted slope or rate of change in the numerical tubule density in the occlusal sites was an increase of 10,640 tubules per mm^2/mm as the distance from the DEJ increased; and in the buccal sites, an increase of 10,080 tubules per mm^2/mm as the distance from the DEJ increased.

Koutsi, et.al. (1994), investigated the tubule density and diameter of deciduous molars and premolars in an attempt to correlate ultrastructure to permeability. 15 primary molars and 10 premolars were stored in phosphate buffered saline containing sodium azide. The roots were removed approximately 1 mm apical to the CEJ using a diamond saw. Four reductions of dentin were made for each tooth: 0 to 30% of the distance from the pulp, 30.1 to 60% from the pulp, 60.1 to 90% from the pulp, and 90 to 100% from the pulp. The smear layer of each sample was removed using 320 grit aluminum oxide sandpaper to create a new smear layer. This was done to create a smear layer that was more easily removed by sonication. Each sample was sonicated for approximately 15 minutes at 70% power to remove the smear layer. After being gold coated, the surfaces were examined in the SEM at 25 kV. At each of the 4 depths, 3 micrographs were taken at 480x and 6 micrographs were taken at 6,000x magnification. The cervical third of the tooth was the area most frequently examined. Tubule density was calculated manually from the micrographs taken at 480x. The tubule diameter was determined from the 6,000x magnification micrographs via image analysis. Numerical tubule density and diameters were presented according to the three depth levels. For the primary molars, they reported superficial dentin with a density of 17,433 per mm^2, outer dentin at 18,075 per mm^2, intermediate dentin at 20,433 per mm^2, and deep dentin at 26,391 per mm^2. Koutsi's group compared these numbers to the findings of Garberoglio and Brannstrom (1976) and Fosse, et.al. (1992) and reported them to be smaller than those for permanent premolars. The tubule diameters were also reported to be smaller than those of permanent teeth at: 0.96 μm, 1.08 μm, 1.10 μm, and 1.29 μm for the above mentioned locations, respectively.

Amory and Yvon (1994), determined correlations between dentin characteristics and shear bond strength. 94 permanent molars were collected and stored in thymol. The roots were first removed from the crown with a diamond saw at the level of the CEJ. The occlusal enamel was removed in a section parallel to the first cut.

A third section was made perpendicular to the first one going through the middle of the crown. Serial sections were made approaching the pulpal wall in steps of 0.1 mm. Dentin measurements were carried out on a surface with an area of approximately 1.5 mm x 0.01 mm, near the edge opposite the tip of a pulp horn. The exposed dentin surface was wet abraded and polished with diamond pastes in felt and sonicated in water to remove the smear layers. Numerical tubule density, tubule diameters and solid dentin surface were measured using a metallographic microscope assisted by image processing equipment. Numerical tubule densities and diameters were presented according to varying distances to the pulp. Near the periphery the numerical tubule density averaged 20,000 per mm^2 and near the pulp it ranged from 42,000 to 70,000 per mm^2. They reported an average tubule diameter of 2.1 μm, and that the tubule diameters increased as the pulp was approached.

Arends, et.al. (1995), assessed the diameter of coronal dentin tubules in vitro as a function of periods of demineralization and air drying under light and scanning electron microscopy. Young premolars stored in water with thymol were sectioned through the pulp parallel to the buccal surface with a thin-bladed saw. 2 cuts perpendicular to the first one were made to produce a 3 x 3 mm block. A final cut was made to expose the dentin surface at a distance of about 1.5 mm from the pulp. The samples were embedded in cold cure acrylic and polished on wet silica paper. Selected samples were demineralized for 1, 2 or 3 weeks and other samples were not subjected to demineralization process but had their smear layers removed via EDTA. Pictures were produced by light and conventional SEM observation at 200x magnification. Image analysis was used to determine the tubule diameters. Sound dentin was found to have tubule diameters of 1.3 +/- 0.2 μm. The authors reported that demineralization increased tubule size initially, but ended up decreasing the tubule size over time; that water losses caused by drying increased tubule size in demineralized dentin; and that tubule diameter in sound dentin was not influenced greatly by

air drying. Their last finding appears to be in agreement with Kinney, et.al. (1995), who found that fully mineralized dentin does not shrink significantly when dried in air.

In summary, from a survey of the literature, it is apparent that several important limitations exist concerning our current knowledge of dentin structures. While an abundance of information regarding many different aspects of permanent tooth dentin is available, there is a comparative lack of general information regarding deciduous tooth dentin. Specifically, there is a lack of significant information regarding microstructure of deciduous tooth dentin as well as the principles of adhesion to deciduous tooth dentin. While most studies related to dentin adhesion relate the findings of permanent dentin and simply apply them to deciduous dentin, there is evidence to suggest a difference (structure, composition, and bonding) between deciduous and permanent tooth dentin. Methods that have been described for the study of dentin microstructure involved procedures that potentially distorted the appearance of the dentin surfaces (e.g. smear layer removal, demineralization, drying). Furthermore, most studies were not able to track specific dentin tubules as would be necessary in order to accurately describe the characteristics of dentin tubules due to the marked variation that has been described. Most studies have characterized tubule size and numerical density in categories of: outer, middle, and deep dentin. Thus, regressions in these parameters with regards to distance from an anatomic landmark (e.g. DEJ or pulp chamber) are not available for permanent or deciduous dentin.

2. STATEMENT OF THE PROBLEM

There is only limited knowledge of dentin microstructural differences associated with position, and most available information is for permanent dentin. Deciduous dentin exhibits similar microstructural features and it is generally assumed that knowledge of permanent dentin can be related or applied to deciduous dentin. However, important differences may be present as indicated by limited studies of tubule size, numerical density, bonding characteristics, and observations of clinical bonding problems.

Thus, there is a need for dentin microstructure study specifically characterizing deciduous dentin. In order to accurately assess the microstructure characteristics, the study needs to be able to control for regional variability and serial specificity to enable the investigation to follow a particular area/group of dentin tubules within the same tooth. The study must also attempt to use specimens under as near environmental conditions as possible so as to avoid potential distortion of the dentin surface.

3. PURPOSE

The purpose of this study is to characterize the microstructure of deciduous tooth dentin of anterior teeth at specific areas and known depths in relation to the DEJ, using a wet-SEM technique and image analysis. The information gained should provide the basis for a better understanding of the microstructure of deciduous dentin and its similarities and differences in relation to permanent dentin. This may in turn, lead to a better understanding of deciduous dentin permeability as well as the development of better bonding/adhesive techniques for the restoration of deciduous teeth and the development of better methods for the study of the microstructure of dentin.

4. MATERIALS & METHODS

4.1 Tooth preparation

10 freshly extracted, non-carious deciduous maxillary anterior teeth with full root development and with no visible signs of root resorption, were collected and stored in a 10% buffered formalin solution. The teeth were recovered from healthy, non-related, children of ages 3-5 years. Reasons for extraction included trauma, esthetic concerns, and occlusal discrepancies. After sterilization by gamma-irradiation following the procedures of White, et.al. (1994), the teeth were labeled and documented by labial view radiographs, producing film images representing the teeth size at a 1:1 ratio.

The teeth were mounted individually on wooden tongue blades in preparation for sectioning. Each tooth was placed with its proximal side (mesial or distal) up and its long axis oriented perpendicularly to the long axis of the tongue blade and then secured with thermoplastic glue. Pen marks were made on the tongue blade to indicate the mesio-distal and labio-lingual orientation of the tooth. The tongue blade/tooth was then secured into the rotating arm of a low speed saw (modified Buehler Isomet Low Speed saw, model# 11-1180, Buehler Ltd., Lake Bluff, IL). Using a circular diamond blade of 0.15 mm thickness and copious filtered water, a 1.0 mm thick slice of tooth was sectioned from the labio-lingual midline in a mesio-distal or distal-mesial direction (Figure 4-1).

Taking great care to recognize the labial-lingual and mesio-distal orientation of the tooth slice, the slice was re-mounted on a new tongue blade parallel to the long axis of the tongue blade and secured in the same manner, this time being placed labial or lingual side up. Once again, pen marks were made on the tongue blade to indicate the orientation of the slice. The diamond saw was used to section the tooth slice in a labial-lingual direction at the DEJ to remove the enamel.

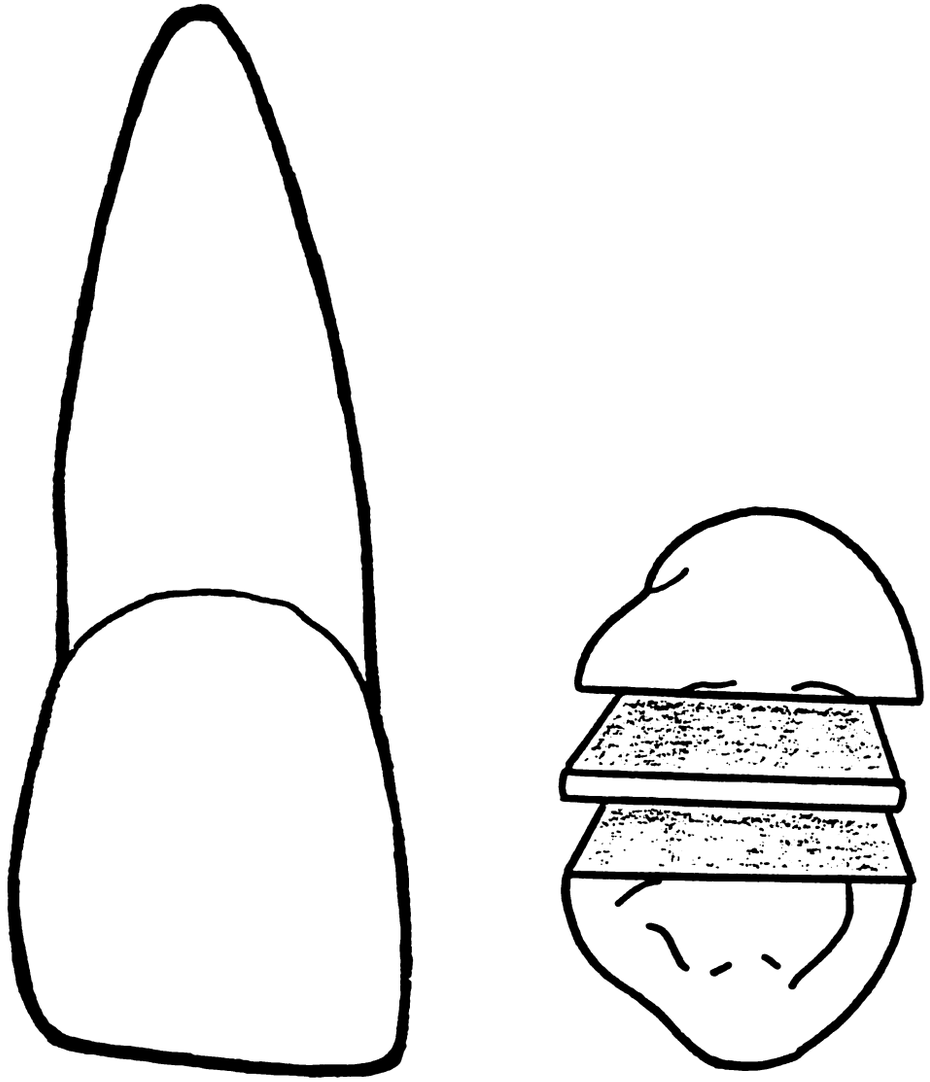

(a) (b)

•Figure 4-1
a) Illustration showing labial view of tooth before sectioning.
b) Illustration showing incisal view of tooth slice after sectioning.

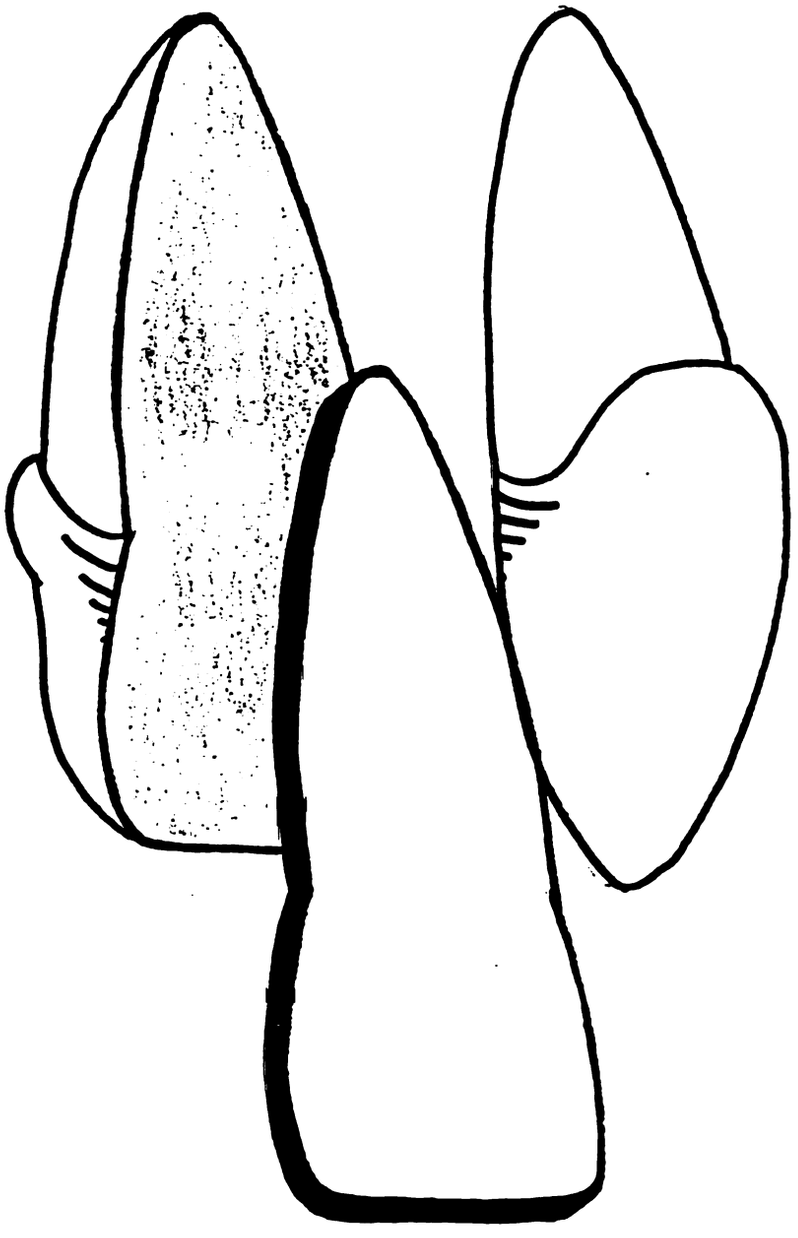

•Figure 4-1
c) Illustration showing profile view of tooth slice after sectioning.

With the enamel removed from the tooth slice, the sample was removed from the tongue blade and re-mounted on and secured to a new tongue blade. The orientation of the sample was perpendicular to the long axis of the tongue blade with the labial or lingual side up and secured in the same manner previously described. The diamond saw blade was used to make cuts 1.0 mm apart, running in a direction from the DEJ to the pulp chamber, producing "matchstick" shaped tooth samples from the slice (Figure 4-2).

Each matchstick was 1.0 mm thick (the thickness of the tooth slice) and 1.0 mm wide and the length ran from the DEJ to the pulp chamber. Two matchsticks were prepared from each tooth, one from the distal corner of the original slice and the other from the mesio-distal mid-point. Once again great care was taken to recognize the mesio-distal and labio-lingual orientations of the matchsticks. Although attempts were made to obtain a third matchstick from the mesial corner, they were not successful due to the small size of the deciduous anterior teeth.

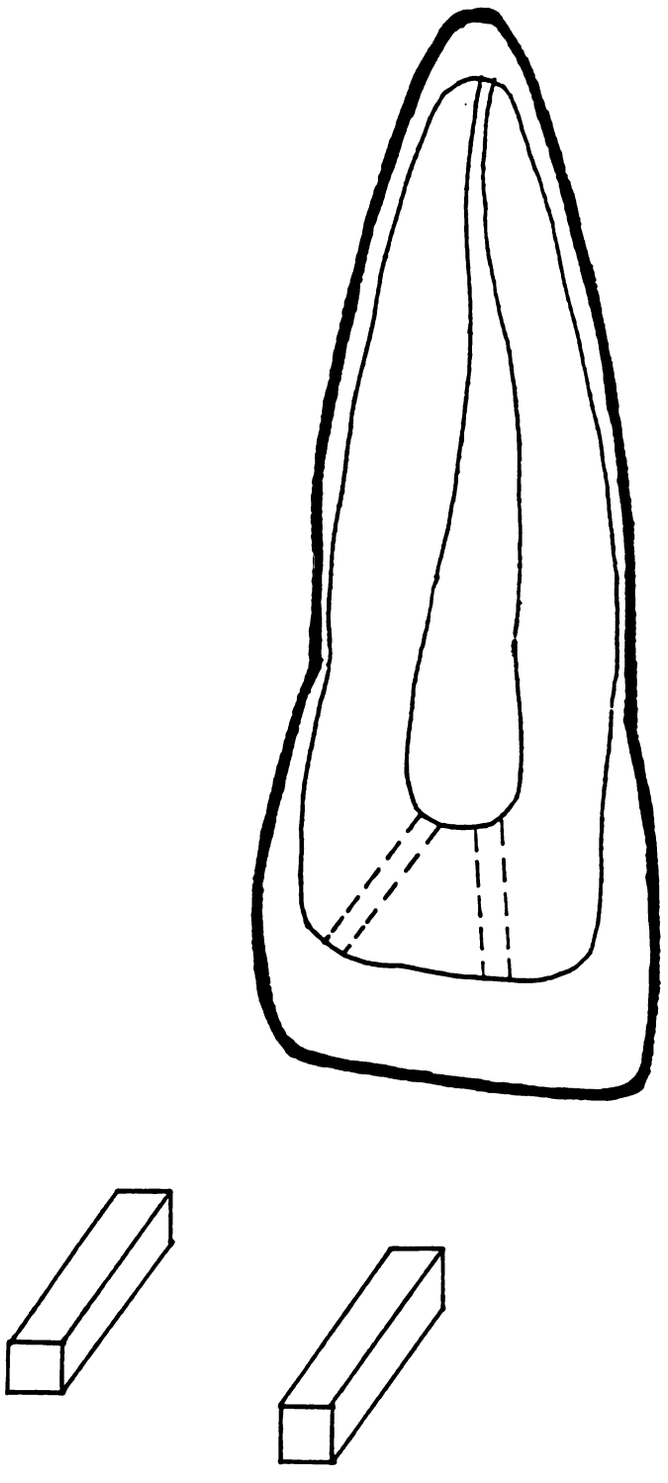

•Figure 4-2
Illustration showing preparation of tooth slice to produce 2 dentin matchsticks.

4.2 Dentin sample preparation

The two matchstick-shaped sections of dentin were then prepared for wet-SEM study. In order to assure that the incisal-apical, mesio-distal and labial-lingual orientations of the matchsticks for each tooth remained constant throughout the study, they were imbedded (invested) in an epoxy matrix for serial study via the following procedure.

A strip of mylar tape was tacked onto a clean glass microscope slide, sticky-side up. In order to prevent any epoxy from penetrating the dentin and occluding the dentin tubules, each matchstick was coated generously with a mixture of clear, quick-dry nail polish (Enamel Top-Coat Quick-dry, Revlon) diluted with acetone (2:1) and allowed to dry. The matchsticks were placed parallel to each other, DEJ-side down onto the mylar tape approximately 2-3 mm apart, once again taking great care to maintain proper labio-lingual and mesio-distal orientations. The matchsticks were secured to the tape using light cured, unfilled adhesive resin (Scotchbond Multipurpose adhesive resin, 3M Dental Products, St. Paul, MN), and their mesio-distal-labial-lingual orientations were indicated with pen marks on the tape.

A polyvinyl chloride (PVC) cylinder (1.25 cm high and 1.5 cm diameter) served as a matrix former for the epoxy resin. The edges of the cylinder were sanded flat on a strip grinder (Buehler Handimet-I Strip Grinder, model# 39-1471, Buehler Ltd., Lake Bluff, IL) so it could seat relatively flush against the flat surface presented by the mylar tape on the glass microscope slide, and the inner surfaces were lubricated with a topical lubricant (White petrolatum U.S.P. topical lubricant, E. Fougera and Co., Melville, NY). The cylinder was placed over the 2 dentin matchsticks and pressed flush against the mylar tape to prevent leakage of the investment epoxy (Figure 4-3).

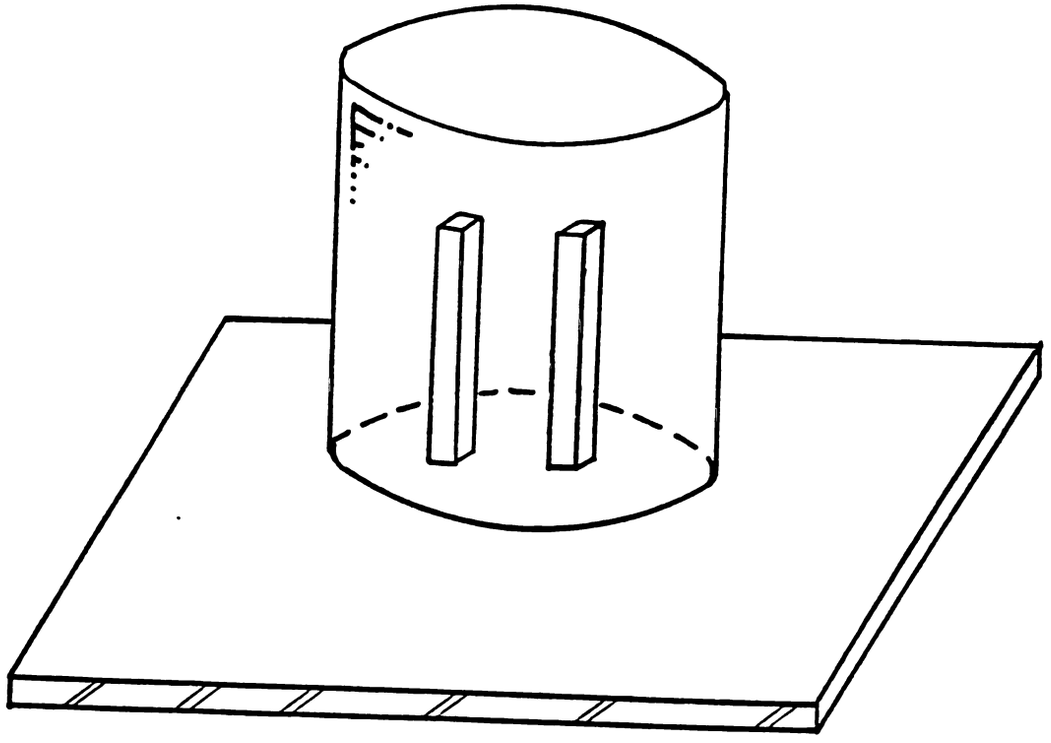

•Figure 4-3
Illustration showing dentin matchsticks in PVC cylinder on microscope slide prior to epoxy investing procedure.

A mixture of cold-cure epoxy resin (Sty-cast, Grace Specialty Polymers, Emerson and Cuming Inc., Woburn, MA) was prepared according to manufacturer's specifications and carefully poured into the cylinder, thus investing the matchsticks. Marks were made on the PVC cylinder to indicate the mesio-distal and labial-lingual orientations, and the sample was set aside and the resin allowed to cure for 24 hours.

Upon complete curing of the epoxy resin, the orientation marks from the PVC cylinder were transferred to the cured epoxy surface, and the epoxy matrix was removed from the PVC cylinder. More permanent orientation grooves were scored into the epoxy using a carbide disk. One groove was scored to indicate the labial side and two grooves were scored to indicate the distal side. The grooves were scored longitudinally on the epoxy cylinder, extending from one end to the other. The DEJ-end of the epoxy matrix was polished using abrasive strips on the strip grinder through 1200 grit and using alumina polishing slurries of 1.0, 0.3, and 0.05 micrometers on polishing felts mounted onto a smooth glass surface (Buehler Texmet polishing cloth, Buehler Ltd., Lake Bluff, IL).

In preparation for serial sectioning, the cylinder of epoxy matrix was mounted on a wooden tongue blade with its long axis parallel to that of the tongue blade and secured with thermoplastic glue. The same low speed diamond saw was used to section off a disk from the DEJ side of the epoxy 0.5 mm from the end. This produced a disk containing 2 squares of dentin 1.0 mm x 1.0 mm, imbedded in an epoxy matrix. The dentin squares were identified as: "distal" and "central", indicating their original positions from the tooth as described earlier. The sectioned disk was placed face down on a clean glass microscope slide. To provide bulk to the disk for easier handling, composite resin (P-50 composite, 3M Dental Products, St. Paul, MN) was placed on the back side of the disk and pressed flush against the back side of the sliced epoxy/dentin disk with a new clean glass microscope slide and light cured. The

resulting sample disk, already having been polished, was placed face down in a beaker of filtered water and ultrasonically cleaned (Neysonic Unit, NEY Corp.) for 45 seconds to remove surface debris. The finished disk was stored in purified and filtered water with 0.02% thymol (Figure 4-4).

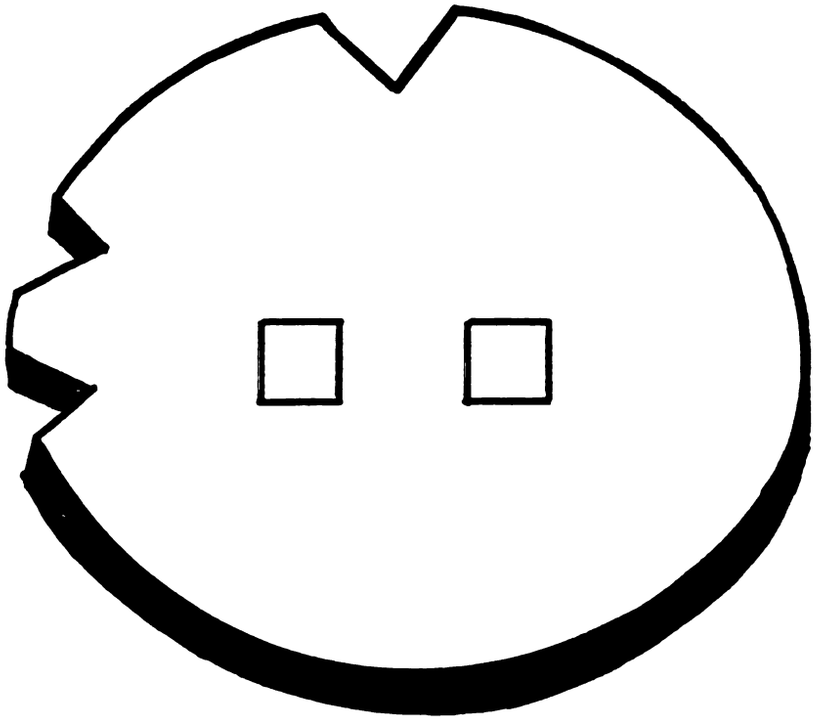

•Figure 4-4
Illustration showing epoxy disk embedded with 2 dentin squares. The two exterior grooves denote the distal side and the single exterior groove denotes the facial side.

Subsequent disks were serially sectioned off of the epoxy cylinder at 0.5 mm increments. By imbedding the matchsticks and sectioning the cylinder as described, it could be ensured that each dentin sample on each slice of epoxy was the desired distance from the DEJ. Each sliced disk was bulked-up with composite, polished, and cleaned as previously described. The disks were stored in order

of increasing distance from the DEJ towards the pulp in separate containers containing the 0.02% thymol solution until the SEM study. The samples were not repolished unless artifact or surface roughness was detected in the SEM. Due to the small length of the deciduous dentin matchsticks (short distance from the DEJ to the pulp), only 3-4 disks could be produced for each tooth.

4.3 SEM study and image analysis

Several problems arise when dealing with biologic samples in SEM studies. There are basically two types of operation modes under which the SEM works, backscattered and secondary. In secondary mode (high resolution), low energy electrons originating near the surface of the sample are collected. Secondary mode is topography-sensitive and is able to image into valleys and holes on the surface. In backscattered mode, the electrons from the primary beam are scattered at high angles, thereby producing a signal that becomes converted to a certain brightness. Backscattered electrons are shielded from the detector by holes, undercuts, or valleys. The backscattered electrons coming off the sample are also dependent on the atomic number of the area being irradiated. This allows the visualization of contrast differences within a relatively flat sample such as a dentin disk, that has areas of different composition; such as tubules and peritubular dentin. Signal collection efficiency is maximized by using a detector that is dedicated to the collection of backscattered electrons (as opposed to secondary electrons). The Robinson backscattered detector is an example. The result of these factors is an image with high contrast, and one in which peritubular dentin will be brighter than intertubular dentin due to its higher mineral content (higher average atomic number), whereas tubules will be black (Marshall, 1989).

Because electrons are scattered by atmosphere and interact strongly with each other, the high vacuum chamber previously mentioned is a requirement for SEM operation. With this in mind, the primary requirements for traditional SEM operation can be discussed. The first, is that the sample has to be electrically

conductive. This is necessary because the electrons need to be conducted away from the sample surface. The second, is that the sample needs to be rigid, to withstand deformation under the high vacuum pressure. The last requirement is that the sample needs to be dry and clean. A dirty sample will contaminate the electron column and obscure the image, and a structure that is not rigid and contains moisture will deform and/or explode under high vacuum (Marshall, 1989).

Biologic samples rarely satisfy these requirements. Regimens to improve the use of biologic samples often result in a markedly distorted sample. It is apparent then, that biologic samples need to be handled differently. Another problem with biologic samples is that they are generally poor electrical conductors. The consequence of this is a local build up of charge on the sample surface that results in charging artifacts, obscuring the image (Marshall, 1989).

The advent of separate electron column and specimen chambers allows for the observation of biologic or non-conducting samples, under backscattered SEM without subjecting the sample to extreme conditions (e.g. high vacuum, extreme preparative regimens). By keeping the filament, lenses, and scanning coils in a high vacuum and the specimen chamber in a relatively low vacuum, this allows for the visualization of these samples in a more natural, unaltered state. An example of this is the CFAS system (Topcon Instruments, Pleasanton, CA). Any accumulation of specimen charging can be almost completely eliminated without significantly affecting the backscattered signal by carefully balancing the pressure in the chamber. A drawback of this type of system is that the resolution is quite far below that of conventional SEM (Marshall, 1989).

With this in mind, the epoxy/dentin disks were prepared for study in the SEM (ISI SX-40A modified with a CFAS system, Topcon Instruments, Pleasanton, CA) in the wet mode by gently wiping the polished sample surface with a cotton swab dipped in filtered water

and air-dried with a quick (1-2 seconds) blast of clean, pressurized air. Starting with the disk closest to the DEJ, the disks were observed at low magnification to recognize the orientation grooves. Use of the SEM in wet mode under extreme vacuum pressure (less than 100 mtorr) resulted in the previously mentioned charging artifact building up and becoming evident on the surface of the dentin samples. In order to prevent charge build-up on the sample, a slow leak of the SEM chamber was established by gradually releasing the bleeder valve of the CFAS module until the pressure stabilized at 100-150 mtorr.

Each square of dentin was first observed at low magnification for orientation. To insure an accurate survey of each dentin square, images were taken from 9 areas in a grid for each square and labeled as: A through I, sequentially. The square was broken down into the following areas: upper left, upper middle, upper right, middle right, middle, middle left, lower left, lower middle, and lower right; much like a tic-tac-toe diagram drawn on a square surface. The upper row of the square (images A, B, and C) corresponded to the labial aspect of the dentin matchstick, the middle row (images D, E, and F) corresponded to the middle of the dentin matchstick (labio-lingually), and the bottom row (images G, H, and I) corresponded to the lingual aspect of the dentin matchstick (Figure 4-5). The images were recorded, winding in a snake like manner and oriented so that images A, F, and G always corresponded to the distal aspect of the dentin matchstick, and C, D, and I always corresponded to the mesial aspect. The images were taken at a magnification of 2000x, therefore each image width was approximately 50 μm (At 2000x, 1 cm on SEM film = 5 μm actual size. Therefore, 5 μm x width of SEM image on film ($\approx$10 cm) is approximately 50 μm).

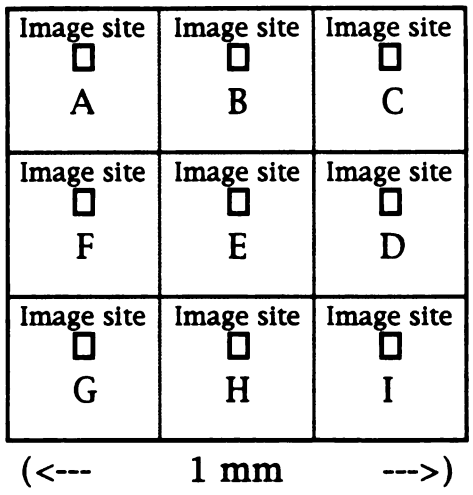

•Figure 4-5
Image locations within dentin sample

Once the desired locations were established under magnification at 2000x and 20 kV, the SEM images were digitized and transferred to the computer screen and recorded using an imaging software system (Advanced Imaging, Kevex Corp., San Carlos, CA). From each epoxy disk, 9 images were taken sequentially from each of the 2 dentin squares (labeled "distal square" and "central square") and recorded. The same procedure was carried out for each of the remaining epoxy disks, with each disk corresponding to an increasing distance from the DEJ.

As working distance is critical to the magnification accuracy in the SEM, a standard working distance (z = 21 mm) was maintained throughout the study. The effect of working distance was evaluated with an atomic force microscope standard containing 5 μm x 5 μm squares. The SEM magnification was calibrated to an accuracy of within 1%. The sensitivity of the working distance was evaluated from distances of 19 mm to 23 mm. A one way ANOVA detected no significant difference between the effect of the different working distances on magnification accuracy.

4.3.1 Storing images:

The image analysis software that was utilized, computed statistics on the basis of a grey scale. The number of bits the computer uses to store the brightness information defines the depth perception of the image. Since computer storage is often organized in bytes, this produces a capacity for 256 brightness or grey levels (Russ, 1990). Corresponding to this numerical greyscale (1 to 255), the low end of the scale (1 to about 125) refers to brightness level of very black to black. The high end of the scale (about 170 to 255) refers to brightness levels of very light grey to white, and the middle of the scale (about 125 to about 175) refers to brightness levels of dark grey to light grey. To maximize the accuracy of the analyses, the SEM images were manipulated and processed prior to being digitized and recorded by the computer in order to approach an ideal range of grey by varying the brightness and contrast on screen. An ideal image would have the maximum contrast between the dentin tubules, peritubular dentin, and intertubular dentin features with very little feature overlap in terms of grey scale values.

In the Advanced Imaging program, under the "fast acquire" command, the SEM images could be viewed on the computer screen and manipulated manually via the brightness and contrast controls on the Robinson Detector module prior to being stored. The ideal contrast and brightness corresponded to a peak in the brightness histogram in the mid-range of the grey scale. Once an acceptable image had been produced on screen, it was labeled, digitized and recorded on floppy disk via the "acquire" command.

4.3.2 Image analysis:

The process of analyzing the data images was based on a system of "painting-in" the desired features on the image on screen with a color, and allowing the computer to calculate a set of statistics for the painted-in features.

Utilizing the Features II program (Features II, Kevex Corp., San Carlos, CA), the recorded, digitized image was recalled onto two screen pages (Kevex software allows for images to be called up on three screen pages). The histogram was examined so that all the data visible on the image fell within the range of the grey scale (numerically 1 (black) to 255 (white)). If any part of the image did not fall within the histogram scale, a "crunch" transformation was carried out on the image to reduce and average out the random noise (Russ, 1990). A transparency sheet was placed on the screen and all tubules were crudely denoted with a dry-erase pen. The sheet was then removed from the screen.

A single color was chosen from the palette, and all the features of interest were painted-in using the rotary dial controller (Kevscan) on the keyboard. Once the desired features were sufficiently painted, the painted image was stored on screen. On command, the computer then transformed the black and white dentin image with the painted-in features, to a display of the painted-in features only. A limitation of using a grey scale criteria is that structurally dissimilar features (e.g., tubules and intertubular dentin) will sometimes be painted-in simultaneously due to their occasional brightness similarities according to a grey scale. Thus, the binary pixel-based representation that results from discrimination of a grey scale image may not perfectly delineate all of the features present. Such a situation is remedied by manipulating the image via image editing (Russ, 1990).

Two examples of image editing are: erosion and dilation. Erosion and dilation are used to smooth feature outlines globally, join broken or discontinuous features, and to separate touching ones. Erosion and dilation operations remove small features or feature irregularities which are presumed to be due to noise or other imaging or object imperfections. Simply put, erosion examines each pixel and changes it from ON to OFF if it has any neighbors that are OFF. Erosion reduces the features all around their periphery, removes features with narrow protuberances, and removes features

connected by a narrow strand. Dilation is the converse of erosion. The combination of erosion and dilation recovers most of the original feature size and produces a smoothed shape. Initial erosion removes small features which may represent noise and also sharp protuberances from the feature outlines. Subsequent dilation does not restore the small features but does fill in any small indentations in the outlines. The resulting feature size is restored to nearly the original value, while the shape is modified to become more rounded and smooth. The process of dilation preceding erosion can be thought of as the opposite process. Small features are not erased, small voids in features are filled in, and breaks or gaps in features are joined (Russ, 1990).

The painted-in image then, was "cleaned-up" or edited using the "erode/dilate" commands. The analysis for intertubular dentin involves the opposite order of dilate/erode and will be further described later. The "cleaned-up" image was then processed by the computer under the "process" command. During the feature processing procedure, the software automatically eliminated any remaining features of very small pixel size (Figure 4-6).

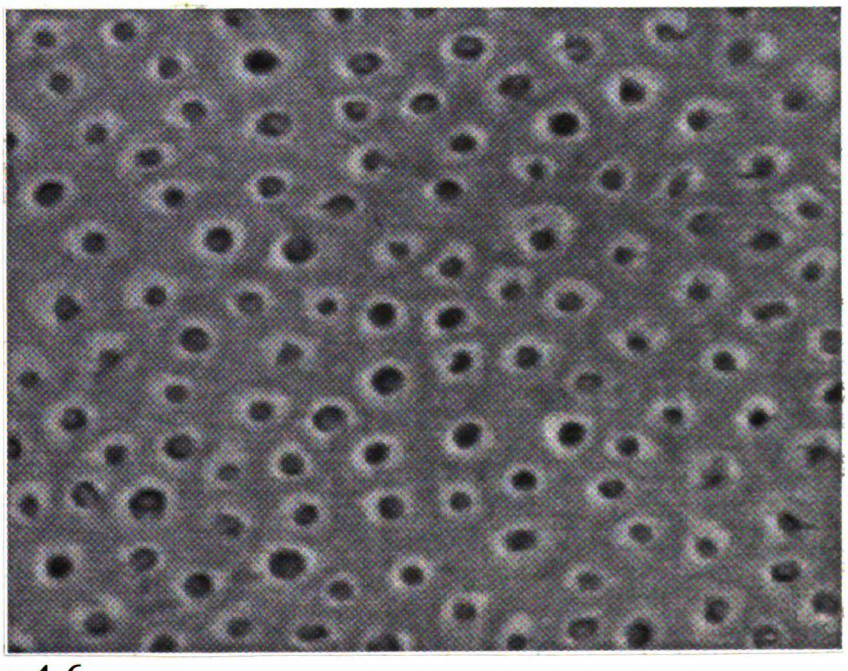

•Figure 4-6
Sequence of images during image analysis.
a) SEM image prior to image analysis.

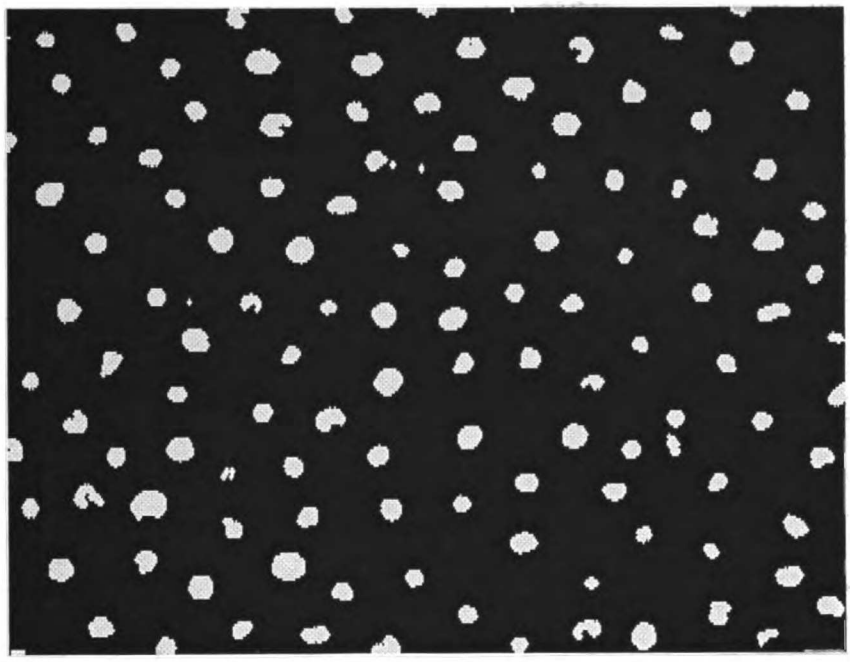

(b)

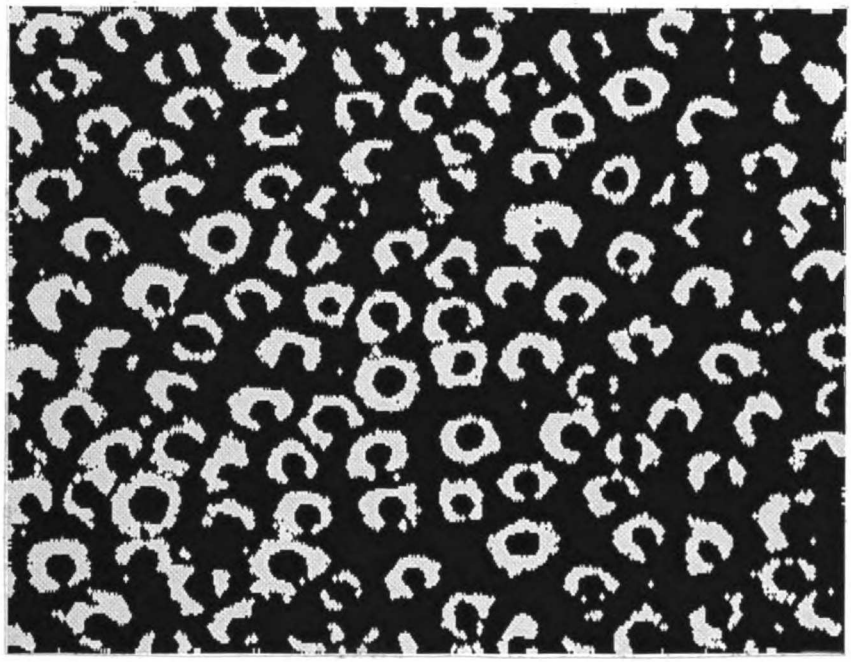

(c)

•Figure 4-6
b) Digitized "dentin tubule features only" image.
c) Digitized "peritubular dentin features only" image.

Following the image processing, the "features" function was used to manually single out and eliminate any remaining undesired features (individually) that had survived the painting, editing, and processing procedure.

The raw data statistics of the processed image were then printed out.

4.4 Individual analyses:

4.4.1 Dentin tubule analysis:

Analysis for the dentin tubules was performed to ascertain the tubule density (number of tubules per mm^2), the tubule diameters, and the tubule areas. As previously described, a transparency sheet was placed on the screen to create a template of the tubules on the image. The image was transformed ("crunch") if necessary so that the range of grey values of the image could be better utilized, and the tubules were painted-in. The goal of painting the desired features was to paint as many and as much of the features as completely as possible without painting-in too many of the non-desired features that happened to exhibit the same grey level. On a black and white screen, dentin tubules generally appear black or on the low/dark end of the grey scale (numerically in the range of 1 to about 125). Once the tubules were sufficiently painted-in, the colored image was stored on screen and transformed by the computer to a features-only image as previously described. The image was subjected to the "erode/dilate" commands to eliminate random noise and the computer was then allowed to process the image.

The processed image was "cleaned up" again using the "features" function to eliminate individual features that were painted in due to their similarity in grey scale to that of tubules, but were actually not tubules. The transparency sheet created before the painting-in stage was placed on the computer screen to serve as a template to discern between tubules and non-tubules during this

procedure. All tubules that appeared completely on screen were included for study. Those tubules that were partially on screen (at the screen edges) were included if it appeared that at least half of the tubule was present on screen. Those tubules that were inadvertently obliterated by debris or investment resin and as a result not painted-in, were noted so they could be included in the total number of tubules count. Following this final elimination stage, the computer was allowed to compute a set of raw data statistics on the remaining features on screen (tubules).

Following acquisition of the tubules raw data statistics, a second step was included to improve the accuracy of the computed tubule diameters and areas. The processed image that had been "cleaned-up" and already had the non-tubules eliminated, was recalled back onto the screen. Due to imperfections in the dentin surface structure as well as impurities incorporated onto the dentin during the sectioning and polishing procedures, some of the tubules may not have been painted-in completely. A polishing impurity for example, appears as a white splotch and may happen to infringe on a tubule (which appears as black). The resultant feature image then presents similar to the shadow of the earth reflecting on the moon thus producing a crescent image. As a result, during the painting-in stage the tubule will not be completely painted or might be completely obliterated unless the painting-in extends into the high end of the grey scale to paint the white-appearing features as well.

Thus, any features (tubules) that appeared as if they were incompletely painted-in, were eliminated manually using the "features" function. This left only those tubules that appeared to be completely painted as the features for which the computer produced a second set of raw data tubule statistics. This procedure was used to provide a more accurate assessment of tubule diameter, since all remaining tubules were fully painted-in.

4.4.2 Peritubular analysis:

Analysis of peritubular dentin was performed to ascertain the width of the peritubular dentin zones. The un-transformed black and white dentin image was again called onto two pages of the computer screen as previously described. The "crunch" transformation was carried out if necessary, and the peritubular dentin features were painted-in. Peritubular dentin presented as a white ring circumferentially associated with the dentin tubules, and corresponded to the extreme high (numerically) end of the grey scale in the range of about 160 to 255. The peritubular dentin features were painted-in as desired and the image was again stored on screen as previously described to produce a screen showing only the painted-in features.

This features-only image was subjected to the "erode/dilate" commands to eliminate random noise, and the image was processed by the computer. The "features" function was then used to manually eliminate individual features that had been painted-in due to their similarities in grey scale brightness to that of peritubular dentin features but were in fact, not peritubular dentin. The transparency sheet produced earlier was placed on the screen and served as a template to identify those features that were associated with an acknowledged tubule and were thus identifiable as peritubular dentin, and to eliminate those features that were not. The computer then produced a set of raw data statistics for the remaining features (peritubular dentin).

4.4.3 Intertubular analysis:

Analysis of intertubular dentin was performed to ascertain the area occupied by intertubular dentin (mm^2). The un-transformed black and white dentin image was again called onto two pages of the computer screen as previously described. The "crunch" transformation was carried out if necessary, and the intertubular dentin features were painted-in. The intertubular dentin features presented in the middle of the grey scale brightness level as dark grey to light grey, in the range of about 120 to 175 (numerically)

compared to the tubules (appear as black) and the peritubular dentin (appear as white) . The intertubular dentin was painted-in as desired and the image was again stored on screen as previously described to produce a screen showing a features-only image.

The features-only image was then subjected to the "erode/dilate" commands to eliminate noise, except this time in the reverse order. The painted-in intertubular dentin feature image presented as the inverse as compared to that for tubules and peritubular dentin. Instead of the image appearing on a blank screen, the intertubular dentin occupied most of the screen area and those features not painted-in occupied only a small portion of the screen. Therefore, to eliminate noise in the image, the "dilate" command was used first, followed by the "erode" command. The resultant image was essentially one large feature, thus the "features" command was not used to eliminate features that were not intertubular dentin. The computer then produced a set of raw data statistics for the intertubular dentin feature.

4.5 Mathematical conversions from the raw data

Raw data available from the computer-produced statistics for each image analysis included: the # of features counted and the % field area occupied by the features. The desired measurements for each of the tubule, peritubular, and intertubular dentin analyses were computed on a spreadsheet (Microsoft Excel 3.0) for each individual image, via the conversions as described in the following section. The appendix contains tables of the raw data.

4.5.1 Dentin tubules:

Data retrieved from the image analysis software for the dentin tubule analysis of each image included: the # of features counted (# of tubules) and the % field area that was occupied by those features. As described earlier, two analyses were completed for each image for the dentin tubules in order to improve the accuracy of the analysis for the tubule diameters, and areas. A corrected % field area for each

individual image was calculated using the data from the two analyses via the following conversion ratio:

$$x \,/\, \text{total \# tubules} = 2^{nd}\ \%\ \text{field area} \,/\, 2^{nd}\ \text{\# tubules}$$

Where:
x = corrected % field area
total # of tubules counted = from raw data
2^{nd} % field area = % field area from the second tubule analysis
2^{nd} # tubules = # of tubules counted from the second tubule analysis

This corrected % field area was a more reliable representation of the % field area occupied by the dentin tubules as it adjusted for those tubules that were incompletely painted in or completely obliterated.

The corrected % field area was then normalized against the total % field area of all the features for each image. The corrected % field area for the tubules was added to the % field area for the peritubular dentin (PT), plus the % field area for the intertubular dentin (IT) to compute a normalized total % field area for each image. The normalized % field area for the tubules was then calculated using the following conversion:

$$x = \text{corrected \% field area} / \text{normalized total \% field area} * 100$$

Where:
X = normalized % field area (tubules)
corrected % field area = as calculated
normalized total % field area = sum of % field area for (tubules, PT, IT)

The normalized % field area was used as a more accurate representation of the actual % field area the tubules occupied, as computed on each analysis.

The total feature area occupied by the dentin tubules for each image was then calculated. It was necessary to calculate this because the image analysis software was not able to produce accurate measurements of the total feature area in the units we desired. In

order to accomplish this, it was first necessary to convert the area of the SEM image and calculate the area of the computer screen image. Visualizing the SEM images at 2000x magnification, 10.0 mm on the SEM screen correlated with 5.0 μm of actual sample size. The conversion to the Kevex computer screen from the SEM at that magnification was 2.5 μm correlating to 10.0 mm. The image area of the Kevex computer screen was measured to be 42,115 mm^2 (236.6 mm x 178.0 mm). Therefore, to convert the area of the image on the Kevex computer screen to μm^2, the following conversion was used:

$$x = 42114.8\ mm^2\ (\ 2.5\ \mu m/10.0\ mm)^2$$
$$x = 2632.175\ \mu m^2$$

Where:
x = area of sample on Kevex screen
42114.8 mm^2 = total available area on Kevex screen
(2.5 μm/10 mm) = SEM-->Kevex screen conversion

The total feature area of the tubules for each image, could then be calculated using the following conversion:

$$x = \text{normalized \% field area} / 100 * 2632.175\ microns^2$$

Where:
x = total feature area of the tubules for that particular image
normalized % field area = the "true" % field area as calculated
2632.175 $microns^2$ = total field area

With this information, the mean feature area per tubule could then be calculated for each image using the following conversion:

$$x = \text{total feature area of the tubule analysis} / \#\ \text{tubules}$$

Where:
x = mean feature area per tubule for that particular image
total feature area = as calculated above
tubules = as known from raw data

The mean tubule diameter for each image could then be computed using the following conversion, assuming all tubules were circular as:

$$x = 2 * SQRT(\text{ mean feature area } / \pi) = 2r = \text{diameter}$$

Where:

x = mean tubule diameter for that particular image
mean feature area = as calculated
area of a circle = πr^2

Finally, the # of tubules per mm^2 was calculated from the total # of tubules for each image and from the size of the image area in μm^2 via the following conversion:

$$x = \#\text{ tubules counted } / 2632.175\ \mu m^2 * 10^6$$

Where:

x = # tubules per mm^2 for that particular image
# tubules / image = as known from raw data
2632.175 μm^2 = total image area

To summarize, the image analysis for the dentin tubules produced raw data that revealed the # of features (tubules) per each image and the % field occupied by those features per each image. The % field area occupied by the tubules was corrected and then normalized against the total % field area occupied by the tubules, PT, and IT. The image size (area) was calculated, and the # of tubules per mm^2 was computed for each image. Using the normalized % field area of the tubules, the total tubule area, the mean tubule area, and the mean tubule diameter was calculated for each image.

4.5.2 Peritubular dentin:

Data from the image analysis software for the peritubular dentin analysis of each image included: the # of features (peritubular dentin) and the % field area occupied by those features. The % field

area was normalized against the total % field area of all the features for each image. The normalized total % field area for each image was recalled as computed above for the dentin tubule analysis and the normalized % field area for the peritubular dentin was then calculated using the following conversion:

x = % field area (PT) / normalized total % field area * 100

Where:
x = normalized % field area (peritubular dentin)
% field area = from raw data
normalized total % field area = sum of % field area for (tubules, PT, IT)

The normalized % field area was used as a more accurate representation of the actual % field area the peritubular dentin occupied, as computed on each analysis.

The total feature area of the peritubular dentin for each image, could then be calculated using the same formula as that of the dentin tubules:

x = normalized % field area (PT) / 100* 2632.175 μm^2

Where:
x = total feature area of the peritubular dentin for that particular image
normalized % field area = as calculated
2632.175 μm^2 = total field area

With this information, the mean feature area of peritubular dentin (per tubule) could then be calculated for each image using the following conversion:

x = total feature area (PT) / # tubules

Where:
x = mean feature area (PT) per tubule for that particular image
total feature area (PT) = as calculated above
tubules = as known from raw data for dentin tubules

The # of tubules was used for this equation instead of the # of peritubular dentin features because on occasion, the ring of peritubular dentin was interrupted due to debris or grey scale differences and thus one complete ring of peritubular dentin might be counted as two or more features.

The mean peritubular width per tubule for each image could then be computed. The formula for the calculation of the mean peritubular width per tubule was derived as follows:

Theoretically, the peritubular radius or width is equal to the radius of the [tubule + peritubular dentin] unit, minus the known radius of the tubule.

r_u = radius of the [dentin tubule + peritubular dentin] unit
r_t = radius of the dentin tubule
R_p = the peritubular radius or width

$$R_p = r_u - r_t$$

MFA_p = mean feature area of peritubular dentin
MFA_t = mean feature area of dentin tubule
MFA_u = mean feature area of [dentin tubule + peritubular dentin] unit

$$MFA_u = MFA_t + MFA_p$$

Using the formula where the area of a circle is equal to (πr^2), the radius is equal to the square root of (the area divided by π):

$$r_t = (MFA_t/\pi)^{1/2}$$

$$r_u = (MFA_u/\pi)^{1/2}$$

This can then be substituted into the equation: $R_p = r_u - r_t$ where:

$$R_p = (MFA_u/\pi)^{1/2} - (MFA_t/\pi)^{1/2}$$

$$= \pi^{-1/2} [\, MFA_u^{1/2} - MFA_t^{1/2} \,]$$

Therefore, substituting for MFA_u as shown above, the formula for peritubular width (R_p) is:

$$R_p = \pi^{-1/2} [\, (MFA_t + MFA_p)^{1/2} - (MFA_t)^{1/2} \,]$$

To summarize, the image analysis for the peritubular dentin produced raw data that revealed the # of features (peritubular dentin) per each image and the % field occupied by those features per each image. The % field area occupied by the peritubular dentin was normalized against the total % field area occupied by the tubules, PT, and IT. Using the normalized % field area of the peritubular dentin, the total peritubular dentin area, the mean peritubular dentin area, and the mean peritubular dentin width was calculated for each image.

4.5.3 Intertubular dentin:

Data from the image analysis software for the intertubular dentin analysis of each image included: the # of features counted, and the % field area occupied by those features. Once again, the % field area occupied by the intertubular dentin was normalized against the total % field area of all the features for each image. The normalized total % field area for each image was recalled as computed above for the dentin tubule analysis and the normalized % field area for the intertubular dentin was then calculated using the following conversion:

x = % field area (IT) / normalized total % field area * 100

Where:
x = normalized % field area (intertubular dentin)
% field area = from raw data
normalized total % field area = sum of % field area for (tubules, PT, IT)

The normalized % field area was used as a more accurate representation of the actual % field area the intertubular dentin occupied, as computed on each analysis.

The total feature area of the intertubular dentin ($mm^{2)}$ for each image, could then be calculated using the same formula for that of the dentin tubules and peritubular dentin:

x = normalized % field area (IT) / 100* 2632.175 μm^2

Where:
x = total feature area of the intertubular dentin per mm^2 for that particular image
normalized % field area = as calculated
2632.175 μm^2 = total field area

To summarize, the image analysis for the intertubular dentin produced raw data that revealed the # of features per each image, and the % field occupied by those features per each image. The % field area occupied by the intertubular dentin was normalized against the total % field area occupied by the tubules, PT, and IT. Using the normalized % field area of the intertubular dentin, the total feature area of the intertubular dentin per mm^2 of dentin was calculated for each image.

Prior to normalizing the quantitative data for each image as described, the values for % field of the dentin tubules, peritubular dentin, and intertubular dentin were added together. If the sum was not 100% +/- 5%, a "painting-in" error was assumed. Due to the grey scale similarities between features described earlier it was possible to paint-in the same feature twice on occasion, resulting in an over- or under-estimation of total feature area. The analysis for dentin tubules dealt with features primarily on the numerically low end or

black end of the grey scale. The analysis of the peritubular dentin dealt with features primarily on the numerically high or white end of the grey scale. Because of this, over- or under-estimation errors between these two types of features was unlikely. The intertubular dentin analysis dealt with features in between the far ends of the grey scale, providing possible interaction with either/both the tubules and the peritubular dentin. With this in mind, any over- or under-estimation error then, was presumed to lie within the intertubular dentin analysis. If the total % field areas did not fall within 100% +/- 5%, the image was re-evaluated and the intertubular dentin analysis was repeated. If the total still did not fall within the acceptable range, the image was deemed unreliable and was not included in the analysis. Overall, the mean total % for the analyses was very close to 100%, at 100.24% with a standard deviation of 0.78%.

5. RESULTS

10 deciduous maxillary anterior teeth were observed in this study. Categorically, there were: 3 left canines, 3 left lateral incisors, 3 right lateral incisors, and 1 right central incisor. The characteristics of numerical tubule density (number per mm^2), tubule diameter (μm), and peritubular width (μm) were quantified for each of the 9 images at each level (with respect to the DEJ) for each tooth.

Each tooth yielded 2 dentin matchsticks, one from the distal direction and one from the central direction. Each dentin matchstick produced samples at 3 levels of depth from the DEJ, at distances of 0.15 mm, 0.8 mm, and 1.45 mm from the DEJ (levels 1, 2 and 3) as seen in figure 6. Due to polishing artifacts and slight imperfections resulting from sample preparation that resulted in images not suitable for grey scale analysis, 54 image analyses for each characteristic for every tooth were not always accomplished. For the analyses of numerical tubule density, peritubular width, and intertubular area, a total of 526, 522, and 515 images were produced and analyzed respectively.

Generally speaking, as the distance from the DEJ increased, the numerical tubule density appeared to increase as well. Within the 9 image areas from each square, there was a high variability of numerical tubule density as shown in Figure 5-1. As the distance from the DEJ increased, the tubule diameters also appeared to increase and the variability didn't seem as large as for numerical tubule density. Lastly, as distance from the DEJ increased, the peritubular width appeared to decrease. As the images from areas A through I were analyzed, it was observed that despite the overall variability within the 1 mm x 1 mm dentin square, the characteristics appeared more similar in certain cluster groups than in others. In other words, when the tic-tac-toe grid of dentin was broken up into rows and columns, the characteristics within rows

appeared more similar to each other versus those in other rows or columns. For all the grids, row A-B-C was always on the labial, row D-E-F was always from the middle, and row G-H-I was always to the lingual. Column A-F-G was always to the distal and column C-D-I was always to the mesial. Because it seemed that the characteristics appeared to have similarities based on positional grouping, it was theorized that the data in each dentin square should be analyzed by groups, either rows or columns. Statistical analysis using multi-factor ANOVA (General Linear Model, The SAS system) however, found that differences between rows and columns were not significant. Therefore, the data were analyzed across all the image sites rather than by rows or columns. However, future studies with more samples should reexamine the row and column differences.

The measurements produced from the 9 images at the 3 levels of each matchstick were averaged to yield one mean value for each of the dentin characteristics at every level (depth from the DEJ) of each of the 2 matchsticks per tooth. Statistical analyses were performed on each of the desired dentin characteristics (numerical density, tubule diameter, peritubular width) separately. For the purpose of the statistical analyses, the 1 central incisor was excluded as it represented a different tooth type.

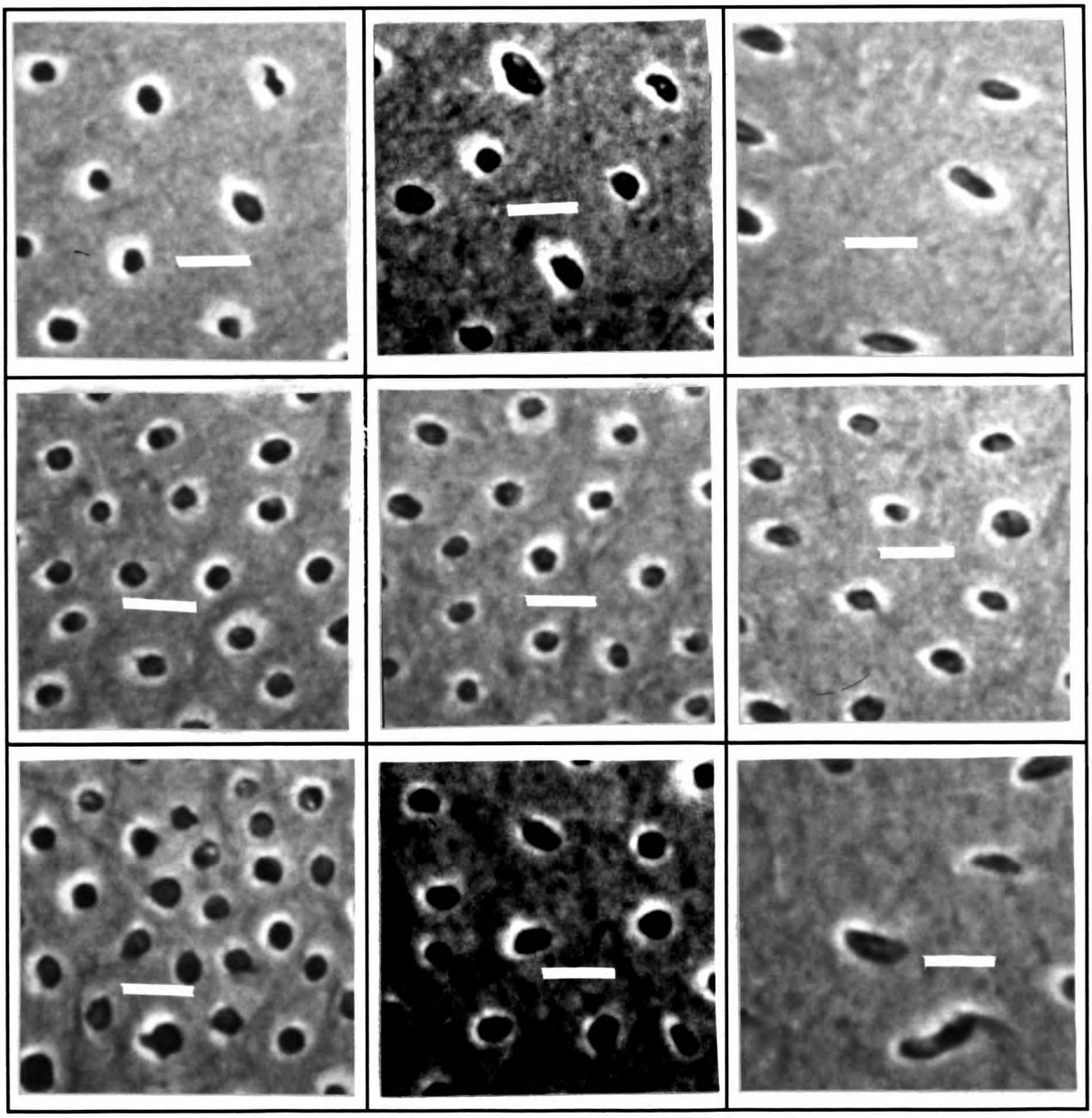

•Figure 5-1
SEM photomicrographs (20 kV, 2000x) arranged within sample dentin square. Legend bar = 5 μm. Tubule density and diameter at different image sites varies within the sample dentin square.

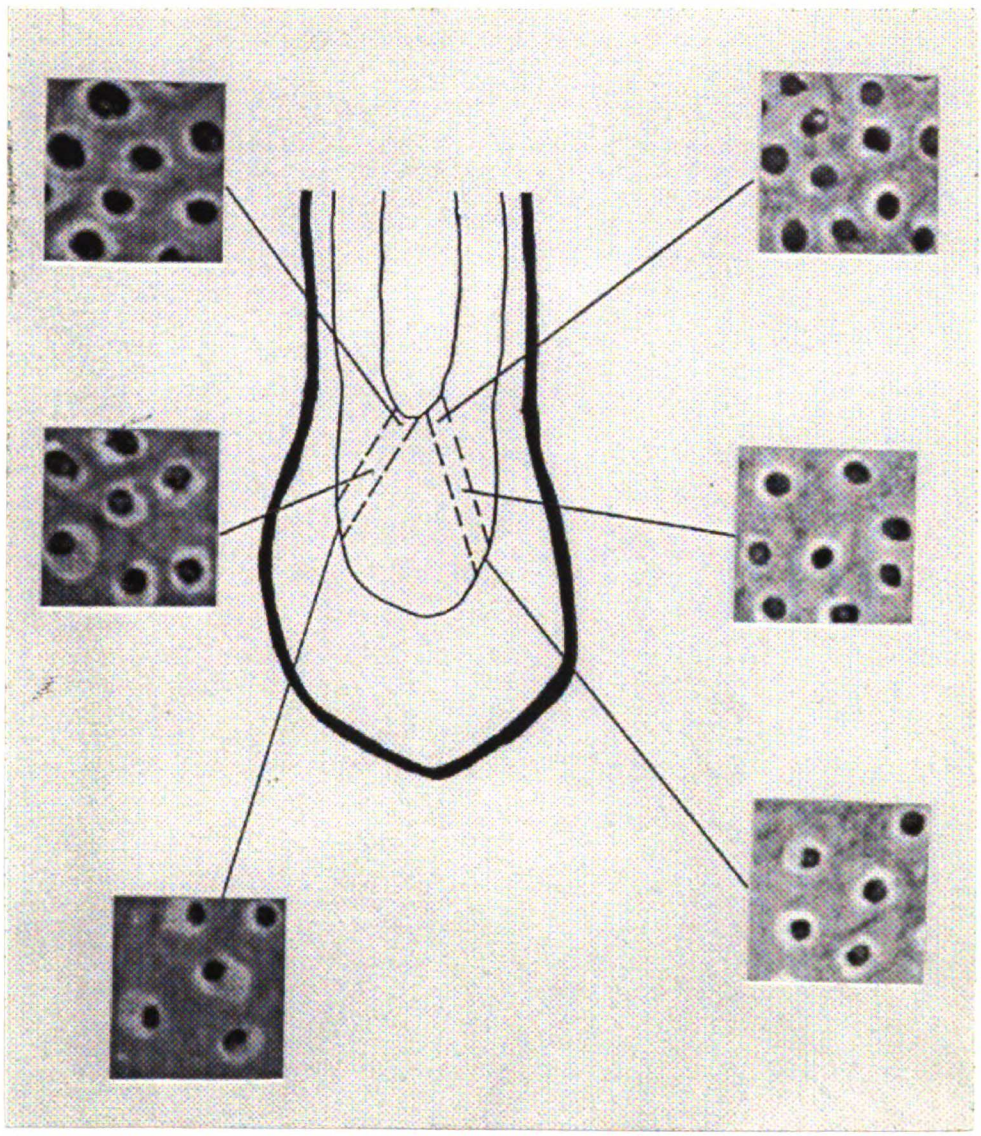

•Figure 5-2
a) SEM photomicrographs taken from the 3 depth levels for the distal and central matchsticks of a canine tooth. Tubule density and diameter increases as the distance from the DEJ increases. Pictures are presented at 92% magnification of the original photomicrographs (20 kV, 2000x).

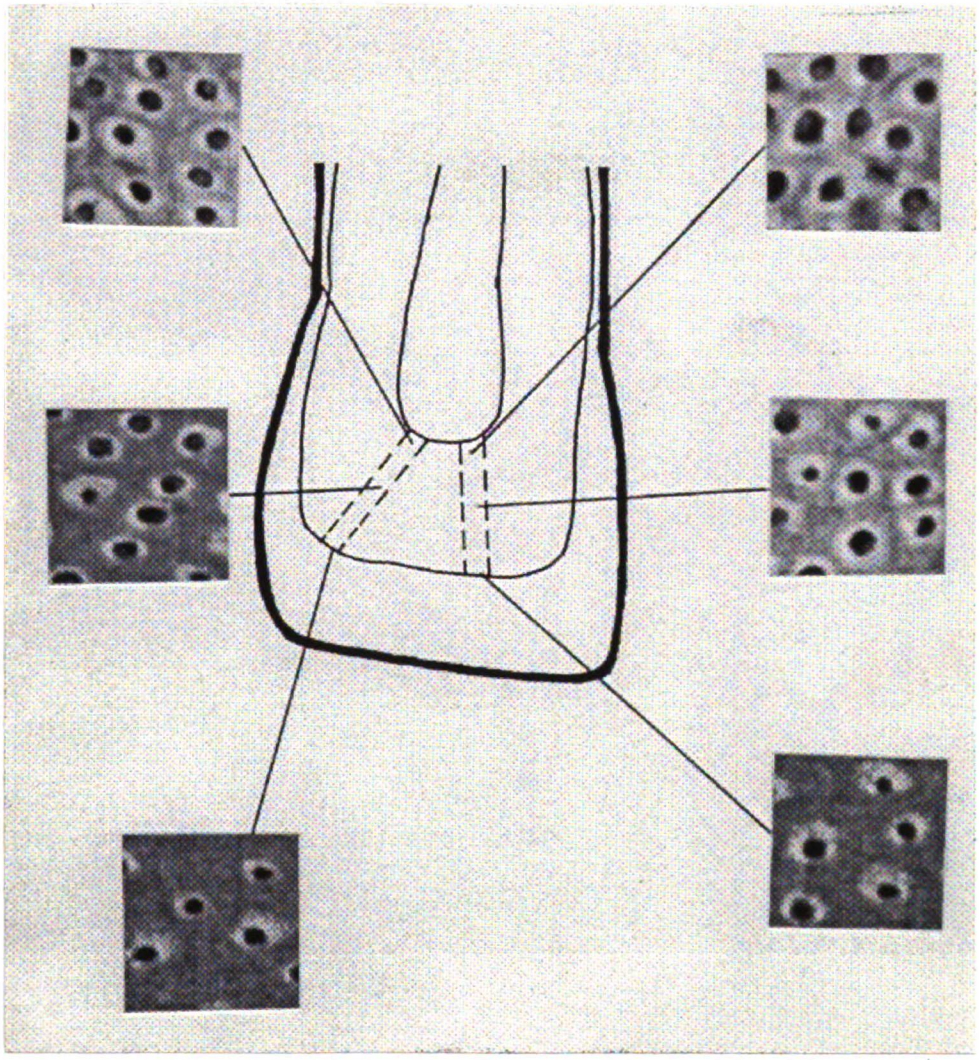

•Figure 5-2
b) SEM photomicrographs taken from the 3 depth levels for the distal and central matchsticks of a lateral incisor. Tubule density and diameter increases as the distance from the DEJ increases. Pictures are presented at 90% magnification of the original photomicrographs (20 kV, 2000x).

5.1 Numerical tubule density

The numerical tubule density data were recorded (Table 5-1) and analyzed statistically for the following variables: tooth (individual), direction (central, distal), level (1, 2, and 3), as well as for any possible interactions between the variables. Data for individual teeth were averaged across all the image sites for each level using a multi-factor ANOVA (General Linear Model, The SAS System). The data were presented with respect to direction within each tooth type.

•Table 5-1

Numerical tubule density (#/mm^2) separated by location within tooth type. (upper value = standard deviation; lower value = robust standard error)

Tooth (location)	0.15 mm from the DEJ	0.8 mm from the DEJ	1.45 mm from the DEJ	Slope (# tub. per mm^2/mm)	R^2
Canines **(Distal)**	17,969 (±6,393) (±3,013)	26,313 (±4,130) (±1,943)	33,278 (±3,899) (±1,838)	11,776	0.997
Canines **(Central)**	23,963 (±8,488) (±4,001)	26,552 (±6,004) (±2,831)	29,732 (±8,005) (±3,774)	4,438	0.997
Lateral incisors **(Distal)**	29,294 (±11,738) (±4,420)	34,586 (±8,360) (±3,116)	39,442 (±13,454) (±5,020)	7,807	0.999
Lateral incisors **(Central)**	38,392 (±10,183) (±3,795)	39,873 (±7,737) (±2,960)	42,427 (±10,000) (±3,836)	3,104	0.977

For both the canines and the lateral incisors, the average numerical tubule density for either direction appeared to increase as the distance from the DEJ increased from 0.15 mm (level 1) to 0.8 mm (level 2) to 1.45 mm (level 3) as shown in Figure 5-2 (matchstick tree). The data suggested that the average numerical tubule density in the lateral incisors was greater than in the canines. It also appeared that in both tooth types, the numerical tubule density in the central matchsticks could be greater than in the distal. Finally, the data seemed to suggest that the rate at which the numerical tubule density increased as the distance from the DEJ increased was higher in the distal matchsticks than in the central.

In the canines, the numerical tubule density of the distal matchstick at levels 1, 2, and 3 was measured to be: 17,969 per mm^2, 26,313 per mm^2, and 33,278 per mm^2, respectively. The standard deviations (with robust standard errors in parentheses) were: 6,393 (3,013), 4,130 (1,943), and 3,899 (1838), respectively. The large standard deviations reflect the wide numerical tubule density variation found within the distal direction of the canines. Robust standard errors take into account any clustering of the data (averaging across sites) and are smaller than the standard errors produced from taking the means of means per tooth because the denominator is then the number of samples rather than the number of teeth. Robust standard errors were used because of the fact that they do take into account the effect of clustering. In the central matchstick, the numerical tubule density at levels 1, 2, and 3 appeared to be higher at: 23,963 per mm^2, 26,552 per mm^2, and 29,732 per mm^2, respectively. The standard deviations (with robust standard errors in parentheses) were: 8,488 (4,001), 6,004 (2,831), and 8,005 (3,774), respectively. Once again, the large standard deviations reflect the wide variation of numerical tubule density within the central direction of the canines. The numerical tubule densities of the different directions were plotted versus distance

from the DEJ (Figure 5-3, error bars represent robust standard errors). Linear regression analysis of the distal matchstick demonstrated that the numerical tubule density increased at a rate of 11,776 tubules per mm^2/mm with an R^2 coefficient of 0.997. The rate of increase for the central matchstick was slightly lower at 4,438 tubules per mm^2/mm with an similar R^2 coefficient of 0.997.

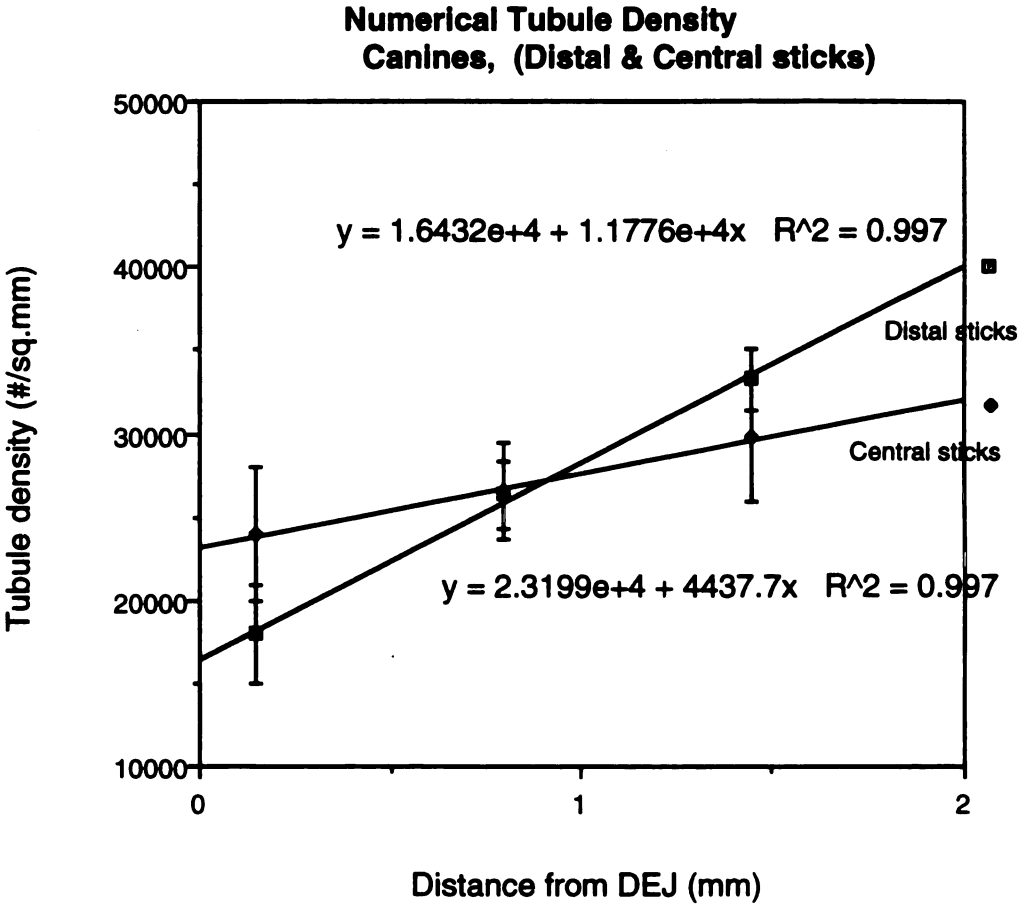

•Figure 5-3
Graph of numerical tubule density ($\#/mm^2$) for the canines separated by distal and central sticks.

In the lateral incisors, the numerical tubule density of the distal matchstick at levels 1, 2, and 3 appeared to be slightly higher than those for the canines at: 29,294 per mm^2, 34,586 per mm^2, and 39,442 per mm^2, respectively. The standard deviations (with robust

standard errors in parentheses) were: 11,738 (4,420), 8,360 (3,116), and 13,454 (5,020), respectively. The large standard deviations reflect the wide variation within the distal matchstick of the lateral incisors. In the central matchstick, the numerical tubule density at levels 1, 2, and 3 appeared to be greater than all of the previously measured data values at: 38,392 per mm^2, 39,873 per mm^2, and 42,427 per mm^2, respectively. Once again, the values presented with large standard deviations (with robust standard errors in parentheses): 10,183 (3,795), 7,737 (2,960), and 10,000 (3,836), respectively. The numerical tubule densities of the different directions were plotted versus distance from the DEJ (Figure 5-4). Linear regression analysis of the distal matchstick demonstrated that the numerical tubule density increased at a rate of 7,807 tubules per mm^2/mm with an R^2 coefficient of 0.999. The rate of increase for the central matchstick was slightly lower at 3,104 tubules per mm^2/mm with a similar R^2 coefficient of 0.977.

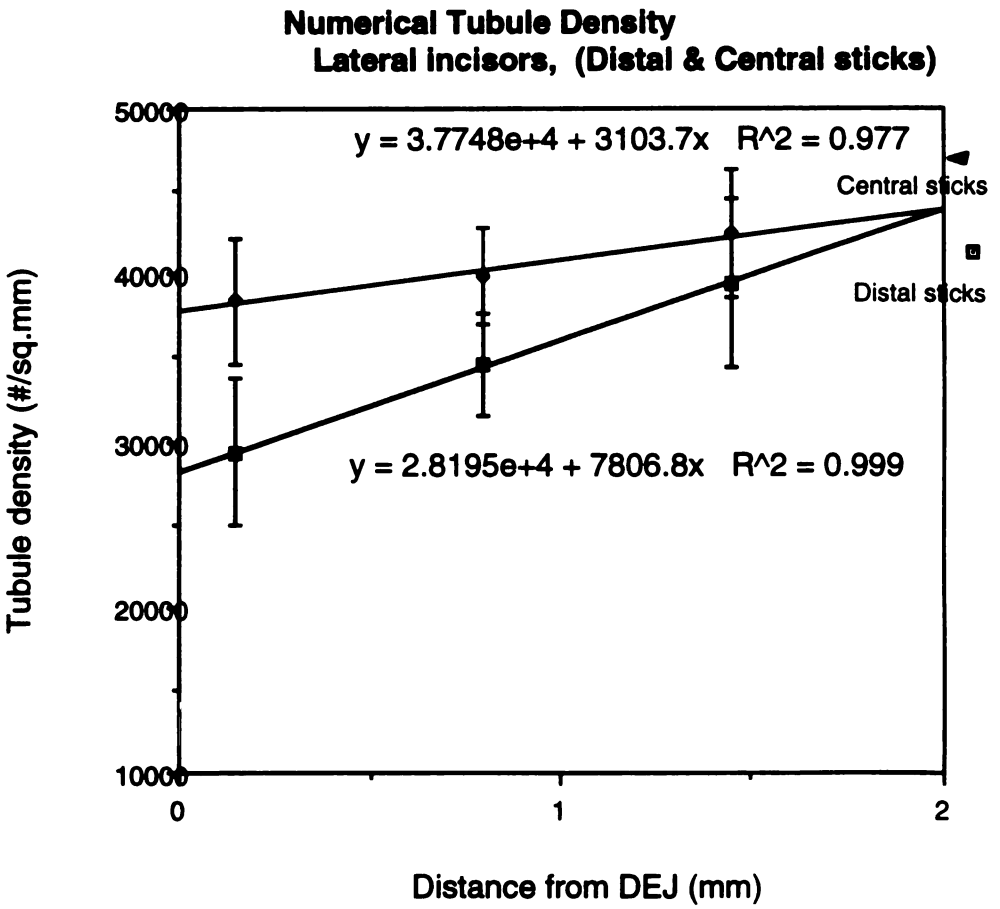

•Figure 5-4
Graph of numerical tubule density (#/mm^2) for the lateral incisors, separated by distal and central sticks.

The numerical tubule densities of the different tooth types were then separated by direction and also plotted versus distance from the DEJ (Figures 5-5 & 5-6) to demonstrate differences in numerical tubule density and rates of change between different tooth types for the same direction.

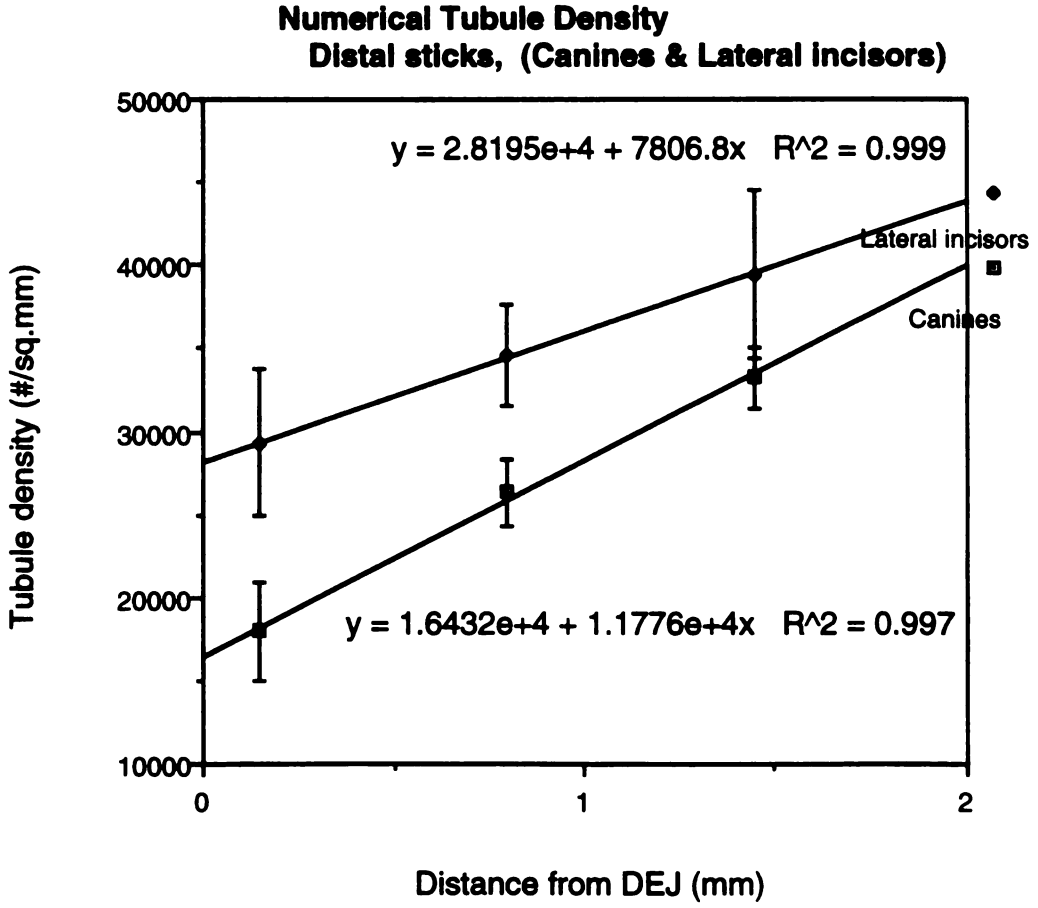

•Figure 5-5
Graph of numerical tubule density (#/mm^2) for the distal sticks separated by tooth type.

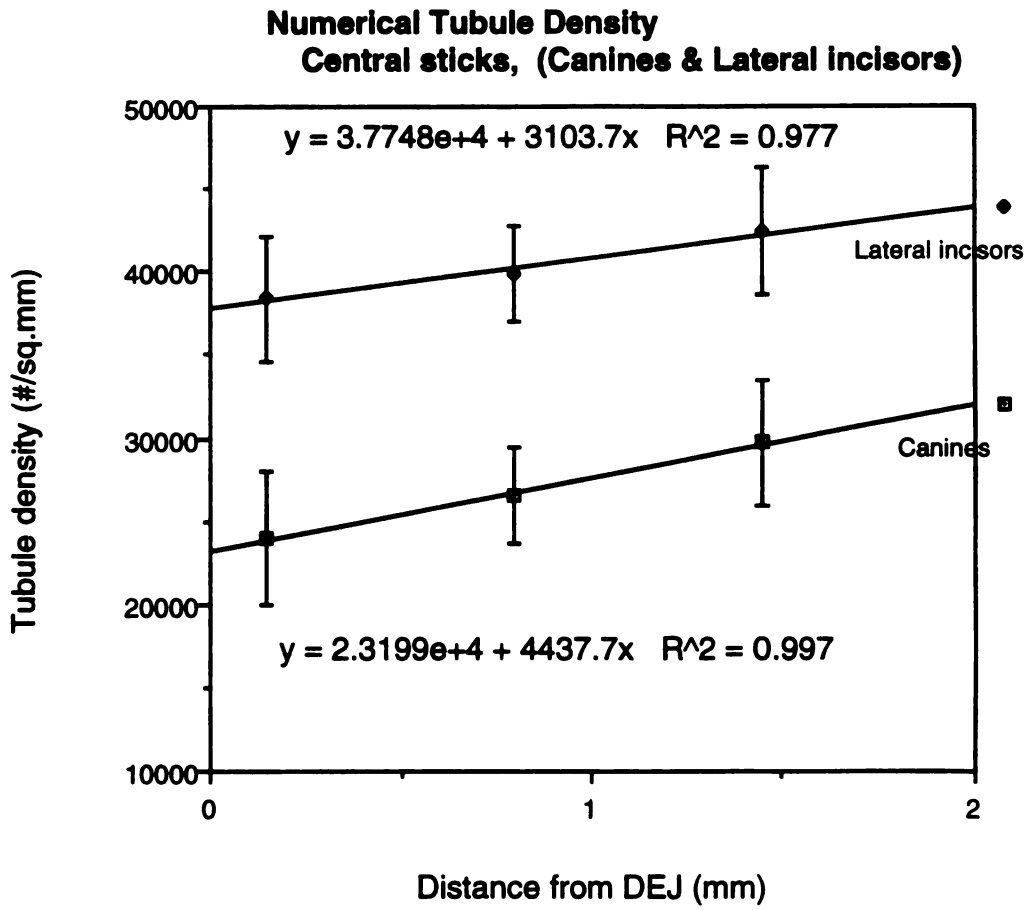

•Figure 5-6
Graph of numerical tubule density for the central sticks separated by tooth type.

The data and the graphs appeared to suggest that the numerical tubule density was different between different directions within and between teeth. The data also seemed to suggest (Figures 5-3 & 5-4) that the central matchsticks had a greater numerical tubule density than the distal matchsticks in both teeth, and that the values found (Figures 5-5 & 5-6) for the lateral incisors were greater than those found for the canines. Statistical analyses were performed to detect any differences in numerical tubule density that were significant at the $p < .05$ level.

Using a multi-factor ANOVA, it was determined that the numerical tubule density in: individual teeth, direction, different tooth types and levels were significantly different ($p < .05$). While no significant interaction was found between: tooth type & level or direction & level, one was found between direction & type ($p < .05$).

Interpreting the interaction between direction & type, the data for the central direction (Figure 5-6) were further examined to determine where any significant differences were. The numerical tubule density in: individual teeth, levels, and tooth type were significantly different ($p < .05$). Tukey's Studentized Range Test revealed that among the different levels in the central matchsticks, while the numerical tubule density in level 3 appeared to be greater than level 2, and level 2 appeared to be greater than level 1, only the difference between level 3 and level 1 was significant ($p < .05$). Furthermore, separating the data between tooth types, Tukey's Studentized Range Test also revealed that amongst the central directions, the numerical tubule density values for the central direction of the lateral incisors (38,392 per mm^2, 39,873 per mm^2, and 42,427 per mm^2) was significantly greater than that of the canines (23,963 per mm^2, 26,552 per mm^2, and 29,732 per mm^2) at $p < .05$.

The data for the distal direction (Figure 5-5) were subsequently analyzed. The numerical tubule density values in individual teeth and levels were significantly different ($p < .05$). Within the distal direction, the difference in numerical tubule density between canines and lateral incisors was not statistically significant. Tukey's Studentized Range Test revealed that for both tooth types, the differences between all the levels, 1, 2, and 3, were significantly different ($p < .05$).

Based on the statistical analysis of the numerical data, the following conclusions can be made. While it appeared that the numerical tubule densities in both directions within the lateral incisors were greater than those found in the canines, the only

significant differences were between the central matchsticks of the canines and lateral incisors. It also appeared that the numerical tubule density at different levels was different. For the central matchsticks, the difference between levels 1 and 3 were statistically significant while in the distal matchsticks, the difference between each of the levels was statistically significant.

Test for Slopes

Due to individual tooth variation, extrapolating information or trends from values found at the y-intercept is not as reliable as the results of the linear regressions would suggest. This is because while great pains were made to accurately assess the samples for level 1 (0.15 mm from the DEJ) at the DEJ this was not deemed realistically possible every time. An example of this is the fact that while the samples may have been flat the DEJ is not. Therefore, different samples may have had different absolute starting points. Examining slopes (rate of change between points) is a better method for extrapolating trends because it enables us to show a direct relationship between known data points and is thus a more reliable way to detect any differences. The data, in this case numerical tubule density, were plotted against the independent variable of distance from the DEJ as shown in Figures 5-3 to 5-6.

A test for slopes for changes in numerical tubule density as a function of distance from the DEJ for different directions within the tooth types was examined first. Within the lateral incisors (Figure 5-4), although the slope for the distal direction appeared to be greater, there was no statistically significant difference between the slope of the central direction (3,104 per mm^2/mm) and the slope of the distal direction (7,807 per mm^2/mm). Therefore, the rate of the tubule density change with distance from the DEJ is not significantly different for directions. As such, the slope for the lateral incisors (combined directions) was calculated, and found to be an increase of 5455 tubules per mm^2/mm. Within the canines however (Figure 5-

3), the slope of the distal direction (11,776 per mm^2/mm) was significantly greater ($p < .05$) than that of the central direction (4,438 per mm^2/mm). A summary of the findings for slope can be seen in Table 5-2.

•Table 5-2
Slopes (numerical tubule density) separated by direction within tooth type.

Tooth	Direction	Slopes (# tub. per mm^2/mm)	Significantly different?	Combined slope value (# tub. per mm^2/mm)
Canines	Distal	11,776	Yes	———
	Central	4,438		
Lateral incisors	Distal	7,807	No	5,455
	Central	3,104		

A test for slopes for changes in numerical tubule density as a function of distance from the DEJ for the different tooth types within the different directions was examined next. Within the central direction (Figure 5-6), there was no statistically significant difference between the slope for the canines and the slope for the lateral incisors. Once again, the slope for the central matchsticks (canines and lateral incisors combined) was calculated and found to be an increase of 3,548 tubules per mm^2/mm. Within the distal direction (Figure 5-5), there was no statistically significant difference between the slope for the canines and the slope for the lateral incisors. The slope for the distal matchsticks (canines and lateral incisors combined) was calculated and found to be an increase of 9,130 tubules per mm^2/mm. Therefore, for either direction, there was no significant difference between the canines and lateral incisors for the rate of change in the tubule density with distance from the DEJ

although it appeared to be greater for the canines in both cases. A summary of the findings for slope can be seen in Table 5-3.

•Table 5-3
Slopes (numerical tubule density) separated by tooth type within direction.

Direction	Tooth	Slopes (# tub. per mm^2/mm)	Significantly different?	Combined slope value (# tub. per mm^2/mm)
Distal	Canines	11,776	No	9,130
	Lateral incisors	7,807		
Central	Canines	4,438	No	3,548
	Lateral incisors	3,104		

5.2 Tubule diameter

Tubule diameter data were recorded (Table 5-4) and analyzed statistically for the variables: tooth (individual), direction (central, distal), level (1, 2, and 3), as well as for any possible interactions between the variables. Data for individual teeth were averaged across all the image sites for each level using a multi-factor ANOVA (General Linear Model, The SAS System). The data presented for each tooth type include both directions.

•Table 5-4
Tubule diameter (μm) separated by tooth type.
(upper value = standard deviation; lower value = robust standard error)

Tooth	0.15 mm from the DEJ	0.8 mm from the DEJ	1.45 mm from the DEJ	Slope (μm/mm)	R^2
Canines	1.58 (±0.20) (±0.05)	1.83 (±0.10) (±0.03)	1.94 (±0.06) (±0.02)	0.28	0.952
Lateral incisors	1.39 (±0.27) (±0.08)	1.68 (±0.24) (±0.07)	1.90 (±0.20) (±0.06)	0.39	0.994

For both the canines and the lateral incisors, the average tubule diameter appeared to increase as the distance from the DEJ increased from 0.15 mm (level 1), to 0.8 mm (level 2), to 1.45 mm (level 3). The data seemed to suggest that the average tubule diameters of the canines were larger than those for the lateral incisors, but that the rate at which the tubule diameters in the lateral incisors increased as distance from the DEJ increased was greater than in the canines.

In the canines, the tubule diameter at levels 1, 2, and 3 was measured to be: 1.58 μm, 1.83 μm, and 1.94 μm, respectively. The standard deviations (with robust standard errors in parentheses) were: 0.20 (0.05), 0.10 (0.03), and 0.06 (0.02), respectively. Relatively small standard deviations reflect that within specific distances from the DEJ, the tubule diameter variation appeared to be small. This is contrary to empirical findings of numerical tubule density which was in fact quite variable. The tubule diameters were plotted versus distance from the DEJ (Figure 5-7). Linear regression analysis of the tubule diameter of the canines demonstrated an

increase of 0.28 μm/mm with respect to distance from the DEJ (R^2 = 0.952).

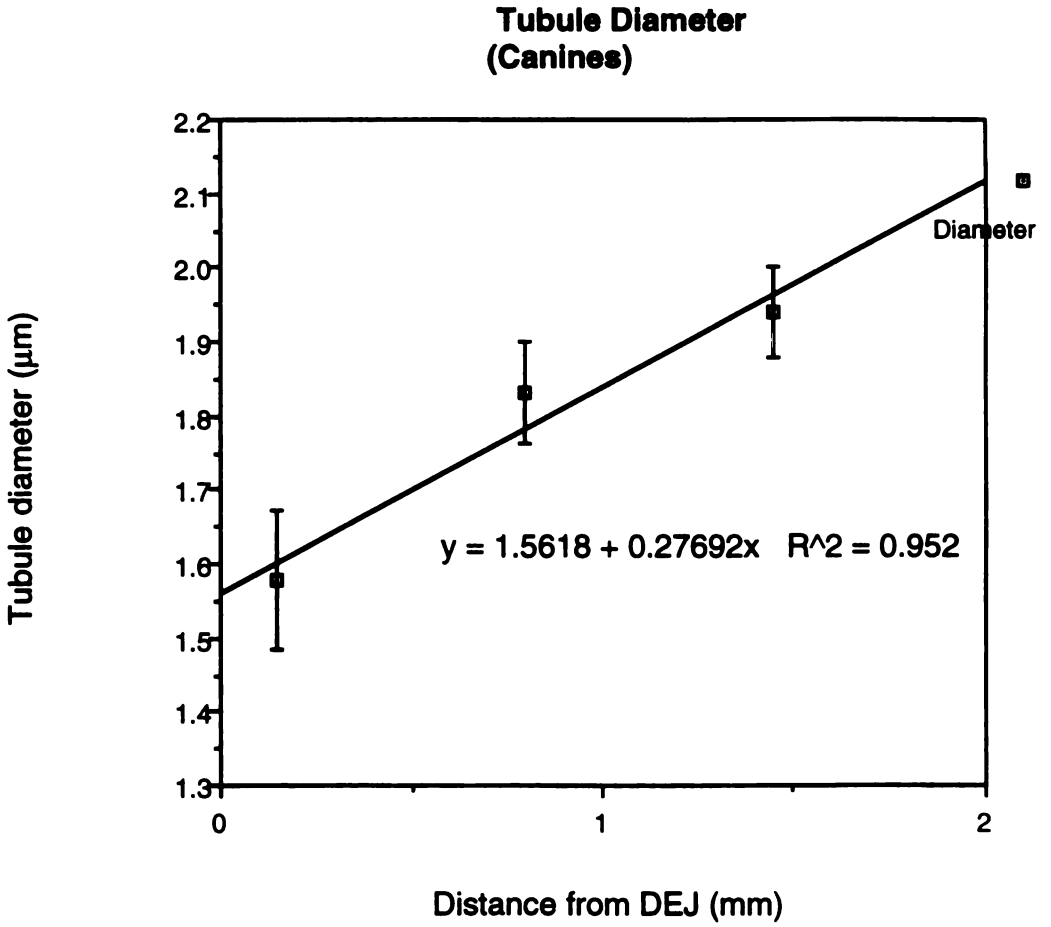

•Figure 5-7
Graph of tubule diameter (μm) for the canines.

In the lateral incisors, the tubule diameter at levels 1, 2, and 3 appeared to be slightly smaller than those for the canines at: 1.39 μm, 1.68 μm, and 1.90 μm, respectively. The standard deviations (with robust standard errors in parentheses) were: 0.27 (0.08), 0.24 (0.07), and 0.20 (0.06), respectively. There appeared to be slightly more variability in the tubule diameters in the lateral incisors compared to the canines. The tubule diameters were plotted versus distance from the DEJ (Figure 5-8). Linear regression analysis of the

distance from the DEJ (Figure 5-8). Linear regression analysis of the tubule diameters demonstrated an increase of 0.39 μm/mm with respect to distance from the DEJ (R^2 = 0.994). Compared to the canines, the tubule diameters of the lateral incisors appeared to increase at a slightly higher rate as distance from the DEJ increased.

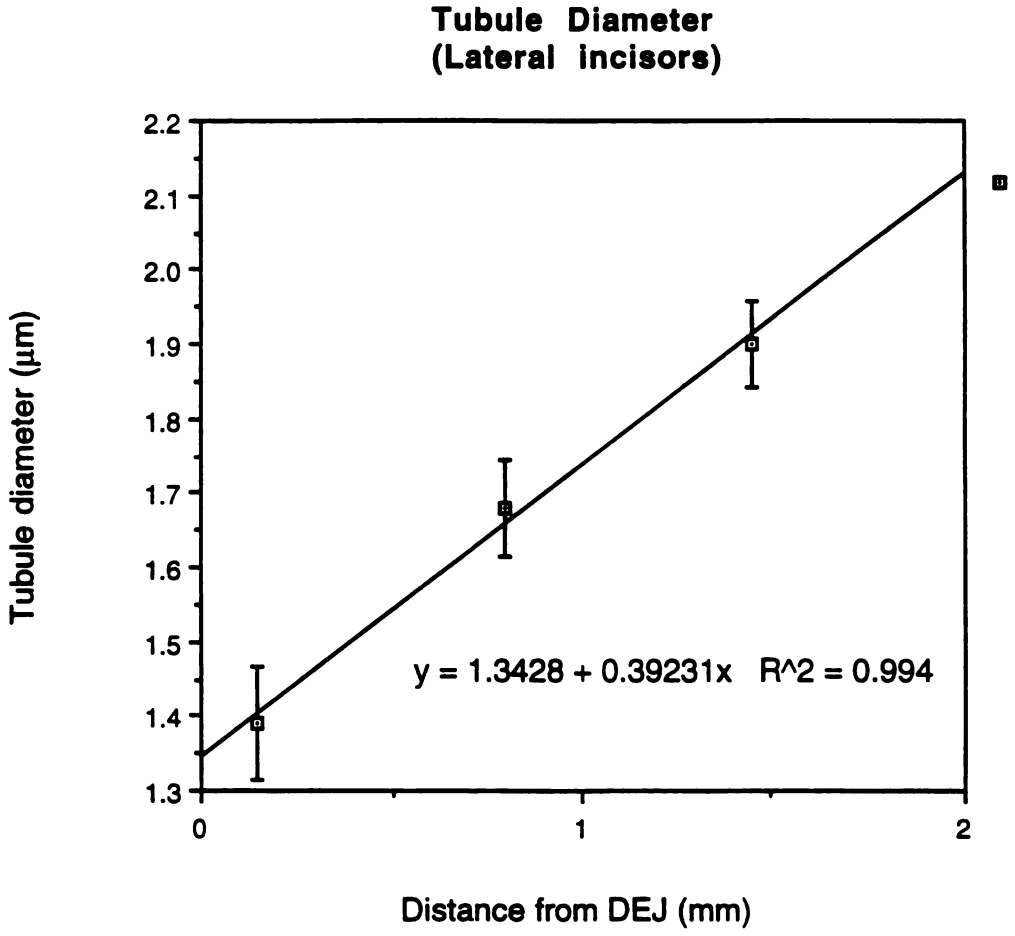

•Figure 5-8
Graph of tubule diameter (μm) for the lateral incisors.

The data and graphs appeared to suggest that the tubule diameters for the different tooth types were different and that those for the canines were slightly higher. It also appeared that the tubule diameters for the lateral incisors increased as the distance from the

DEJ increased at a higher rate than the canines. Statistical analyses were performed to detect any differences for tubule diameter that were significant at the $p < .05$ level.

Using a multi-factor ANOVA, it was determined that the tubule diameters in individual teeth, directions, and levels were significantly different ($p < .05$). The difference in tubule diameters between the canines and the lateral incisors however, was not statistically significant. A significant interaction was found between tooth type & slice ($p < .05$).

The data were examined according to tooth type via multi-factor ANOVA. For the lateral incisors, differences in the tubule diameters of individual teeth, levels and direction were significant ($p < .05$). Tukey's Studentized Range Test was performed to determine where there were significant differences. In the lateral incisors, the tubule diameters at level 3 were significantly greater than level 2, diameters at level 3 were significantly greater than level 1, and diameters at level 2 were significantly greater than level 1 ($p < .05$). The diameters of the central direction were significantly greater than those from the distal direction ($p < .05$).

For the canines, while the difference in tubule diameter for different directions was not significant, differences in the tubule diameters of individual teeth and levels were statistically significant ($p < .05$). Tukey's Studentized Range Test was performed and determined that in the canines, the tubule diameters at level 3 were significantly greater than level 2, diameters at level 3 were significantly greater than level 1, and diameters at level 2 were significantly greater than level 1 ($p < .05$).

To summarize, the tubule diameters at different levels were significantly different and no significant difference was detected between the canines and the lateral incisors. Within the canines, there was no significant difference between the tubule diameters of the central and distal directions. However, in the lateral incisors, the

tubule diameters of the central direction were significantly greater than those of the distal direction.

Test for slopes

A test for slopes for changes in the tubule diameters versus distance from the DEJ detected a significant difference between the canines and the lateral incisors ($p < .05$). A test for slopes for the same characteristics for direction within the tooth types revealed no statistically significant difference.

Therefore, it appears that the rate of change of tubule diameter as the distance from the DEJ increased was significantly different for the different tooth types (greater in the lateral incisors, $p < .05$). The rate of the change of the tubule diameter with distance from the DEJ was not significantly different for different directions of teeth. A summary of the results for slopes can be seen in Table 5-5.

•Table 5-5
Slopes (tubule diameter) separated by tooth type.

Tooth	Slopes (μm/mm)	Significantly different?
Canines	0.28	Yes
Lateral incisors	0.39	

5.3 Peritubular width

Peritubular width data were recorded (Table 5-6) and analyzed statistically for the variables: tooth (individual), direction (central, distal), type (canines, lateral incisors), level (1, 2, and 3 corresponding to the distances 0.15 mm, 0.8 mm, and 1.45 mm from

the DEJ), as well as for any possible interactions between the variables. Data for individual teeth were averaged across all the image sites for each level using a multi-factor ANOVA (General Linear Model, The SAS System).

•Table 5-6
Peritubular width (μm) separated by tooth type.
(upper value = standard deviation; lower value = robust standard error)

Tooth	0.15 mm from the DEJ	0.8 mm from the DEJ	1.45 mm from the DEJ	Slope (μm/mm)	R^2
Canines	0.92 (±0.14) (±0.05)	0.90 (±0.10) (±0.03)	0.75 (±0.06) (±0.02)	-0.13	0.837
Lateral incisors	0.62 (±0.19) (±0.05)	0.57 (±0.05) (±0.02)	0.55 (±0.10) (±0.02)	-0.05	0.942

For both the canines and the lateral incisors, the average peritubular width appeared to decrease as the distance from the DEJ increased from 0.15 mm (level 1), to 0.8 mm (level 2), to 1.45 mm (level 3). The average peritubular width in the canines appeared to be thicker than that in the lateral incisors, and the rate at which the peritubular width decreased as distance from the DEJ increased appeared greater in the canines as well.

In the canines, the peritubular width at levels 1, 2, and 3 was measured to be: 0.92 μm, 0.9 μm, and 0.75 μm, respectively. The standard deviations (with robust standard errors in parentheses) were: 0.14 (0.05), 0.10 (0.03), and 0.06 (0.02), respectively. The peritubular widths were plotted versus distance from the DEJ (Figure

5-9). Linear regression analysis of the peritubular width of the canines demonstrated a decrease of 0.13 μm/mm with respect to distance from the DEJ (R^2 = 0.837).

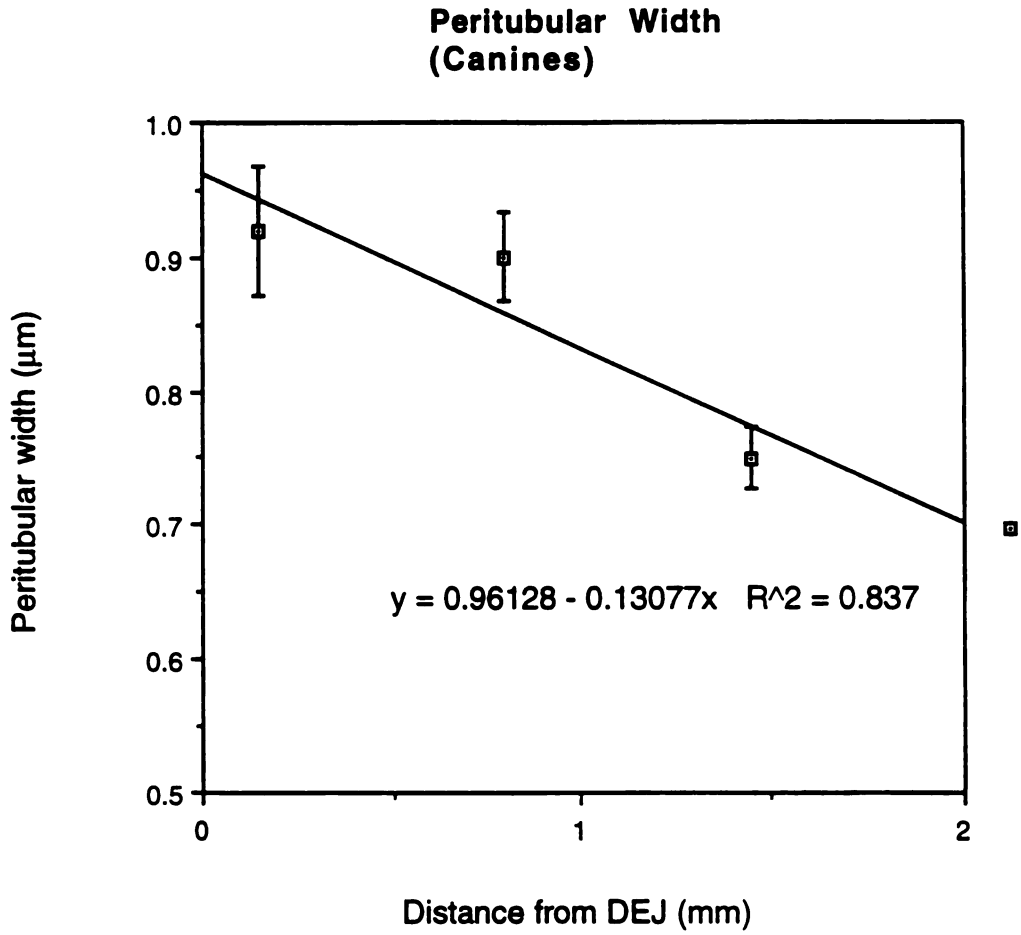

•Figure 5-9
Graph of peritubular width (μm) for the canines.

In the lateral incisors, the peritubular width at levels 1, 2, and 3 was measured to be: 0.62 μm, 0.57 μm, and 0.55 μm, respectively. The standard deviations (with robust standard errors in parentheses) were: 0.19 (0.05), 0.05 (0.02), and 0.10 (0.02), respectively. The variation in peritubular width appeared to be similar in both tooth types. The peritubular widths were plotted versus distance from the

DEJ (Figure 5-10). Linear regression analysis of the peritubular widths of the lateral incisors demonstrated a decrease of 0.05 μm/mm with respect to distance from the DEJ (R^2 = 0.942).

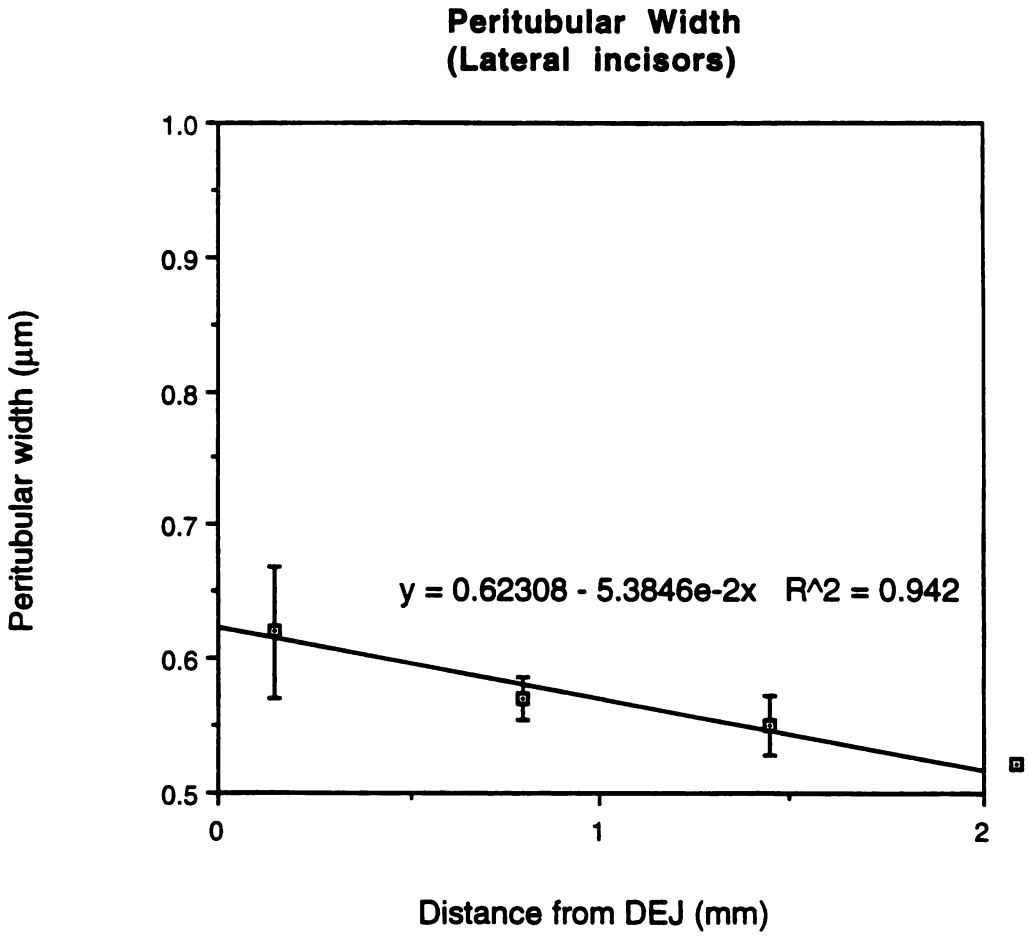

•Figure 5-10
Graph of peritubular width (μm) for the lateral incisors.

The data and the graphs suggested that the peritubular width in the canines was greater than that in the lateral incisors. The data also seemed to suggest that the rate at which the peritubular width decreased as distance from the DEJ increased was greater in the

canines as well. Statistical analyses were performed to detect any differences that were significant at the $p < .05$ level.

Using a multi-factor ANOVA, it was determined that the peritubular widths in individual teeth, tooth types, and levels were significantly different ($p < .05$). No significant interactions were detected. Tukey's Studentized Range Test was performed and found that while the peritubular width at level 1 appeared greater than level 2, and the width at level 2 appeared greater than level 3, only the peritubular width at level 1 was significantly greater than level 3 ($p < .05$). The peritubular width values for the canines were found to be significantly greater than those found for the lateral incisors ($p < .05$).

Test for slopes

A test for slopes found that for peritubular width versus distance from the DEJ, the rates at which the peritubular width decreased were not statistically different between the canines and the lateral incisors. As such, the slope for the canines and lateral incisors combined was calculated and found to be a decrease of 0.08 μm/mm. A summary of the results for slopes can be seen in Table 5-7.

•Table 5-7

Slopes (peritubular width) separated by tooth type.

Tooth	Slopes (μm/mm)	Significantly different?	Combined slope value (μm/mm)
Canines	-0.13	No	-0.08
Lateral incisors	-0.05		

5.4 Microcanals

The presence of microcanals was incidentally recorded in the course of this investigation. The microcanals presented distinctly as very large dentin tubules located within the intertubular matrix and were surrounded by a cuff of hypermineralized matrix resembling peritubular dentin. The location of the microcanals was constant, appearing in the midpoint facio-lingually of the dentin as seen in Figure 5-11. When more than one microcanal was present, they were arranged in a mesio-distal line, again within the midpoint facio-lingually. These features were approximately 5 to 10 times the size of the normal dentin tubules (Figure 5-12). Microcanals presented in 4 out of 20 teeth in this study (the additional 10 teeth were used in preliminary study). Within an individual tooth, as many as 15 microcanals and as few as 1 were detected. Serial sectioning demonstrated that when present, the microcanals coursed themselves similarly to normal dentinal tubules, traveling from the DEJ and continuing through the dentin matrix all the way to the pulp. Upon closer observation, the presence of collagen-like fibrils was detected. The microcanals presented in 2 out of 5 central incisors and 2 out of 11 lateral incisors. No microcanals were found in any of the canine teeth.

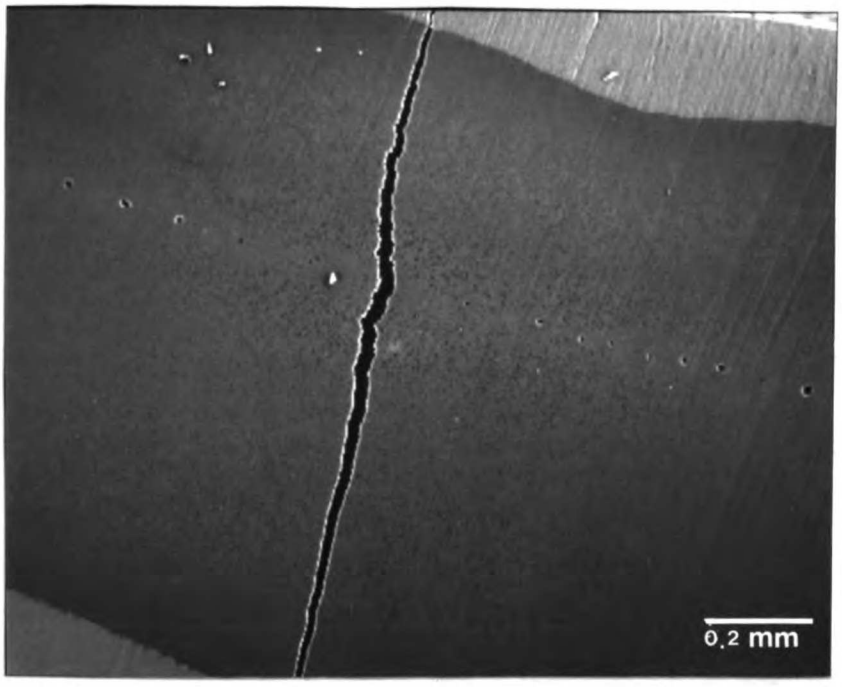

•Figure 5-11
SEM photomicrograph (20kV, 75x) showing microcanals situated in a mesio-distal direction at the midpoint faciolingually. Legend bar = 0.2 mm.

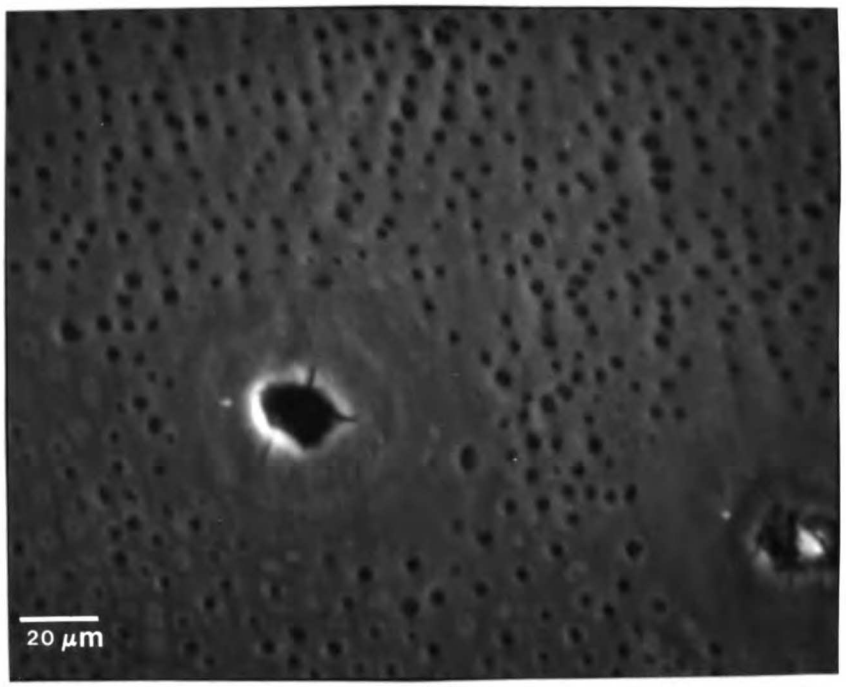

(a)

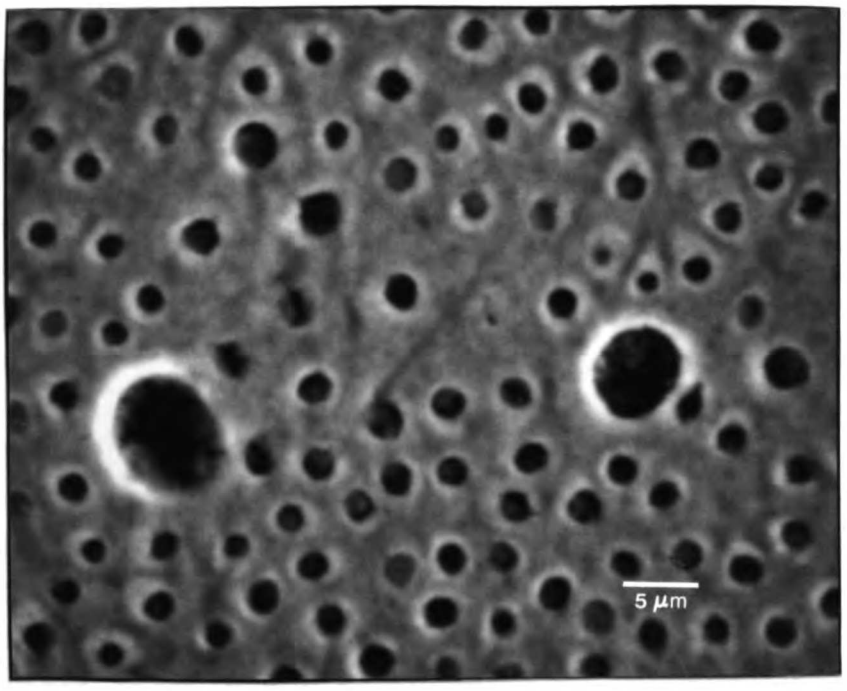

(b)

•Figure 5-12
a) SEM photomicrograph (20 kV, 500x) showing microcanals situated amongst normal dentin tubules. Legend bar = 20 μm.
b) SEM photomicrograph showing different set of microcanals in a different tooth situated amongst normal dentin tubules. Legend bar = 5 μm.

6. DISCUSSION

Of the three hard tissue components of teeth (enamel, dentin and cementum), dentin is perhaps the most complex and important structure. Modification of the physical and chemical nature of dentin plays a key role in the development and progression of caries, dental pain and sensitivity, preventive therapy, and restorative dentistry. A better understanding of the nature of dentin will have significant consequences regarding current and future methods of dental restoration, tooth protection, and the repair of dental structure as the result of pathology or trauma. Much progress in improving the bond between dentin and restorative materials has been made and research continues in this area. A better understanding of bonding to dentin should lead to improved resin-based restorations. Such achievements are important because the clinical success of restorations is dependent on more efficient bonding ability, sufficient bond strength, and the prevention of microleakage. (Marshall, 1993).

Although a significant amount of research has been devoted to dentin, little effort has been made to differentiate between the dentin of permanent teeth and that of deciduous teeth. Not only is there a lack of general information regarding deciduous dentin, there is also a lack of significant information specifically in the area of the microstructure of deciduous dentin and the principles of adhesion to deciduous dentin. Research on permanent dentin has involved procedures that may potentially distort and obscure the appearance of the dentin surface structure. Most studies have not made strong attempts to track a specific group of dentin tubules and monitor any changes along the tubules course from the DEJ to the pulp. Furthermore, most studies have characterized the microstructure of dentin in terms of general spatial locations (i.e., outer, middle, deep dentin) and have not analyzed changes in the microstructure with regards to specific anatomic landmarks (e.g., pulp, DEJ).

In this study, the microstructure of deciduous teeth was specifically investigated. By carefully sectioning the teeth to produce dentin matchsticks of a specific width and girth, attempts were made to follow a given group of dentin tubules and observe any changes in the characteristics (numerical tubule density, tubule diameter, peritubular width) along the tubules course from the DEJ to the pulp (Figure 4-2). The sections were made at specific distances from the DEJ to establish a regression of the changes in these parameters with regards to a specific anatomic landmark. To minimize alteration of the dentin surface structure, the samples were not subjected to demineralization, and were studied in the wet mode of an SEM. Image analysis provided an efficient and reliable method of quantifying the desired characteristics.

6.1 Dentin tubules

6.1.1 Numerical tubule density

The data for numerical tubule density (Table 5-1), exhibited a tremendous amount of variation, but generally fell within the range of previous authors' findings for deciduous and/or permanent teeth (Table 1-1).

The analysis of the data showed that near the DEJ, the numerical tubule density of deciduous dentin appears to be greater than that for permanent dentin. As distance from the DEJ increased, the numerical tubule density of deciduous dentin appears to approach the values reported for permanent dentin. However, this observation must be made with caution for several reasons. Most previous studies did not define what part of the tooth was being investigated, nor was it always clear at what intervals in relation to the DEJ the measurements were made. It is very likely that "outer", "middle" and "inner" dentin does not accurately reflect the same intervals at which the measurements for deciduous dentin were made in this study. When comparing data, consideration must also be given to the fact that although attempts were made to account for variation within a group of tubules and location in this study, previous investigations did not attempt to account for this. As

deciduous teeth are smaller than permanent teeth, the thickness of permanent dentin from the DEJ to the pulp is also greater than it is in deciduous dentin. Measurements in permanent dentin could be made at more and deeper levels (distances from the DEJ) rather than the 3 levels in this study. It stands to reason that if deciduous dentin was thicker, more levels could have been studied leading to the likelihood that even greater values for numerical tubule density might have been measured if it were possible to get 4 or 5 mm from the DEJ. Because the experimental methods differed, direct comparisons of the dentin microstructure must be made with care.

However, there are several studies in particular, that may be pertinent in making comparisons to this study (Figure 6-1).

•Figure 6-1
Illustration showing numerical changes in tubule density and their associated slopes in the canines and lateral incisors. Rounded values are shown.

Garberoglio and Brannstrom (1976), reported the numerical tubule density of permanent teeth at specific 0.5 mm intervals as distance from the pulp increased (Table 6-1). They determined that near the DEJ (3.0 mm from the pulp) the numerical tubule density was 19,000-20,000 tubules per mm^2, in the middle (2.0 mm from the pulp) it was 23,000-30,000 tubules per mm^2, and near the pulp (1.0 mm from the pulp) it was 30,000-40,000 tubules per mm^2. By making their measurements at specific intervals from an anatomic position (pulp), they were able to plot their data in a linear regression to assess the rate of change of numerical tubule density as the distance from the pulp increased. The values for numerical tubule density for deciduous canines and lateral incisors in this study would seem to suggest a higher number of tubules per mm^2 in deciduous teeth compared to permanent teeth. Using the values they found in their study, a linear regression analysis showed numerical tubule density increased at a rate of 8,571 tubules per mm^2/mm (Table 6-2). While it isn't known at which site they observed their dentin samples, their slope lies within the range of slopes found for canines and lateral incisors in the current study. Their slope value was greater than those found for the lateral incisors and the central matchsticks of the canines; but less than that found for the distal matchsticks of the canines. As stated earlier however, any comparisons should be made with caution due to the thickness of permanent dentin and differences in experimental design.

•Table 6-1

Comparison of current data for numerical tubule density (#/mm^2) to that reported by various authors.

*(C = central matchsticks; D = distal matchsticks)

**(O = occlusal sites; B = buccal sites)

Investigators	Tooth	Superficial	Outer	Middle	Inner
*Current study (deciduous)	Canines (D)		17,969	26,313	33,278
	Canines (C)		23,963	26,552	29,732
	Lateral incisors (D)		29,294	34,586	39,442
	Lateral incisors (C)		38,392	39,873	42,427
			(0.15 mm from DEJ)	(0.8 mm from DEJ)	(1.45 mm from DEJ)
Brannstrom & Garberoglio, 1976			19,000-20,000	23,000-30,000	30,000-40,000
			(3 mm from pulp)	(2 mm from pulp)	(1 mm from pulp)
**Olsson, et.al., 1993	Third molars (O)		24,500	40,400	51,100
	Third molars (B)		18,200	30.900	43,400
Koutsi et.al., 1994 (deciduous)	Molars	17,433	18,075	20,433	26,391

•Table 6-2a

Comparison of current data for slopes (numerical tubule density) to that reported by various authors, separated by tooth type.

Investig.	Tooth	Location	Slopes (# per mm^2/ mm)
Current study	Canines	Distal	11,776
		Central	4,438
Current study	Lateral incisors	both	5,455
Garberoglio & Brannstrom, 1976	Premolars		8,571
Olsson, et.al., 1993	Third molars	Occlusal	10,640
		Buccal	10,080

•Table 6-2b

Comparison of current data for slopes (numerical tubule density) to that reported by various authors, separated by direction.

Investig.	Location	Tooth	Slopes (# per mm^2/ mm)
Current study	Distal	both	9,130
Current study	Central	both	3,548
Garberoglio & Brannstrom, 1976		Premolars	8,571
Olsson, et.al., 1993	Occlusal	Third molars	10,640
	Buccal		10,080

A second pertinent study was performed by Koutsi, et.al. (1994) on deciduous molar teeth. They characterized the numerical tubule density in the buccal direction in terms of general locations in relation to the pulp: superficial (90-100% distance from the pulp), outer (60.1-90% from the pulp), intermediate (30.1-60% from the pulp), and deep (0-30% from the pulp). The values reported were: 17,433 per mm^2, 18,075 per mm^2, 20,433 per mm^2, and 26,391 per mm^2, respectively (Table 6-1). Once again, any comparisons to the data in the current study must be made with caution. However it appears that the numerical tubule density in deciduous anterior teeth is greater than that found in deciduous posterior teeth. Koutsi's group did not relate their data in terms of specific intervals from an anatomic landmark, rather they discussed their data in terms of % distance from the pulp. For the purpose of comparing slopes, the data in the current study can be discussed in terms of % distance as well. Most of the deciduous dentin matchsticks had a length of 2 mm. Knowing that the matchsticks were sectioned at 0.65 mm increments (0.5 mm + 0.15 mm blade thickness), the distances from the DEJ could be changed to % distance from the DEJ (7.5%, 40%, and 72.5%). Slope values in terms of % distance from the DEJ could then be estimated from the data in the current study and compared to that estimated from Koutsi, et.al.'s (1994) study as seen in Table 6-3. Similar to the findings of Garberoglio and Brannstrom (1976), the %-estimated slope for the deciduous molars in Koutsi, et.al.'s (1994) study was greater than that for the lateral incisors and the central matchsticks in the canines; but much less than that found for the distal matchsticks of the canines.

•Table 6-3a
Comparison of current data for slopes (by %) of numerical tubule density to that reported by Koutsi, et.al. (1994) separated by tooth type.

Investig.	Tooth	Location	Slopes (# tubules/ % distance from DEJ)
Current study	Canines	Distal Central	23,552 8,875
Current study	Lateral incisors	both	10,911
Koutsi, et.al., 1994	Molars		12,516

•Table 6-3b
Comparison of current data for slopes (by %) of numerical tubule density to that reported by Koutsi, et.al. (1994) separated by direction.

Investig.	Location	Teeth	Slopes (# tubules/ % distance from DEJ)
Current study	Distal	both	18,260
Current study	Central	both	7,095
Koutsi, et.al., 1994		molars	12,516

Another significant study was performed by Schellenberg, et.al. (1992), who studied differences in numerical tubule density between different permanent teeth. While measurements were made only at one distance from the pulp, a significant difference was detected between maxillary and mandibular molars. This finding suggests that the numerical tubule density differs in different tooth types.

Secondly, they found at the pulp chamber, that the numerical tubule densities of the facial/lingual walls were significantly greater than those of the mesial/distal walls, suggesting that there is a difference in numerical tubule density according to location within teeth. Again because they were unable to control for precise distance from the pulp, these findings need to be interpreted with caution.

Lastly, Olsson, et.al.'s (1993) data on the occlusal and buccal sites of third molars can be compared to the findings in the current study. While they did not state exactly at what distance from the DEJ they initiated their observations, they were able to observe the dentin samples at 1.25 mm increments thereafter. Once again, similar to the findings reported by Garberoglio and Brannstrom (1976), near the DEJ, the numerical tubule density found for deciduous teeth appears to be greater than that found for permanent teeth. Using their data for a linear regression analysis, the slope values found in their study were greater than those found for the lateral incisors and the central matchsticks of the canines, but less than those found for the distal matchsticks of the canines.

It was expected that the values for numerical tubule density at different distances from the DEJ in the current study would be different; that the values for different directions might be different; and that the values for different teeth might be different. Statistical analysis of the data attempted to confirm this. The values for numerical tubule density did in fact increase as the distance from the DEJ increased. However, only within the distal matchsticks were the differences in tubule density between all depths significantly different. In the central matchsticks, only the difference between level 1 (0.15 mm from the DEJ) and level 3 (1.45 mm from the DEJ) were significant. Between different tooth types, the only significant difference was that the values from the central matchsticks of the lateral incisors was greater than those from the central matchsticks of the canines. While not all of the differences in numerical tubule density in this study were statistically significant, it is likely that this may be attributed to a small sample size. Other factors that may

have contributed were biological variation within and between teeth, inaccurate initial sectioning (at the DEJ), and possible operator error during the image analysis process.

The rate of change of numerical tubule density as distance from the DEJ increases is a characteristic that is not often investigated in dentin tubule studies. Identifying dentin microstructural characteristics at specific distances from the DEJ provides valuable information, but is not necessarily the best way to compare differences between or within teeth. It is difficult to establish the position of a slice of dentin exactly at the DEJ, for reasons that include the fact that the DEJ is not a straight, static line, and the thickness of the cutting blade must be taken into account. The possible result is that while it is likely that with care, the initial slice of dentin should still be within 0.15 mm (blade thickness) from the DEJ, it is not completely accurate to say that the tubule density for example, is a certain value at precisely "x" mm from the DEJ. It is possible that the measurements made at 1.0 mm from the DEJ on one dentin matchstick may not be exactly the same distance from the DEJ as measurements made at 1.0 mm from the DEJ on another dentin matchstick. It is possible however, to take microstructural measurements at specific distance intervals thereafter. By following this procedure of measurements at specific intervals, it is possible to assess the slope or rate of change of numerical tubule density. Because it is fairly straightforward to take measurements at specific intervals, differences in slope (rate of change) may be a more accurate method of assessing dentin tubule characteristics rather than the absolute number (numerical tubule density, tubule diameter, peritubular width) at a specific location. In this study, between different tooth types, no statistically significant difference was found between slopes for numerical tubule density. However, within the canines the slope in the distal direction was significantly greater than that found in the central direction. Once again, a small sample size may have contributed to the lack of significant differences in slopes between and within teeth. The significant difference within the canines however, is worth exploring. At first,

no difference in slopes was expected. However referring back to the description of the process of dentinogenesis, due to the cylindrical nature of tooth anatomy (versus spherical) the odontoblasts move obliquely as they migrate apically. This pattern causes the odontoblasts to track in an S-shaped curve as they make accommodations for the more occlusally/incisally located odontoblasts (Moss-Salentijn and Hendricks-Klyvert, 1985). A look at the basic coronal anatomy of canines versus lateral incisors may provide insight as to the statistically significant findings that were made (Figure 6-2).

The incisal edge (enamel profile) of the lateral incisor is relatively flat and unchanging from proximal end to end. The incisal edge of the canine however, is much more angled. As the incisal edge traces from the mid-incisal point, there is a gradual but definite apical sloping as it approaches the proximal angle. The outer enamel shape belies the shape of the DEJ, thus belying the shape of the dentin profile. Overall then, in the distal matchstick of the canines, the tooth shape changes more rapidly and the cells are forced to migrate within a more constricted volume. This probably leads to the increased rate of change in numerical tubule density in the distal versus the central matchsticks of the canines.

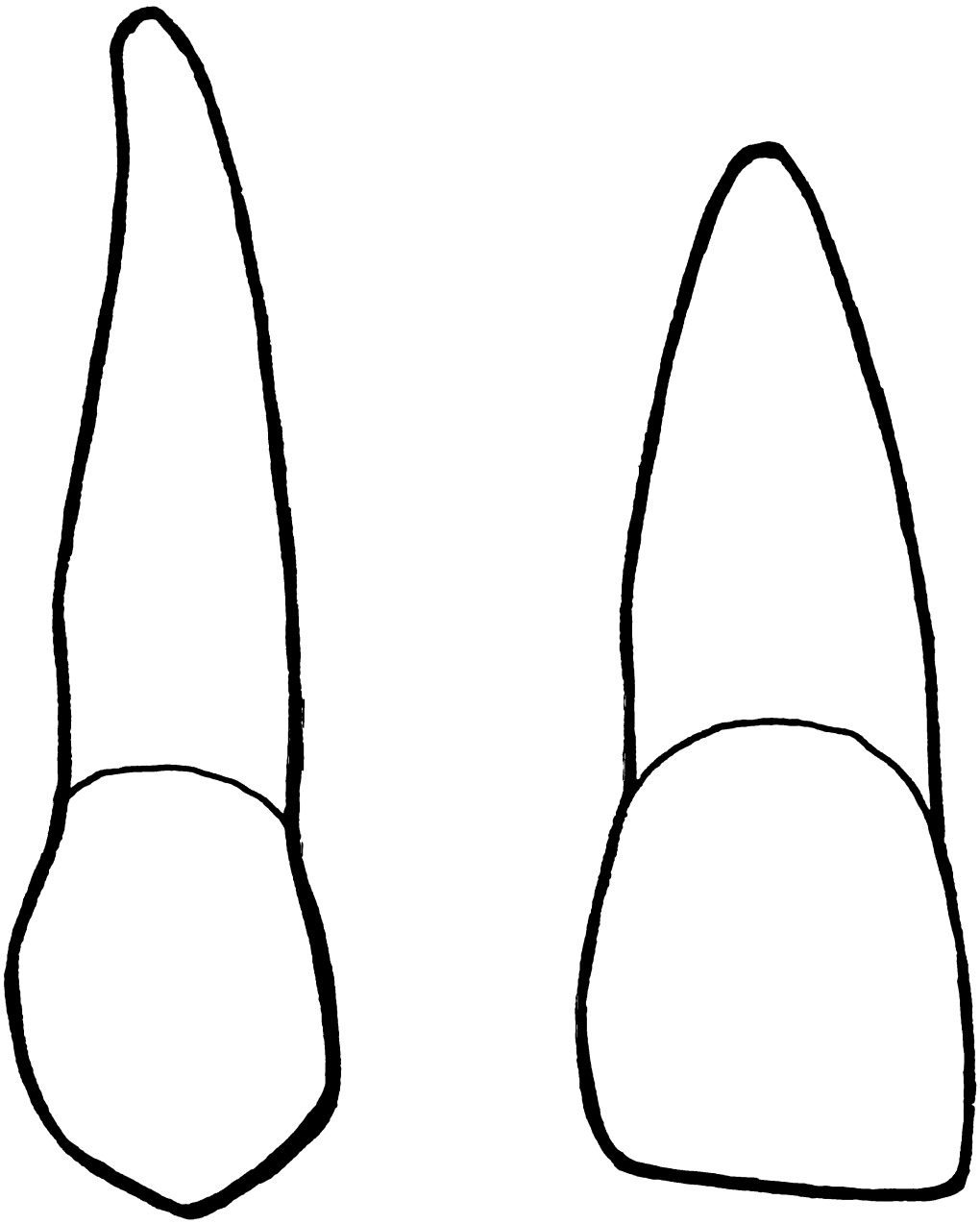

•Figure 6-2
Illustration showing labial view of a canine and lateral incisor to depict differences in coronal anatomy outline.

Based on a comparison of the data from this study to that of previous works, several conclusions become apparent. The numerical tubule density in the deciduous anterior teeth is greater than that found for the deciduous molars. The lateral incisors had a higher numerical tubule density than the canines, and the canines had a higher numerical tubule density than did the molars; suggesting a trend of decreasing numerical tubule density as tooth position proceeds posteriorly. It appears that the canines pose as a transition from anterior to posterior teeth. It also appears that the numerical tubule density of deciduous anterior teeth is greater than that found in permanent teeth as well. It is difficult to understand why numerical tubule density is greater in deciduous anterior teeth versus posterior teeth, and greater in deciduous teeth versus permanent teeth. One possibility would be that embryologically, tooth buds start out with a predetermined number of odontoblasts per unit area and that the numerical tubule density at any point is related to the total surface area of the coronal structure. In other words, as the crown of a deciduous tooth is generally smaller than that of a permanent tooth, it has less total surface area in which the odontoblasts can produce dentin, resulting in a higher numerical tubule density. The same can be said of the coronal structure of a deciduous anterior tooth having a smaller total surface area than a deciduous molar, resulting in a higher numerical tubule density in the anterior tooth.

A second possibility is that the number and size of odontoblasts is related to the time required for tooth development. If a tooth has a relatively short time in which to develop, it is likely that more and larger odontoblasts would be required for the process of dentinogenesis. For the time allotted between hard tissue formation to tooth eruption, deciduous anterior teeth must develop much faster than any other teeth in either dentition. Deciduous central and lateral incisors begin hard tissue formation at around 3-4 months *in utero* and erupt at around 6-7 months of age. Deciduous second

molars begin formation at around 5 months *in utero* and erupt at around 20 months (Braham and Morris, 1985). Permanent incisors on the other hand, begin formation at around 3-4 months post-natally and erupt at around 7 years of age, while permanent third molars begin formation at around 10 years and erupt at around 17-21 years (McDonald and Avery, 1988). It seems logical then, that because deciduous anterior teeth must develop much more quickly, that more and stronger "manpower" would be required to get the job done. It might also be hypothesized that microcanals may be in fact, giant dentin tubules with a comparatively large odontoblastic potential to assist in the relatively rapid tooth development of deciduous anterior teeth.

A third possibility is that teeth tend to end up with a particular tubule density near the pulp. This can be related to a possible protective mechanism for the oral cavity. As anterior teeth are the most anterior exposed hard tissue in the oral cavity, they may also serve as temperature sentries. Having more tubules near the pulp might allow anterior teeth to be more sensitive to extreme temperature changes due to liquids or food as the stimuli enter the oral cavity. This mechanism, along with sensation from the peri- and intra-oral soft tissues may thus act as protective mechanism for the oral cavity. These possibilities need to be further explored however, before a definitive relationship can be assumed.

When the values found for slopes are compared, it appears that the rate of increase in numerical tubule density as the distance from the DEJ increases, is markedly greater within the distal direction of the deciduous canines. The discrepancy found between the distal matchsticks of the canines is most likely due to the anatomic uniqueness of the coronal structure of canine teeth and the curvature of the DEJ as described earlier. It appears then, that overall anatomic morphology plays an important role in affecting changes in numerical tubule density.

6.1.2 Tubule diameter

The data for tubule diameter (as shown in Table 5-4), exhibited somewhat less variation relative to that found for numerical tubule density, and once again generally fell within the range of the findings of previous authors. The values for tubule diameter of the canines at distances of 0.15 mm, 0.8 mm and 1.45 mm from the DEJ were: 1.58 μm, 1.83 μm, and 1.94 μm, respectively; and increased at a rate of 0.28 μm/mm. The values for the lateral incisors were: 1.39 μm, 1.68 μm, and 1.90 μm, respectively; and increased at a rate of 0.39 μm/mm.

As noted for numerical tubule density, previous reports of tubule diameter were in relation to general locations of "outer", "middle", and "inner" permanent tooth dentin. The tubule diameter of "outer" dentin has been reported in the range of 0.5 μm to 1.0 μm (Ten Cate, 1994; Garberoglio and Brannstrom, 1976; Tronstad, 1973), "middle" dentin in the range of 1.1 μm, to 1.2 μm (Ten Cate, 1994; Garberoglio and Brannstrom, 1976), and "inner" dentin in the range of 1.6 μm, to 2.5 μm (Ten Cate, 1994; Garberoglio and Brannstrom, 1976). The data in this study suggested that, near the DEJ, the tubule diameter of deciduous dentin is greater than that for permanent dentin. As the distance from the DEJ increased, the tubule diameter of deciduous dentin appears to approach the values reported for permanent dentin. Once again, this observation must be made with caution because it is unclear at what intervals in relation to the DEJ the previous authors made their measurements. It is very likely that what they considered to be "outer", "middle", and "inner" dentin does not reflect the same intervals at which the measurements for deciduous dentin were made in this study. Another consideration when comparing data is the fact that while in this study, attempts were made to account for variation within a group of tubules and location, previous reports did not. Lastly, the methods for quantifying tubule diameter differed. Therefore, any direct comparisons must be made with care.

Two studies may be pertinent in making comparisons to the data in this study. Garberoglio and Brannstrom (1976) reported the tubule diameter of permanent teeth at specific 0.5 mm intervals as distance from the pulp increased (Table 6-4). They determined that near the DEJ (3.0 mm from the pulp) the tubule diameter was 0.8 μm, in the middle (2.0 mm from the pulp) the tubule diameter was 1.1 μm, and near the pulp (1.0 mm from the pulp) the tubule diameter was 1.6 μm. By making their measurements at specific intervals from an anatomic position (i.e. pulp or DEJ), they were able to plot their data in a linear regression to assess the rate of change of tubule diameter as the distance from the pulp increased. Because of this, any comparison to the data from the current study should be made with relative confidence to the findings of Garberoglio and Brannstrom (1976), as opposed to the data reported by other authors who did not report their findings at specific intervals. The values for tubule diameter for deciduous canines and lateral incisors in this study suggest a larger diameter of tubules in deciduous teeth compared to permanent teeth. As stated earlier, this comparison must be made with caution. Their findings can be adapted to a linear regression to produce a slope value for tubule diameter (Table 6-5). The slope for tubule diameter in the deciduous lateral incisors was similar to that found for premolars by Garberoglio and Brannstrom, and both were larger than that found for deciduous canines.

•Table 6-4

Comparison of current data for tubule diameter (μm) to that reported by various authors.

Investigators	Tooth	Superficial	Outer	Middle	Inner
Current study (deciduous)	Canines		1.58	1.83	1.94
	Lateral incisors		1.39 (0.15 mm from DEJ)	1.68 (0.8 mm from DEJ)	1.90 (1.45 mm from DEJ)
Brannstrom & Garberoglio, 1976			0.8 (3 mm from pulp)	1.1 (2 mm from pulp)	1.6 (1 mm from pulp)
Koutsi et.al., 1994 (deciduous)	Molars	0.96	1.08	1.10	1.29

•Table 6-5

Comparison of current data for slopes of tubule diameter (μm) to that reported by various authors.

Investig.	Tooth	Location	Slopes (μm/mm)
Current study	Canines	both	0.28
Current study	Lateral incisors	both	0.39
Garberoglio & Brannstrom, 1976	Premolars		0.37

Another pertinent study was performed by Koutsi, et.al. (1994) on deciduous molar teeth. As in their method for numerical tubule density, they characterized the tubule diameter in terms of general

locations in relation to the pulp: superficial (90-100% distance from the pulp), outer (60.1-90% from the pulp), intermediate (30.1-60% from the pulp), and deep (0-30% from the pulp). The values reported were: 0.96 μm, 1.08 μm, 1.1 μm, and 1.29 μm, respectively (Table 6-4). Once again, while any comparisons to the data in the current study must be made with caution, the findings suggest that the tubule diameters in deciduous anterior teeth are larger than those in deciduous posterior teeth. As described earlier, the data from the current study can be transformed to % distance from the DEJ so that the slopes may be compared (Table 6-6). It appears that the rate that tubule diameters in deciduous molars increases is only slightly greater than that in deciduous anterior teeth.

•Table 6-6
Comparison of current data for slopes (by %) of tubule diameter (μm) to that reported by Koutsi, et.al. (1994).

Investig.	Tooth	Location	Slopes (μm/mm)
Current study	Canines	both	0.28
Current study	Lateral incisors	both	0.39
Koutsi, et.al., 1994	molars		0.41

Based on the numerical data it was expected that the values for tubule diameter at different distances from the DEJ should be different, and that the values for different tooth types might be different. The data suggested this and statistical analysis attempted to confirm this. The differences in tubule diameter between each level (distance from the DEJ) were significant and no significant difference was detected between the canines and lateral incisors.

Within the lateral incisors however, the tubule diameters of the central direction were significantly greater than those of the distal direction. Several reasons for this discrepancy may be possible, the small sample size, and that the method for computing the tubule diameters assumed that the dentin tubules were perfect circles. However, the tubules did not always appear as perfect circles. Although attempts were made to account for this, polishing debris and artifacts may have interfered with the ability of the image analysis software to assess % field area occupied by the tubules. Any discrepancies could also be attributed to operator error in the image analysis process.

As with numerical tubule density, the rate of change of tubule diameter is a characteristic that is rarely investigated in dentin tubule studies. As stated earlier, the slope or rate of change in tubule diameter may be a more accurate assessment than the absolute value of the tubule diameters. In this study, the rates of change of tubule diameter between the different directions within teeth were not significantly different. However, the rate of increase in tubule diameter in the lateral incisors was significantly greater than that in the canines. Again going back to the process of dentinogenesis, because the lateral incisors have a broader, relatively flatter incisal edge compared to canines; as the odontoblasts migrate from the DEJ to the pulp they are less encumbered by any possible crowding than those in canines (Figure 6-2). As a result, if odontoblasts expand as they approach the pulp, they are freer to expand without having to compete for intertubular space as much as are those in canines. Conversely, it is possible that the increase in tubule diameter is not due to odontoblast expansion but rather is due to a decrease in the amount of peritubular dentin deposition. Ten Cate (1994) pointed out that peritubular dentin is deposited within the dentin tubule, that the amount of peritubular dentin deposition is in fact what causes differences in tubule diameter, and refers to peritubular dentin as intratubular dentin. In other words, it is possible that all dentin tubules/odontoblasts originate with roughly the same diameter, and that changes in the diameter as the distance

from the DEJ increases are the result of changes in the amount of peritubular dentin deposition as opposed to tubule expansion by the odontoblast. There are a couple of possible reasons for this. One is that changes in tubule diameter/peritubular dentin deposition are a process of maturation. Hojo (1990) demonstrated that as tooth age and tooth wear increased, tubule diameter decreased. He attributed this finding to tooth wear and subsequent exposure of the dentin to minerals in the diet. It is thought that such exposure would result in remineralization and deposition of peritubular dentin. A second possibility is somewhat related to that demonstrated by Hojo and is that intertubular dentin acts as a mineral reservoir. As the numerical tubule density increases as depth increases, there is less solid dentin matrix available from which to draw mineral. This may result in less peritubular dentin which would lead to larger tubule diameters.

Thus several conclusions can be drawn. It appears that the tubule diameters for deciduous anterior teeth are larger than those for deciduous molars. It also appears that the tubule diameters for deciduous anterior teeth are larger than those for permanent teeth. The differences between tubule diameters for deciduous and permanent teeth might be explained by differences in peritubular dentin deposition, tooth age, and the amount of available mineral. If dentin tubule diameter is dependent on the deposition of the highly mineralized peritubular dentin, then it would seem that if there were less mineral in deciduous teeth versus permanent teeth that would result in larger tubules in deciduous teeth. Hirayama (1994) suggested that the concentrations of Ca and P might be lower in deciduous teeth compared to permanent teeth. However, this theory is in conflict with the conclusions reported by Hirayama, et.al. (1986), that peritubular dentin in deciduous teeth is 2 to 5 times thicker than that in permanent teeth, and the data from this study that showed peritubular width to be at least as great as that for permanent teeth. Therefore, the difference in tubule diameter between deciduous and permanent teeth is more likely due to the requirement for more and larger tubules in deciduous teeth that is

related to the time allotted for tooth development as was discussed earlier.

The rate that tubule diameters change in relation to the DEJ does not appear to be markedly different for deciduous or permanent teeth. However, the slope for tubule diameter in deciduous lateral incisors was significantly greater than that for deciduous canines. As stated above, if in fact mineral content differs between permanent and deciduous teeth, it is possible that the mineral content varies at different depths within the coronal structure of teeth, and differs between tooth types as well. Hardness, a characteristic that is often correlated with mineral content, has been shown to decrease from the DEJ to the pulp, and has been previously associated with numerical tubule density (Pashley, et.al., 1985). However, recent work by Kinney, et.al. (1996) reported that the decrease in dentin hardness as the pulp is approached, is due to changes in the hardness/composition of the intertubular dentin. Their findings seem to lend support to the possibility that mineral content does differ, and these differences could be the cause of the difference in slope found for deciduous canines and lateral incisors.

6.2 Peritubular width

The data for peritubular width (as shown in Table-13), generally fell within the range of the findings in the literature. The values for the canines at distances of 0.15 mm, 0.8 mm, and 1.45 mm from the DEJ were: 0.92 μm, 0.90 μm, and 0.75 μm, respectively, and decreased at a rate of 0.13 μm/mm. The values for the lateral incisors were: 0.62 μm, 0.57 μm, and 0.55 μm, respectively and decreased at a rate of 0.05 μm/mm.

Peritubular width has not been studied as extensively as numerical tubule density and tubule diameter (Table 6-7). Allred (1968), reported that peritubular width ranged from 1.0 to 2.0 μm in molar and premolar teeth, and Ten Cate (1994), reported the

peritubular width near the DEJ to be approximately 0.75 μm and near the pulp 0.044 μm (most likely at the predentin-dentin border). Hirayama, et.al. (1986), reported that the peritubular dentin found in deciduous teeth was 2 to 5 times thicker than that found in permanent dentin.

•Table 6-7
Comparison of current data for peritubular width (μm) to that reported by Ten Cate (1994).
*(Probably at the pre-dentin border)

Investigators	Tooth	Outer	Middle	Inner
Current study (deciduous)	Canines	0.92	0.90	0.75
	Lateral incisors	0.62 (0.15 mm from DEJ)	0.57 (0.8 mm from DEJ)	0.55 (1.45 mm from DEJ)
Ten Cate, 1994		0.75		0.044*

From the data in this study, it was expected that the values for peritubular width at different distances from the DEJ should be different, that the directions might be different, and that the tooth types might be different. Statistical analysis attempted to confirm this. While the peritubular width decreased as distance from the DEJ increased, only the difference between level 1 (0.15 mm from the DEJ) and level 3 (1.45 mm from the DEJ) was significant. The peritubular width for the canines was significantly greater than that of the lateral incisors. No significant difference in the rate of peritubular width decrease was detected nor expected. Several possible theories exist to explain these findings. Once again, a small sample size may have contributed to the non-significant differences between values at some of the distances from the DEJ. The method for quantifying peritubular width also assumed the tubule and

peritubular dentin to be a circular unit and in some cases, the peritubular band was not of uniform thickness around a particular tubule. Polishing debris and artifacts may have obscured some of the peritubular features during the image analysis. Finally, operator error also may have contributed to any unexpected findings.

Referring back to the theory mentioned earlier concerning how peritubular dentin width affects changes in tubule diameter, the slopes of the tubule diameters and peritubular widths were compared. When tubule diameter is halved to become tubule radius, the resultant slope can be compared to that for peritubular width since we consider the tubule and peritubular dentin unit to be a circle. As seen in Table 6-8, if the slope values for tubule diameter are halved, they seem to approach the absolute value of the slope value for the canines and are slightly larger than that found for the lateral incisors.

•Table 6-8
Comparison of current data for slopes of tubule diameter to that of peritubular width.

Tooth type	Tubule diameter slope (μm/mm)	Tubule radius slope (diameter/2)	Peritubular width slope (μm/mm)
Canines	0.28	0.14	-0.13
Lateral incisors	0.39	0.195	-0.05

It appears that the absolute value of the rate that the tubule diameters increase is similar to the absolute value of the rate that peritubular width decreases, as the distance from the DEJ increases. In other words, it appears that as the tubule diameters increase, the peritubular dentin width decreases at a similar rate. This similarity would seem to support the theory that the dentin tubules all start

out at a similar diameter and that the increase in tubule diameter as the distance from the DEJ increases can be accounted for by a decrease in the amount of peritubular dentin deposition within the tubule. Differences in the extent of peritubular dentin deposition are likely due to the amount of mineral available within the dentin matrix or are related to tooth maturity/wear. As the numerical tubule density increases near the pulp, there is less solid dentin matrix and less cell activity, and perhaps then there is less mineral available for peritubular dentin deposition.

6.3 Microcanals

As stated earlier, the presence of microcanals was incidentally observed and their presence and characteristics were recorded as described in the results section. Similar to their description by previous authors, microcanals did not occur in every tooth (4 out of 20) and when they did, they ranged in prevalence from 1 to 15. The literature regarding microcanals has not been able to provide a definitive explanation as to their origin or function. Microcanal origination has been theorized to be the result of odontoblast crowding and necrosis (Dyngeland, 1988) or the result of a disturbance during dentinogenesis and subsequent imperfection (Agematsu, et.al., 1990).

Observations made in this study seem to agree with those made previously, in that the microcanals do in fact resemble large dentin tubules. They were surrounded by a cuff of hypermineralized matrix resembling peritubular dentin, and appeared to track from the DEJ all the way to the pulp. The position of the microcanals was consistently in the labio-lingual midline. When more than one microcanal was present, they were always in a line mesio-distally.

Several questions thus arise. What would cause odontoblasts to produce such large, hypertrophied tubules? What process occurs during odontoblast crowding and is this in fact the result of odontoblast crowding? If they are the result of an imperfection,

what is the nature of the imperfection? Lastly why would this only occur some of the time? It appears that these features can appear in deciduous and permanent teeth (Agematsu, et.al., 1990; Hals, 1984), with an incidence of 0 to 30 when they do appear (Hals, 1983). They are always found in the labio-lingual mid-line and if more than one appears, they run in a straight line mesio-distally (Agematsu, et.al., 1990). The diameter of the microcanals has been reported between 6.0 and 7.5 μm (Agematsu, et.al., 1990). Their origin has been speculated to be related to a defect resulting from odontoblast crowding (Agematsu, et.al., 1990) or accumulation and necrosis of odontoblasts (Dyngeland, 1988). Thus, while their morphological appearance would seem to suggest that they resemble normal dentin tubules of an enlarged nature; their odd yet specific positioning might seem to suggest their origin might be due to an interference or disruption during dentinogenesis as odontoblasts migrate apically, rather than as simply an imperfection (which could occur anywhere). None of the currently available literature however, has been able to specifically establish the prevalence of microcanals, provide a definitive explanation for their origin, or determine if they are more likely to occur in deciduous or permanent teeth, or anterior or posterior teeth. Current literature would seem to suggest that they might be more prevalent in deciduous anterior teeth.

6.4 Clinical implications

Based on the results from this study, several points become apparent. Deciduous teeth appear to have a higher numerical tubule density than do permanent teeth. Deciduous anterior teeth also appear to have a higher numerical tubule density than do deciduous molars. The tubule diameters found in deciduous anterior teeth appear to be larger than those found in deciduous molars and permanent teeth. These findings can have significant implications in the area of restorative dentistry. It is known that bonding restorative resins to dentin is dependent on the amount of solid dentin available (Suzuki and Finger, 1988). It stands to reason then, that when there are more and larger tubules in a given sample there

is less solid dentin available for bonding, and as a result, bond strength decreases. As discussed in the section regarding differences in bond strength, there is a body of literature showing that bond strength to deciduous dentin is significantly less than bond strength to permanent dentin. The data in this study and previous works suggest that the numerical tubule density in deciduous teeth is greater than that of permanent teeth and perhaps can explain the reason for the difference in bond strengths. Furthermore, Marshall, et.al. (1995) demonstrated that peritubular dentin etches faster than intertubular dentin. Remembering that deciduous dentin was found to have larger tubule diameters to begin with, and that peritubular dentin was at least as thick in deciduous versus permanent teeth in this study and has been reported by Hirayama, et.al. (1986) as even thicker for deciduous teeth, acid etching prior to bonding would result in even larger tubules in deciduous dentin thus further decreasing the amount of solid dentin available for bonding. Therefore, peritubular width may also help explain the difference in bond strengths.

The existence of more and larger dentin tubules may also play a role in tooth sensitivity and trauma as well. It hasn't yet been demonstrated that deciduous teeth are more susceptible to tooth sensitivity. However, having more and larger conduits (dentin tubules) to the pulp would seem a likely cause for an increased risk of transmission of noxious stimuli. Exposure of dentin tubules due to trauma would seem to have more deleterious effects in deciduous teeth also, due in fact to the more and larger tubules. Current treatment recommendations for minor/shallow dentin fractures of deciduous teeth call for smoothing of sharp or rough enamel and dentin edges only (Andreasen and Andreasen, 1994). If deciduous teeth are more susceptible to noxious substance transmission through more and larger tubules, modifications of the recommendations might be necessary. Revised recommendations might include: bonding a resin layer to protect and occlude the exposed tubules or application of high concentration topical fluoride to promote mineralization.

Regarding peritubular width changes, this study suggests that peritubular dentin width decreases as dentin tubule diameter increases with distance from the DEJ. This seems to support Ten Cate's (1994) theory that peritubular dentin is deposited within the lumen of the dentin tubules and that as the amount of peritubular dentin decreases, the tubule diameter increases. An association of bond strength to numerical tubule density and tubule diameter has been demonstrated (Suzuki and Finger, 1988), and peritubular width also appears to play a role. As the peritubular width decreases and the tubule diameter increases with depth, there is less solid dentin available for bonding. This would support the theory that deep dentin has a lower bond strength than peripheral dentin.

There is an outward flow of fluid within the dentin tubules that tends to create a wet surface which may result in decreased bond strength as well (Kanca, 1992). This wetness increases with depth, probably as the result of increased tubule diameters as well as a closer distance from the pulp. It is likely that the larger tubules and/or microcanals in deciduous dentin might also result in a wetter substrate than permanent dentin, which would contribute to decreased bond strength.

Microcanals present a perplexing enigma to the field of dentin studies. Whether or not they are a feature more common in deciduous teeth, their existence may have several important implications. The first and most obvious is that their extremely large size would result in a tremendous decrease in the amount of solid dentin available for bonding as well as higher wetness, resulting in a lower bond strength to dentin with microcanals. Secondly, their large size may be the source of idiopathic tooth sensitivity as discussed earlier in the section regarding numerical tubule density and tubule diameter. Lastly, exposure of microcanals due to trauma may result in significant pulpal pathology as they would seem to serve as a "freeway" to the pulp for noxious stimuli.

7. CONCLUSIONS

The numerical tubule density of deciduous anterior teeth was found to increase in all teeth as the distance from the DEJ increased. The rate of change (slope) in numerical tubule density appears to be dependent on different locations within teeth. Deciduous teeth have higher numerical tubule densities than those reported in the literature for permanent teeth.

Tubule diameter increased in all teeth as distance from the DEJ increased. The rate of change did not differ with direction, but was different between tooth types. Deciduous teeth appear to have greater tubule diameters than those reported for permanent teeth.

Peritubular width was found to decrease in all teeth as distance from the DEJ increased. The rate of change did not differ between tooth types. The decreasing slope for peritubular width corresponded to the increasing slope for tubule diameter, suggesting an interdependent relationship between the two features.

Microcanals appear to be more than just a sporadically appearing feature in deciduous teeth. These features resemble markedly enlarged dentin tubules in structure and morphology, however their origin or purpose is not clearly understood. They may be more common in deciduous teeth and may have important implications in resin bonding, trauma, and sensitivity.

To summarize from a clinical standpoint, the practitioner who routinely restores deciduous teeth is faced with several factors that make them more difficult to effectively restore compared to permanent teeth. Pediatric patients often present as behavior management problems for whom the words "open your mouth please" and "hold still" seem to be foreign concepts. As a result, their oral cavity region may be sometimes considered a "moving target" which often makes it difficult to establish and maintain proper tooth

isolation prior to the restoration process. Deciduous teeth are also more difficult to handle than permanent teeth due to their relatively small size. Once adequate tooth preparation has been completed, the clinician is faced with a dentin substrate that has more and larger tubules compared to permanent dentin, along with the occasional presence of giant, space-occupying microcanals. The data and the literature has also demonstrated that peritubular dentin in deciduous teeth is at least as thick or thicker than that found in permanent teeth. These features in combination with resin bonding procedures utilizing acid etching, will result in much less solid dentin available for bonding in deciduous versus permanent dentin. The unique characteristics of the more and larger tubules and microcanals in deciduous dentin may also lead to a wetter substrate in which bonding must be accomplished compared to permanent dentin as well. These factors may be the basis for understanding the reasons behind the decreased bond strength to deciduous dentin compared to permanent dentin that has been reported.

The information gathered in this study helps to provide the basis for a better understanding of deciduous dentin microstructure and how it relates to permanent dentin. There appear to be some features and characteristics unique to deciduous dentin. However, much more research is needed in order to establish a thorough understanding of these features and differences that exist within and between the dentitions.

8. FUTURE STUDIES

Despite the vast amount of current research dedicated to the structure and characteristics of dentin, much more information is required before a thorough understanding of the dentin substrate can be attained. Future studies will have major implications regarding dentin bonding, sensitivity, remineralization and permeability. Studies concentrating on the microstructure of dentin must take into account the microstructural characteristics at specific distances from known anatomic landmarks (i.e. DEJ, pulp) and the rate at which they increase or decrease in size. It is clear that characteristics are somewhat site-specific, therefore it is imperative to have a good understanding of how the characteristics change in relation to different directions and specific intervals of depth. Better techniques to improve the accuracy of "starting at the DEJ" need to be explored. Using the DEJ as a starting landmark may be more relevant than using the pulp because of the fact that dentinogenesis initiates at the DEJ, therefore it would seem logical to attempt to follow the pathway of odontoblast migration.

Most of the available information on dentin deals with permanent tooth dentin, yet there is evidence that in fact deciduous and permanent dentin are not identical. While the current study was able to lay the basis for research on deciduous dentin, a much larger sample size is needed before definitive statements can be made. Future studies aimed at replicating the current experimental design should look to improve the ability to follow a group of tubules as they course from the DEJ to the pulp, try to account for the large variation within a single tooth (image more sites), increase the sample size (particularly to include central incisors as they are the most anterior tooth), compare deciduous anterior versus molar teeth, and improve image analysis techniques. Investigations should specifically attempt to provide data for all teeth so that a correlation between numerical tubule density/tubule diameter may be made in reference to how long it takes for each type of tooth to develop from initial to complete calcification.

It has been discussed that as the amount of available dentin decreases (peripheral versus inner dentin), bond strength can decrease up to between 30-50% (Suzuki and Finger, 1988; Causton, 1984). As stated earlier, the data obtained would seem to suggest that deciduous dentin has a greater number of tubules per mm^2 and larger tubule diameters than does permanent dentin. If this is true, that may help to explain the fact that bond strengths to deciduous dentin have been shown to be much less than that to permanent dentin. Lower bond strength to deciduous dentin has been the source of frustration to those practitioners who routinely restore deciduous teeth. In particular, as it is difficult to restore teeth in the very young and uncooperative patient in the first place, ideally a restoration would be placed once with confidence in sufficient bond strength to maintain the restoration. Unfortunately however, in those particular patients the restorations seem to have a relatively high failure rate. With that in mind, future studies should attempt to draw a definitive comparison/contrast regarding the site specific characteristics of deciduous and permanent dentin and the rate of changes in the characteristics in relation to distances from the DEJ. At the same time, bond strength tests versus tubule density and depth in deciduous teeth should be done as well. Definitively exploring differences between and among anterior and posterior teeth would also help to establish a better understanding, as there are some data that suggest differences between tooth types as well.

Recent improvements in dentin bonding systems have led to the implication that the resin/dentin bond might be stronger than the shear strength of dentin (Gwinnett, 1994). However, Watanabe, et.al. (1996), recently demonstrated that the shear strength of permanent dentin differed according to tubule direction and that it was much greater than the values reported for shear bond strength tests. Shear strength tests for deciduous dentin should be carried out in comparison to those for permanent dentin to assess the relationship between dentin shear strength and shear bond strength. Hardness tests on deciduous dentin such as those described by

Kinney, et.al. (1996) should also lead to a better understanding of the behavior of the dentin/resin interface.

The mechanism of peritubular dentin deposition has been presented via several theories. Prevailing among these, is that dentin tubules may start out at a certain size and changes in the diameter occur as peritubular dentin gets deposited within the lumen of the tubules. The data in this study seem to support this theory. Future studies should concentrate on establishing the direct relationship between tubule diameter and peritubular dentin width. The mechanisms governing peritubular dentin deposition should be explored. Such investigations should include young versus old teeth to assess possible differences in peritubular dentin deposition.

Few studies have concentrated on differences in mineral content between deciduous and permanent teeth. There is some evidence suggesting not only differences between the dentitions, but also differences between tooth types and within different depths of teeth. These differences may reflect differences in intertubular dentin composition. A more thorough understanding of mineral distribution and differences may allow for a better understanding of the origin of tubule diameter differences and the mechanism of peritubular dentin deposition.

Despite the use of the wet-SEM to view the dentin samples in their minimally altered, non-desiccated, fully mineralized state, the SEM in the wet-mode still necessitates that the delicate dentin sample be subjected to a vacuum (albeit a relatively low vacuum). Any stress placed on such biological samples may potentially distort the appearance of the samples. Recent work with the atomic force microscope (Marshall, 1993) may provide a way of performing dentin characterization studies without having to subject the dentin sample to any vacuum whatsoever and without the risk of possible desiccation. Future studies should continue to concentrate on observing both deciduous and permanent dentin in their least altered form (i.e. wet, fully mineralized, atmospheric pressure).

The existence of microcanals in deciduous as well as permanent teeth is a subject that has been barely explored. Because of their large size when present, microcanals should be considered a major component of the microstructure of dentin. The possibility of the existence of as many as 30 microcanals (Hals, 1983), running from the DEJ to the pulp as well as their large diameters indicate that they may have significant implications regarding permeability, bonding, sensitivity, and trauma. Current information has not been able to definitively explain their prevalence in either permanent or deciduous teeth. Very few theories exist regarding their origin or function. It is unclear whether they are in fact enlarged dentin tubules or the result of odontoblast crowding and subsequent necrosis. Studies should concentrate on the careful microstructural and chemical analysis of the microcanals to determine whether they are normal or abnormal dentin tubule structures. Future studies also should make attempts to determine the prevalence of microcanals, and whether there is a difference in those occurring in deciduous or permanent teeth.

9. REFERENCES

Agematsu H.
"Studies on the fine structure of microcanals in deciduous coronal dentin"
Shikwa Gakuho
1988 88:1375-1402.

Agematsu H; Watanabe H; Yamamoto H; Fukuyama M; Kanazawa T; Miake K.
"Scanning electron microscope observations of microcanals and continuous zones of interglobular dentin in human deciduous incisal dentin"
Bulletin of Tokyo Dental College
1990 May 31(2):163-73.

Allred H.
"The differential staining of peritubular and intertubular matrices in human dentine"
Archives of Oral Biology
1968 Jan 13(1):1-12.

Amory C; Yvon J.
"Shear bond strength of a light-cured resin composite vs. dentin characteristics"
Dental Materials
1994 May 10(3):203-9.

Andreasen JO; Andreasen FM.
Textbook and Color Atlas of Traumatic Injuries to the Teeth
1994 Mosby, St. Louis

Arends J; Ruben J; Jongebloed WL.
"Dentine caries in vivo. Combined scanning electron microscopic and microradiographic investigation"
Caries Research
1989 23(1):36-41.

Arends J; Stokroos I; Jongebloed WG; Ruben J.
"The diameter of dentinal tubules in human coronal dentine after demineralization and air drying. A combined light microscopy and SEM study"
Caries Research
1995 29(2):118-21.

Asmussen E; Ino S.
"Adhesion of restorative resins to dentin: Chemical and physiochemical aspects"
Oper Dent (Suppl)
1992 5:68-74.

Atkins CO Jr.; Rubenstein L; Avent M.
"Preliminary clinical evaluation of dentinal and enamel bonding in primary anterior teeth"
Journal of Pedodontics
1986 Spring 10(3):239-46.

Berkovitz BKB; Boyde A; Frank RM; Hohling HJ; Moxham BJ; Nalbandian J; Tonge CH.
Teeth
1989 Springer-Verlag, Berlin, Germany

Bordin-Aykroyd S; Sefton J; Davies EH.
"In vitro bond strengths of three current dentin adhesives to primary and permanent teeth"
Dental Materials
1992 Mar 8(2):74-8.

Bowen RL; Cobb EN; Rapson JE.
"Adhesive bonding of various materials to hard tooth tissues: improvement in bond strength to dentin"
J Dent Res
1982 a 61:1070-76.

Bowen RL; Cobb EN; Setz LE.
"Adhesive bonding to dentin and enamel"
Dentistry
1982 b 2:11-13.

Bradford EW.
"The interpretation of decalcified sections of human dentine"
Br Dent J
1955 98:153

Braham RL; Morris ME.
Textbook of Pediatric Dentistry
1985 Williams and Wilkins, Baltimore

Brannstrom M; Garberoglio R.
"The dentinal tubules and the odontoblast processes. A scanning electron microscope study"
Acta Odontologica Scandinavica
1972 Sep 30(3):291-311.

Carrigan PJ; Morse DR; Furst ML; Sinai IH.
"A scanning electron microscope evaluation of human dentinal tubules according to age and location"
Journal of Endodontics
1984 Aug 10(8):359-63.

Causton BE.
"Improved bonding of composite restorative to dentine"
Br Dent J
1984 156:93-95.

Donly KJ; Keprta M; Stratmann R.
"An in vitro comparison of acid etched vs. nonacid etched dentin bonding agents/composite interfaces over primary dentin"
Ped Dent
1991 13(4):204-7.

Driessens FCM; Verbeeck RMH.
Biominerals
1990 CRC Press, Boca Raton

Dyngeland T.
"Transmission of electron microscope study of giant tubules in bovine dentin"
Scandinavian Journal of Dental Research
1988 Aug 96(4):293-303.

Dyngeland T; Fosse G.
"Scanning electron microscopic, light microscopic and microradiographic study of giant tubules in bovine dentin"
Scandinavian Journal of Dental Research
1986 a Aug 94(4):285-98.

Dyngeland T; Fosse G.
"Light microscopic study of giant tubules in bovine dentin"
Scandinavian Journal of Dental Research
1986 b Oct 94(5):381-93.

Dyngeland T; Fosse G; and Justesen NPB.
"Histochemical study of giant tubule content in dentin of unerupted cow incisors"
Scand J Dent Res
1984 92:177-82.

Elkins CJ; McCourt JW.
"Bond strength of dentinal adhesives in primary teeth"
Quintessence International
1993 Apr 24(4):271-3.

Fagan TR; Crall JJ; Jensen ME; Chalkley Y; Clarkson B.
"A comparison of two dentin bonding agents in primary and permanent teeth"
Pediatric Dentistry
1986 Jun 8(3):144-6.

Foreman PC; Soames JV.
"Comparative study of the composition of primary and secondary dentin"
Caries Research
1989 23:1-4.

Fosse G; Saele PK; Eide R.
"Numerical density and distributional pattern of dentin tubules"
Acta Odontologica Scandanavica
1992 Aug 50(4):201-10.

Garberoglio R; Brannstrom M.
"Scanning electron microscope investigation of human dentinal tubules"
Archives of Oral Biology
1976 21(6):355-62.

Gwinnett AJ.
"A new method to test the cohesive strength of dentin"
Quintessence Int
1994 25:215-218.

Gwinnett AJ, Kanca J.
"Micromorphological relationship between resin and dentin in vivo and in vitro"
Am J Dent
1992 5:29-32.

Hals E.
"Observations on giant tubules in human coronal dentin by light microscopy and microradiography"
Scandinavian Journal of Dental Research
1983 Feb 91(1):1-7.

Hals E.
"Microradiographic and polarized light study of red deer root dentin with special reference to occurrence of giant tubules"
Scandinavian Journal of Dental Research
1984 Jun 92(3):183-9.

Hals E; Dyngeland T.
"Column-like structures following the course of dentinal tubules in bovine, red deer, and rat teeth"
Scandinavian Journal of Dental Research
1988 Dec 96(6):489-99.

Heyman HO; Bayne SC.
"Current concepts in dentin bonding: focusing on dentinal adhesion factors"
JADA
1993 124:27-36.

Hirayama A.
"Experimental Analytical electron microscopic studies on the quantitative analysis of elemental concentrations in biological thin specimens and its application to dental science"
Shikwa Gakuho
1990 90:1019-1036.

Hirayama A; Yamada M; Miake K.
"An electron microscope study on dentinal tubules of human deciduous teeth"
Shikwa Gakuho
1986 88:1021-1031.

Hojo T.
"Scanning electron microscope quantitative study of changes with age in closing pattern of openings of dentinal tubules on worn occlusal surfaces of Japanese permanent mandibular incisors"
Scanning Microscopy
1990 Dec 4(4):1049-53.

Kanca III, J.
"Improving bond strength through acid etching of dentin and bonding to wet dentin surfaces"
JADA
1992 Sep 123:35-43.

Ketterl W.
"Studie uber das Dentin der permanenten Zahne des Menschen"
Stoma
1961 14:79-112.

Kinney JH; Balooch M; Haupt DL Jr.; Marshall SJ; Marshall GW .
"Mineral distribution and dimensional changes in human dentin during demineralization"
Journal of Dental Research
1995 May 74(5):1179-84.

Kinney J; Balooch M; Marshall GW; Marshall SJ.
"Atomic-force microscope study of dimensional changes in human dentine during drying"
Archs Oral Biol
1993 38(11):1003-1007.

Kinney JH; Balooch M; Marshall SJ; Marshall GW; Weihs TP.
"Hardness and Young's modulus of human peritubular and intertubular dentine"
Archs Oral Biol
1996 vol. 41(1):9-13.

Kodaka T; Mori R; Miyakawa M.
"Sequential Observations followed by acid etching on the enamel surfaces of human teeth under scanning electron microscopy at low vaccum"
Microscopy Research and Technique
1993 24:429-436.

Kodaka T; Toko T; Debari K; Hisamitsu H; Ohmori A; Kawata S.
"Application of the environmental SEM in human dentin bleached with hydrogen peroxide in vitro"
Journal of Electron Microscopy
1992 Oct 41(5):381-6.

Koutsi V; Noonan RG; Horner JA; Simpson MD; Matthews WG: Pashley DH.
"The effect of dentin depth on the permeability and ultra structure of primary molars"
Pediatric Dentistry
1994 Jan-Feb 16(1):29-35.

Kubota K; Ajisaka M; Inoue Y; Yamaguchi S; Hasegawa I.
"Scanning electron microscopic observation of longitudinally sectioned dentinal tubules"
J of Nihon University School of Dentistry
1969 Dec 11(4):140-3.

Kubota K; Sekikawa M; Shimamura M; Nakajima T.
"A scanning electron microscope consideration of the structure of peritubular dentin"
Journal of Nihon University School of Dentistry
1978 Dec 20(1-4):1-5.

Marshall GW Jr.
Introduction to SEM and X-ray Microanalysis
1989

Marshall GW Jr.
"Dentin microstructure and characterization"
Quintessence International
1993 Sep 24(9):606-17.

Marshall GW Jr.; Balooch M; Tench RJ; Kinney JH; Marshall SJ.
"Atomic force microscopy of acid effects on dentin"
Dental Materials
1993 Jul 9(4):265-8.

Mazzeo N; Ott NW; Hondrum SO.
"Resin bonding to primary teeth using three adhesive systems"
Pediatric Dentistry
1995 Mar-Apr 17(2):112-5.

McDonald RE; Avery DR.
Dentistry for the Child and Adolescent
1988 Mosby, St. Louis.

Mendis BRRM; Darling AI.
"Distribution with age and attrition of peritubular dentine in the crowns of human teeth"
Archs Oral Biol
1979 vol. 24:131-139.

Meyer W.
Lehrbuch der normalen Histologie und Entwicklungsgechichte der Zahne des Menschen
1951 Verlag Carl Hanser, Munchen

Miller J.
"Large tubules in dentine"
J of Dent Children
1981 July-Aug. 269-271.

Mjor IA; Fejerskov O.
Histology of the Human Tooth
1979 Munksgaard, Copenhagen

Moss-Salentijn L; Hendricks-Klyvert M.
Dental and Oral Tissues: An Introduction, 2nd edition
1985 Lea & Febiger, Philadelphia

Nakabayashi N, Ashizawa M, Nakamura M.
"Identification of a resin-dentin hybrid layer in vital human dentin created in vivo: durable bonding to vital dentin"
Quintessence Int
1992 23:135-41.

Olsson S; Olio G; Adamczack E.
"The structure of dentin surfaces exposed for bond strength measurements"
Scand J Dent Res
1993 101:180-4.

Panighi M; G'Sell C.
"Effect of the tooth microstructure on the shear bond strength of a dental composite"
Journal of Biomedical Materials Research
1993 Aug 27(8):975-81.

Pashley DH.
"Smear Layer: Physiological Considerations"
Operative Dentistry
1984 Suppl 3: 13-29.

Pashley DH.
"Dentin: a dynamic substrate- A review"
Scan Micros
1989 3:161-176.

Pashley DH.
"Clinical considerations of microleakage"
J of Endodontics
1990 16(2):70-77.

Pashley DH.
"Clinical correlations of dentin structure and function"
Journal of Prosthetic Dentistry
1991 Dec 66(6):777-81.

Pashley DH; Andringa HJ; Derkson GD; Derkson ME; Kalathoor SR.
"Regional variability in the permeability of human dentine"
Arch Oral Biology
1987 32:519-523.

Pashley DH; Michelich V; Kehl T.
"Dentin permeability: effects of smear layer removal"
Journal of Prosthetic Dentistry
1981 Nov 46(5):531-7.

Pashley D; Okabe A; Parham P.
"The relationship between dentin microhardness and tubule density"
Endod Dent Traumatol
1985 1:176-179.

Reinhardt JW; Chan DCN; Boyer DB.
"Shear strengths of ten commercial dentin bonding agents"
Dent Mater
1987 3:43-45.

Retief DH; Rozalia SM; Russell CM; Denys FR.
"Phosphoric acid as a dentin etchant"
Am J Dent
1992 5:24-28.

Russ JC.
Computer-Assisted Microscopy: The Measurement and Analysis of Images
1990 Plenum Press, New York

Salama FS; Tao L.
"Comparison of Gluma bond strength to primary vs. permanent teeth"
Pediatric Dentistry
1991 May-Jun 13(3):163-6.

Schellenberg U; Krey G; Bosshardt D; Ramachandran Nair PN.
"Numerical density of dentinal tubules at the pulpal wall of human permanent premolars and third molars"
Journal of Endodontics
1992 18(3):104-109.

Shellis RP.
"Dental tissues"
Dental anatomy and embryology, Osborn JW editor
Oxford: Blackwell Scientific Publications
1981 p. 155-210.

Suzuki T; Finger WJ.
"Dentin adhesives: site of dentin vs. bonding of composite resins"
Dental Materials
1988 4:379-383.

Ten Cate AR.
Oral Histology. Development, Structure, and Function.
1994 Mosby-Year Book Inc., St. Louis.

Tidmarsh BG; Arrowsmith MG.
"Dentinal tubules at the root ends of apicected teeth: a scanning electron microscope study"
International Endodontic Journal
1989 Jul 22(4):184-9.

Toda Y; Kageyama M; Nagai S; Miyazaki S; Takagi H; Sugisawa H; Takehana S.
"Scanning electron microscope observations of dentinal tubules in interglobular dentin"
Journal of Nihon University School of Dentistry
1981 Jun 23(2):71-8.

Tronstad L.
"Ultrastructural observation on human coronal dentin"
Scand Dent J
1973 81:101-111.

Van der Graaf ER; Ten Bosch JJ.
"Changes in dimensions and weight of human dentine after different drying procedures and during subsequent rehydration."
Archs Oral Biol
1993 38:97-99.

Walls AW; McCabe JF; Murray JJ.
"Factors influencing the bond strength between glass polyalkenoate (ionomer) cements and dentine"
Journal of Oral Rehabilitation
1988 Nov 15(6):537-47.

Watanabe LG; Marshall GW; Marshall SJ.
"Dentin shear strength: Effects of tubule orientation and intratooth location"
Dental Materials
1996 March 12:109-115.

White JM; Goodis HE; Marshall SJ; Marshall GW.
"Sterilization of teeth by gamma radiation"
J Dent Res
1994 Sep 73(9):1560-7.

Wright JT; and Gantt DG.
"The ultrastructure of the dental tissues in dentinogenesis imperfecta in man"
Arch Oral Biol 1985 30:201-206.

APPENDIX A

Spreadsheets containing raw data for sample teeth.

D2-tubule density

Sites	holes per mm 2	Sites	holes per mm 2	Sites	holes per mm 2				
D2D1A		D2D2A	27353.80	D2D3A	40650.79		Average	Average	Average
D2D1C		D2D2B	34572.17	D2D3C	55087.52		D2D-level 1	D2D-level 2	D2D-level 3
D2D1B	12917.07	D2D2C	44070.02	D2D3B	50528.56		26159.79	37400.42	39764.33
D2D1D	27353.80	D2D2D	36091.83	D2D3D	61546.06				
D2D1F	31912.77	D2D2E	41030.71	D2D3F	44829.85				
D2D1E	29253.37	D2D2F	31152.94	D2D3E	44829.85				
D2D1G	18235.87	D2D2G	34572.17	D2D3G	17855.96				
D2D1I	30773.03	D2D2H	42550.36	D2D3I	24314.49				
D2D1H	32672.60	D2D2I	45209.76	D2D3H	18235.87				
D2B1A	52808.04	D2B2A	54327.69	D2B3A	53567.87		Average	Average	Average
D2B1C	26593.98	D2B2B	43690.10	D2B3C	45209.76		D2D-level 1	D2B-level 2	D2B-level 3
D2B1B	47869.16	D2B2C	28493.55	D2B3B	52808.04		44281.08	39468.84	45842.95
D2B1D	41410.62	D2B2D	48249.07	D2B3D	54327.69				
D2B1F	52808.04	D2B2E	60026.40	D2B3F	57367.01				
D2B1E	44449.93	D2B2F	58886.66	D2B3E	43310.19				
D2B1G	42930.28	D2B2G	19755.53	D2B3G	22794.84				
D2B1I	45589.67	D2B2H	18235.87	D2B3I	46349.50				
D2B1H	44070.02	D2B2I	23554.66	D2B3H	36851.65				

D2-tubule diam.

Sites	Hole Diameter	Sites	Hole Diameter	Sites	Hole Diameter		Average D2-level 1	Average D2-level 2	Average D2-level 3
							1.04	1.43	1.60
D2D1A		D2D2A	1.41	D2D3A	1.45				
D2D1C		D2D2B	1.43	D2D3B	1.46				
D2D1B	0.69	D2D2C	1.38	D2D3C	1.51				
D2D1E	0.84	D2D2D	1.48	D2D3D	1.58		Average	Average	Average
D2D1F	0.93	D2D2E	1.37	D2D3E	1.36		D2D-level 1	D2D-level 2	D2D-level 3
D2D1D	0.66	D2D2F	1.34	D2D3F	1.35		0.88	1.34	1.46
D2D1I	1.29	D2D2G	1.19	D2D3G	1.56				
D2D1G	0.92	D2D2H	1.20	D2D3H	1.42				
D2D1H	0.83	D2D2I	1.27	D2D3I	1.47				
D2B1A	1.26	D2B2A	1.53	D2B3A	1.67		Average	Average	Average
D2B1C	1.09	D2B2B	1.47	D2B3C	1.59		D2B-level 1	D2B-level 2	D2B-level 3
D2B1B	1.12	D2B2C	1.73	D2B3B	1.68		1.17	1.53	1.74
D2B1D	1.50	D2B2D	1.58	D2B3D	1.91				
D2B1E	1.07	D2B2F	1.74	D2B3E	2.36				
D2B1F	1.28	D2B2E	1.58	D2B3F	1.83				
D2B1G	0.99	D2B2G	1.27	D2B3G	1.53				
D2B1I	1.01	D2B2H	1.22	D2B3I	1.50				
D2B1H	1.16	D2B2I	1.63	D2B3H	1.58				

D2-PT width

Sites	PT width microns	Sites	PT width microns	Sites	PT width microns		Average D2-level 1	Average D2-level 2	Average D2-level 3
							0.69	0.51	0.48
D2D1A		D2D2A	0.44	D2D3B	0.39				
D2D1C		D2D2B	0.42	D2D3A	0.45				
D2D1B	0.68	D2D2C	0.41	D2D3C	0.40				
D2D1D	0.78	D2D2D	0.52	D2D3E	0.40		Average	Average	Average
D2D1F	0.81	D2D2E	0.46	D2D3D	0.46		D2D-level 1	D2D-level 2	D2D-level 3
D2D1E	0.88	D2D2F	0.66	D2D3F	0.57		0.79	0.47	0.48
D2D1G	0.56	D2D2G	0.45	D2D3H	0.44				
D2D1I	0.81	D2D2H	0.47	D2D3G	0.62				
D2D1H	1.03	D2D2I	0.41	D2D3I	0.57				
D2B1A	0.39	D2B2A	0.42	D2B3B	0.43		Average	Average	Average
D2B1C	0.72	D2B2B	0.47	D2B3A	0.49		D2B-level 1	D2B-level 2	D2B-level 3
D2B1B	0.67	D2B2C	0.62	D2B3C	0.43		0.60	0.54	0.49
D2B1D	0.54	D2B2D	0.55	D2B3E	0.56				
D2B1F	0.45	D2B2E	0.52	D2B3D	0.55				
D2B1E	0.65	D2B2F	0.49	D2B3F	0.51				
D2B1G	0.64	D2B2G	0.66	D2B3H	0.49				
D2B1I	0.73	D2B2H	0.57	D2B3G	0.48				
D2B1H	0.64	D2B2I	0.58	D2B3I	0.48				

D2-IT area

Sites	IT-area micron 2	Sites	IT-area micron 2	Sites	IT-area micron 2		Average area µ2 D2 (IT)-level 1	Average area µ2 D2 (IT)-level 2	Average area µ2 D2 (IT)-level 3
							2188.63	2152.96	2061.55
D2D1A		D2D2A	2333.64	D2D3A	2167.25				
D2D1C		D2D2B	2260.89	D2D3C	2020.41				
D2D1B	2517.56	D2D2C	2191.69	D2D3B	2108.37				
D2D1D	2361.67	D2D2D	2154.57	D2D3D	1830.22				
D2D1F	2202.22	D2D2E	2189.25	D2D3F	2064.57				
D2D1E	2215.95	D2D2F	2176.57	D2D3E	2192.29				
D2D1G	2477.18	D2D2G	2320.86	D2D3G	2344.27				
D2D1I	2091.11	D2D2H	2232.50	D2D3I	2286.81				
D2D1H	2069.14	D2D2I	2223.62	D2D3H	2431.87				
D2B1A	2177.40	D2B2A	1999.04	D2B3A	1858.73				
D2B1C	2278.11	D2B2B	2103.28	D2B3C	2068.06				
D2B1B	2035.62	D2B2C	2114.75	D2B3B	1928.57				
D2B1D	2059.41	D2B2D	1913.99	D2B3D					
D2B1F	2109.61	D2B2E	1777.40	D2B3F	1676.13				
D2B1E	2115.57	D2B2F	1727.76	D2B3E	1543.61				
D2B1G	2172.93	D2B2G	2360.32	D2B3G	2341.72				
D2B1I	2043.10	D2B2H	2420.65	D2B3I	2048.32				
D2B1H	2091.45	D2B2I	2252.45	D2B3H	2135.05				

D4-tubule density

Sites	holes per mm 2	Sites	holes per mm 2	Sites	holes per mm 2				
D4D1A	42550.36	D4D2A	27733.72	D4D3A	41410.62		Average	Average	Average
D4D1C	53187.95	D4D2B	37231.57	D4D3C	49008.90		D4D-level 1	D4D-level 2	D4D-level 3
D4D1B	46729.42	D4D2C	36851.65	D4D3B	56987.09		50908.47	31701.71	58042.41
D4D1D	57367.01	D4D2D	41790.53	D4D3D	54327.69				
D4D1F	66864.86	D4D2E	39890.96	D4D3F	63825.54				
D4D1E	66484.94	D4D2F	37611.48	D4D3E	67624.68				
D4D1G	56987.09	D4D2G	17476.04	D4D3G	75602.88				
D4D1I	36471.74	D4D2H	21655.10	D4D3I	50148.64				
D4D1H	31532.86	D4D2I	25074.32	D4D3H	63445.63				
D4B1A	55087.52	D4B2A	37611.48	D4B3A	54707.61		Average	Average	Average
D4B1C	49388.81	D4B2B	32672.60	D4B3C	43310.19		D4B-level 1	D4B-level 2	D4B-level 3
D4B1B	50908.47	D4B2C	25454.23	D4B3B	50908.47		46687.20	35205.36	49515.45
D4B1D	53947.78	D4B2D	47109.33	D4B3D	56607.18				
D4B1F	54327.69	D4B2E	42550.36	D4B3F	63065.72				
D4B1E	55847.35	D4B2F	38751.22	D4B3E	53567.87				
D4B1G	41790.53	D4B2G	20135.44	D4B3G	48628.99				
D4B1I	21655.10	D4B2H	28493.55	D4B3I	27733.72				
D4B1H	37231.57	D4B2I	44070.02	D4B3H	47109.33				

D4-tubule diam.

Sites	Hole Diameter	Sites	Hole Diameter	Sites	Hole Diameter		Average D4-level 1	Average D4-level 2	Average D4-level 3
							1.72	1.58	1.97
D4D1A	1.42	D4D2A	1.60	D4D3A	1.65				
D4D1C	1.95	D4D2B	1.57	D4D3C	2.50				
D4D1B	1.62	D4D2C	1.52	D4D3B	1.86				
D4D1E	1.77	D4D2D	1.44	D4D3D	2.52		Average	Average	Average
D4D1F	1.67	D4D2F	1.57	D4D3E	2.18		D4D-level 1	D4D-level 2	D4D-level 3
D4D1D	1.94	D4D2E	1.65	D4D3F	1.71		1.70	1.50	2.10
D4D1I	1.72	D4D2G	1.25	D4D3H	2.17				
D4D1G	1.53	D4D2I	1.53	D4D3G	1.74				
D4D1H	1.62	D4D2H	1.33	D4D3I	2.56				
D4B1B	1.65	D4B2A	1.78	D4B3A	1.78		Average	Average	Average
D4B1C	1.66	D4B2C	1.51	D4B3B	1.76		D4B-level 1	D4B-level 2	D4B-level 3
D4B1A	1.66	D4B2B	1.70	D4B3C	1.82		1.75	1.67	1.84
D4B1E	1.84	D4B2D	1.67	D4B3D	1.93				
D4B1F	1.73	D4B2F	1.77	D4B3E	1.97				
D4B1D	1.83	D4B2E	1.93	D4B3F	2.08				
D4B1H	1.55	D4B2G	1.41	D4B3G	1.77				
D4B1I	2.19	D4B2I	1.69	D4B3H	1.73				
D4B1G	1.65	D4B2H	1.53	D4B3I	1.68				

D4-PT width

Sites	PT width microns	Sites	PT width microns	Sites	PT width microns		Average D4-level 1	Average D4-level 2	Average D4-level 3
							0.45	0.60	0.46
D4D1A	0.47	D4D2A	0.69	D4D3B	0.46				
D4D1C	0.35	D4D2B	0.69	D4D3A	0.44				
D4D1B	0.50	D4D2C	0.69	D4D3C	0.60				
D4D1D	0.52	D4D2D	0.59	D4D3E	0.55		Average	Average	Average
D4D1F	0.45	D4D2E	0.54	D4D3D	0.40		D4D-level 1	D4D-level 2	D4D-level 3
D4D1E	0.39	D4D2F	0.44	D4D3F	0.55		0.45	0.58	0.51
D4D1G	0.47	D4D2G	0.47	D4D3H	0.56				
D4D1I	0.51	D4D2H	0.50	D4D3G	0.53				
D4D1H	0.40	D4D2I	0.64	D4D3I	0.46				
D4B1A	0.54	D4B2A	0.59	D4B3B	0.51		Average	Average	Average
D4B1C	0.35	D4B2B	0.65	D4B3A	0.40		D4B-level 1	D4B-level2	D4B-level 3
D4B1B	0.51	D4B2C	0.84	D4B3C	0.47		0.46	0.61	0.42
D4B1D	0.39	D4B2D	0.44	D4B3E	0.29				
D4B1F	0.48	D4B2E	0.64	D4B3D	0.40				
D4B1E	0.41	D4B2F	0.51	D4B3F	0.31				
D4B1G	0.49	D4B2G	0.81	D4B3H	0.43				
D4B1I	0.44	D4B2H	0.59	D4B3G	0.38				
D4B1H	0.49	D4B2I	0.43	D4B3I	0.59				

D4-IT area

Sites	IT-area micron 2	Sites	IT-area micron 2	Sites	IT-area micron 2		Average area µ2 D4 (IT)-level 1	Average area µ2 D4 (IT)-level 2	Average area µ2 D4 (IT)-level 3
D4D1A	2143.11	D4D2A	2126.90	D4D3A	2081.57		1936.15	2093.02	1662.92
D4D1C	1853.36	D4D2B	1961.99	D4D3C	1240.25				
D4D1B	1974.92	D4D2C	1993.99	D4D3B	1718.85				
D4D1D	1577.99	D4D2D	2034.94	D4D3D	1058.91				
D4D1F	1714.12	D4D2E	2020.36	D4D3F	1591.51				
D4D1E	1736.13	D4D2F	2165.53	D4D3E	1135.85				
D4D1G	1915.67	D4D2G	2458.23	D4D3G	1401.35				
D4D1I	2067.20	D4D2H	2390.84	D4D3I	1369.50				
D4D1H	2248.07	D4D2I	2222.63	D4D3H	1208.74				
D4B1A	1778.32	D4B2A	1953.56	D4B3A	1879.54				
D4B1C	2059.81	D4B2B	2026.31	D4B3C	1949.79				
D4B1B	1886.59	D4B2C	2097.04	D4B3B	1816.88				
D4B1D	1871.82	D4B2D	1997.19	D4B3D	1763.45				
D4B1F	1820.88	D4B2E	1725.09	D4B3F	1679.80				
D4B1E	1819.16	D4B2F	2011.89	D4B3E	1907.54				
D4B1G	2036.57	D4B2G	2251.73	D4B3G	1987.89				
D4B1I	2209.33	D4B2H	2198.87	D4B3I	2163.71				
D4B1H	2137.74	D4B2I	2037.30	D4B3H	1977.35				

D5-tubule density

Sites	holes per mm 2	Sites	holes per mm 2	Sites	holes per mm 2				
D5D1A	29633.29	D5D2A	32672.60	D5D3A	45589.67		Average	Average	Average
D5D1C	47489.24	D5D2B	34192.26	D5D3C	50148.64		D5D-level 1	D5D-level 2	D5D-level 3
D5D1B	31912.77	D5D2C	38371.31	D5D3B	53567.87		32545.96	43690.10	46444.48
D5D1D	46729.42	D5D2D	52428.13	D5D3D					
D5D1F	31912.77	D5D2E	50528.56	D5D3F	44070.02				
D5D1E	42170.45	D5D2F	44829.85	D5D3E	44449.93				
D5D1G	14436.73	D5D2G	43690.10	D5D3G	40270.88				
D5D1I	22414.92	D5D2H	49008.90	D5D3I	43690.10				
D5D1H	26214.06	D5D2I	47489.24	D5D3H	49768.73				
D5B1A	32292.69	D5B2A	47109.33	D5B3A	48628.99		Average	Average	Average
D5B1C	55847.35	D5B2B		D5B3C	40650.79		D5B-level 1	D5B-level 2	D5B-level 3
D5B1B	54707.61	D5B2C	41030.71	D5B3B	41410.62		46054.01	45779.63	39447.73
D5B1D	49008.90	D5B2D		D5B3D					
D5B1F	29253.37	D5B2E		D5B3F	41790.53				
D5B1E	52428.13	D5B2F	45589.67	D5B3E					
D5B1G	33812.34	D5B2G	49388.81	D5B3G	17855.96				
D5B1I	53187.95	D5B2H		D5B3I	46349.50				
D5B1H	53947.78	D5B2I		D5B3H					

D5-tubule diam.

Sites	Hole Diameter	Sites	Hole Diameter	Sites	Hole Diameter		Average D5-level 1	Average D5-level 2	Average D5-level 3
							1.61	1.98	2.07
D5D1A	1.49	D5D2A	1.58	D5D3B	1.75				
D5D1C	1.66	D5D2B	1.74	D5D3A	1.70				
D5D1B	1.45	D5D2C	1.77	D5D3C	1.96				
D5D1D	1.67	D5D2D	2.21	D5D3D			Average	Average	Average
D5D1F	1.40	D5D2E	1.95	D5D3F	1.68		D5D-level 1	D5D-level 2	D5D-level 3
D5D1E	1.46	D5D2F	1.78	D5D3E	2.38		1.45	1.93	1.97
D5D1G	1.17	D5D2G	1.83	D5D3H	1.90				
D5D1I	1.36	D5D2H	2.00	D5D3I	2.44				
D5D1H	1.37	D5D2I	2.49	D5D3G	1.93				
D5B1A	1.37	D5B2A	1.71	D5B3A	1.92		Average	Average	Average
D5B1C	2.21	D5B2B		D5B3C	2.47	*	D5B-level 1	D5B-level 2	D5B-level 3
D5B1B	1.65	D5B2C	2.59	D5B3B	2.50		1.77	2.09	2.19
D5B1D	2.06	D5B2D		D5B3E					
D5B1E	1.79	D5B2F	2.05	D5B3F	2.53				
D5B1F	1.43	D5B2E		D5B3D					
D5B1G	1.40	D5B2G	2.02	D5B3G	2.81				
D5B1H	2.02	D5B2I		D2B3H	1.58				
D5B1I	1.98	D5B2H		D2B3I	1.50				

D5-PT width

Sites	PT width microns	Sites	PT width microns	Sites	PT width microns		Average D5-level 1	Average D5-level 2	Average D5-level 3
							0.54	0.56	0.58
D5D1A	0.56	D5D2A	0.59	D5D3B	0.52				
D5D1C	0.61	D5D2B	0.44	D5D3A	0.50				
D5D1B	0.48	D5D2C	0.51	D5D3C	0.45				
D5D1D	0.54	D5D2D	0.48	D5D3E	0.62		Average	Average	Average
D5D1F	0.62	D5D2E	0.64	D5D3D			D5D-level 1	D5D-level 2	D5D-level 3
D5D1E	0.44	D5D2F	0.56	D5D3F	0.67		0.57	0.54	0.53
D5D1G	0.47	D5D2G	0.62	D5D3H	0.49				
D5D1I	0.68	D5D2H	0.61	D5D3G	0.44				
D5D1H	0.72	D5D2I	0.45	D5D3I	0.55				
D5B1A	0.69	D5B2A	0.53	D5B3B	0.70		Average	Average	Average
D5B1C	0.34	D5B2B		D5B3A	0.52		D5B-level 1	D5B-level 2	D5B-level 3
D5B1B	0.44	D5B2C	0.68	D5B3C	0.61		0.50	0.59	0.66
D5B1D	0.39	D5B2D		D5B3E					
D5B1F	0.67	D5B2E		D5B3D					
D5B1E	0.45	D5B2F	0.49	D5B3F	0.48				
D5B1G	0.64	D5B2G	0.67	D5B3H					
D5B1I	0.45	D5B2H		D5B3G	1.00				
D5B1H	0.45	D5B2I		D5B3I					

D5-IT area

Sites	IT-area micron 2	Sites	IT-area micron 2	Sites	IT-area micron 2		Average area µ2 D5 (IT)-level 1	Average area µ2 D5 (IT)-level 2	Average area µ2 D5 (IT)-level 3
							2031.36	1732.96	1684.86
D5D1A	2218.94	D5D2A	2116.06	D5D3A	1941.44				
D5D1C	1814.60	D5D2B	2147.61	D5D3C	1780.81				
D5D1B	2244.78	D5D2C	2012.49	D5D3B	1774.82				
D5D1D	1902.52	D5D2D	1544.20	D5D3D					
D5D1F	2176.25	D5D2E	1547.12	D5D3F	1803.38				
D5D1E	2157.14	D5D2F	1853.09	D5D3E	1425.50				
D5D1G	2497.71	D5D2G	1779.49	D5D3G	1972.74				
D5D1I	2288.30	D5D2H	1580.19	D5D3I	1503.21				
D5D1H	2203.39	D5D2I	1515.04	D5D3H	1787.14				
D5B1A	2127.20	D5B2A	1886.73	D5B3A	1744.86				
D5B1C	1663.59	D5B2B		D5B3C	1491.45				
D5B1B	1913.83	D5B2C	1308.19	D5B3B	1326.38				
D5B1D	1814.61	D5B2D		D5B3D					
D5B1F	2167.59	D5B2E		D5B3F	1572.91				
D5B1E	1852.26	D5B2F	1766.81	D5B3E					
D5B1G	2126.93	D5B2G	1471.53	D5B3G	1778.60				
D5B1I	1715.73	D5B2H		D5B3I					
D5B1H	1679.06	D5B2I		D5B3H					

E1-tubule density

Sites	holes per mm 2	Sites	holes per mm 2	Sites	holes per mm 2				
E1D1A	28113.63	E1D2A	32292.69	E1D3A	42170.45		Average	Average	Average
E1D1C	38371.31	E1D2B	38371.31	E1D3C	46729.42		E1D-level 1	E1D-level 2	E1D-level 3
E1D1B	34192.26	E1D2C	41790.53	E1D3B	45969.59		30730.82	34952.08	44745.42
E1D1D	44070.02	E1D2D	47489.24	E1D3D	44449.93				
E1D1F	36091.83	E1D2E	46349.50	E1D3F	56607.18				
E1D1E	25074.32	E1D2F	42170.45	E1D3E	50908.47				
E1D1G	23174.75	E1D2G	19755.53	E1D3G	40650.79				
E1D1I	22035.01	E1D2H	22414.92	E1D3I	39511.05				
E1D1H	25454.23	E1D2I	23934.58	E1D3H	35711.91				
E1B1A	49008.90	E1B2A	48249.07	E1B3A	34952.08		Average	Average	Average
E1B1C	48249.07	E1B2B	44070.02	E1B3C	27353.80		E1B-level 1	E1B-level 2	E1B-level 3
E1B1B	46349.50	E1B2C	44829.85	E1B3B	28873.46		37928.08	41579.47	35458.64
E1B1D	34572.17	E1B2D	41790.53	E1B3D	36471.74				
E1B1F	23554.66	E1B2E	39131.14	E1B3F	42170.45				
E1B1E	25834.15	E1B2F	50908.47	E1B3E	34192.26				
E1B1G		E1B2G	31532.86	E1B3G	37231.57				
E1B1I		E1B2H	35332.00	E1B3I	37611.48				
E1B1H		E1B2I	38371.31	E1B3H	40270.88				

E1-tubule diam.

Sites	Hole Diameter	Sites	Hole Diameter	Sites	Hole Diameter		Average E1-level 1	Average E1-level 2	Average E1-level 3
							1.72	1.75	1.93
E1D1A	1.75	E1D2A	1.80	E1D3A	1.71				
E1D1B	1.98	E1D2B	1.76	E1D3B	1.79				
E1D1C	1.85	E1D2C	1.58	E1D3C	2.08				
E1D1D	1.37	E1D2D	1.67	E1D3D	1.81		Average	Average	Average
E1D1E	1.65	E1D2E	1.43	E1D3E	1.75		E1D-level 1	E1D-level 2	E1D-level 3
E1D1F	1.72	E1D2F	1.57	E1D3F	1.76		1.54	1.56	1.78
E1D1G	1.25	E1D2G	1.37	E1D3G	1.69				
E1D1H	1.14	E1D2H	1.38	E1D3H	1.68				
E1D1I	1.18	E1D2I	1.49	E1D3I	1.74				
E1B1A	1.71	E1B1B	1.73	E1B3C	2.79		Average	Average	Average
E1B2A	2.41	E1B2B	2.48	E1B1C	1.93		E1B-level 1	E1B-level 2	E1B-level 3
E1B3A	2.42	E1B3B	2.67	E1B2C	2.37		1.98	1.94	2.09
E1B1D	1.59	E1B2D	1.69	E1B3F	2.02				
E1B1E	1.85	E1B2E	1.91	E1B3D	1.96				
E1B1F	1.90	E1B2F	1.83	E1B3E	1.98				
E1B1G		E1B2G	1.72	E1B3G	1.82				
E1B1H		E1B2H	1.74	E1B3H	1.91				
E1B1I		E1B2I	1.69	E1B3I	2.04				

E1-PT width

Sites	PT width microns	Sites	PT width microns	Sites	PT width microns		Average E1-level 1	Average E1-level 2	Average E1-level 3
							0.44	0.43	0.43
E1D1A	0.39	E1D2A	0.46	E1D3B	0.41				
E1D1C	0.47298	E1D2B	0.63	E1D3A	0.42				
E1D1B	0.34	E1D2C	0.539198	E1D3C	0.50643				
E1D1D	0.37	E1D2D	0.47	E1D3E	0.37		Average	Average	Average
E1D1F	0.45191	E1D2E	0.40	E1D3D	0.43		E1D-level 1	E1D-level 2	E1D-level 3
E1D1E		E1D2F	0.352097	E1D3F	0.36414		0.44	0.48	0.41
E1D1G	0.50	E1D2G	0.44	E1D3G	0.41				
E1D1I	0.47672	E1D2H	0.57	E1D3I	0.44297				
E1D1H	0.49	E1D2I	0.502797	E1D3H	0.29				
E1B1A	0.32	E1B2A	0.59	E1B3B	0.51		Average	Average	Average
E1B1C	0.39289	E1B2B	0.54	E1B3A	0.51		E1B-level 1	E1B-level 2	E1B-level3
E1B1B	0.57	E1B2C	0.40254	E1B3C	0.55017		0.45	0.37	0.45
E1B1D	0.40	E1B2D	0.33	E1B3E	0.39				
E1B1F	0.5638	E1B2E	0.31	E1B3D	0.52				
E1B1E	0.47	E1B2F	0.303119	E1B3F	0.35881				
E1B1G		E1B2G	0.29	E1B3H	0.32				
E1B1I		E1B2H	0.28	E1B3G	0.38				
E1B1H		E1B2I	0.263332	E1B3I	0.46252				

E1-IT area

Sites	IT-area micron 2	Sites	IT-area micron 2	Sites	IT-area micron 2		Average area µ2 E1 (IT)-level 1	Average area µ2 E1 (IT)-level 2	Average area µ2 E1 (IT)-level 3
E1D1A	2256.22	E1D2A	2142.85	E1D3A	2065.78		2171.84	2057.98	1978.05
E1D1C	2010.91	E1D2B	1913.34	E1D3C	1709.00				
E1D1B	2132.95	E1D2C	2019.16	E1D3B	1988.91				
E1D1D	2225.30	E1D2D	1968.68	E1D3D	1973.93				
E1D1F	2120.60	E1D2E	2150.11	E1D3F	1911.33				
E1D1E		E1D2F	2182.95	E1D3E	1977.74				
E1D1G	2389.05	E1D2G	2423.42	E1D3G	2102.24				
E1D1I	2423.99	E1D2H	2338.30	E1D3I	2068.48				
E1D1H	2398.54	E1D2I	2325.68	E1D3H	2257.97				
E1B1A	2075.40	E1B2A	1351.50	E1B3A	1774.32				
E1B1C	1897.55	E1B2B	1483.96	E1B3C	1776.22				
E1B1B	1847.03	E1B2C	1698.29	E1B3B	1818.30				
E1B1D	2226.20	E1B2D	2154.07	E1B3D	1955.86				
E1B1F	2187.22	E1B2E	2109.48	E1B3F	1979.56				
E1B1E	2214.81	E1B2F	2008.76	E1B3E	2096.01				
E1B1G		E1B2G	2287.10	E1B3G	2116.50				
E1B1I		E1B2H	2246.37	E1B3I	1946.66				
E1B1H		E1B2I	2239.62	E1B3H	2086.17				

G4-tubule density

Sites	holes per mm 2	Sites	holes per mm 2	Sites	holes per mm 2				
G4D1A	19755.53	G4D2A	15956.39	G4D3A	14816.64		Average	Average	Average
G4D1C	29633.29	G4D2B	19755.53	G4D3C	12917.07		G4D-level 1	G4D-level 2	G4D-level 3
G4D1B	24694.41	G4D2C	17476.04	G4D3B	14816.64		25496.45	24652.19	21612.88
G4D1D	26214.06	G4D2D	28113.63	G4D3D	15196.56				
G4D1F	23934.58	G4D2E	29253.37	G4D3F	23934.58				
G4D1E	23554.66	G4D2F	22035.01	G4D3E	15576.47				
G4D1G	32292.69	G4D2G	32292.69	G4D3G	36851.65				
G4D1I	19755.53	G4D2H	32292.69	G4D3I	28493.55				
G4D1H	29633.29	G4D2I	24694.41	G4D3H	31912.77				
G4B1A	28873.46	G4B2A	33052.51	G4B3A	33052.51		Average	Average	Average
G4B1C	39511.05	G4B2B	40650.79	G4B3C	41410.62		G4B-level 1	G4B-level 2	G4B-level 3
G4B1B	38751.22	G4B2C	49008.90	G4B3B	42170.45		36134.04	46138.44	47784.73
G4B1D	44449.93	G4B2D	52048.21	G4B3D	56227.26				
G4B1F	37231.57	G4B2E	50908.47	G4B3F	45589.67				
G4B1E	37231.57	G4B2F	45589.67	G4B3E	52428.13				
G4B1G	38751.22	G4B2G	45969.59	G4B3G	52428.13				
G4B1I	24694.41	G4B2H	47109.33	G4B3I	53567.87				
G4B1H	35711.91	G4B2I	50908.47	G4B3H	53187.95				

G4-tubule diam.

Sites	Hole Diameter	Sites	Hole Diameter	Sites	Hole Diameter		Average G4-level 1	Average G4-level 2	Average G4-level 3
							1.35	1.74	2.00
G4D1A	1.40	G4D2A	1.61	G4D3A	2.08				
G4D1C	1.31	G4D2B	1.72	G4D3B	1.98				
G4D1B	1.40	G4D2C	1.80	G4D3C	1.78				
G4D1D	1.37	G4D2D	1.79	G4D3E	2.05		Average	Average	Average
G4D1F	1.48	G4D2E	1.96	G4D3F	2.01		G4D-level 1	G4D-level 2	G4D-level 3
G4D1E	1.36	G4D2F	2.01	G4D3D	2.03		1.36	1.79	1.97
G4D1G	1.34	G4D2G	1.72	G4D3G	1.85				
G4D1I	1.27	G4D2H	1.82	G4D3I	2.01				
G4D1H	1.33	G4D2I	1.66	G4D3H	1.93				
G4B1A	1.33	G4B2A	1.68	G4B3A	1.86		Average	Average	Average
G4B1C	1.40	G4B2B	1.70	G4B3C	1.92		G4B-level 1	G4B-level 2	G4B-level 3
G4B1B	1.37	G4B2C	1.72	G4B3B	1.87		1.35	1.70	2.03
G4B1D	1.45	G4B2D	1.61	G4B3D	2.17				
G4B1F	1.30	G4B2E	1.76	G4B3F	1.85				
G4B1E	1.42	G4B2F	1.72	G4B3E	1.86				
G4B1G	1.46	G4B2G	1.72	G4B3G	1.85				
G4B1I	1.30	G4B2H	1.63	G4B3I	2.55				
G4B1H	1.10	G4B2I	1.76	G4B3H	2.31				

G4-PT width

Sites	PT width microns	Sites	PT width microns	Sites	PT width microns		Average G4-level 1	Average G4-level 2	Average G4-level 3
G4D1A	0.99	G4D2A	0.48	G4D3A	0.96		0.96	0.66	0.72
G4D1C	1.10	G4D2B	0.47	G4D3C	0.70				
G4D1B	1.12	G4D2C	0.54	G4D3B	0.91				
G4D1D	1.34	G4D2D	0.85	G4D3D	0.91		Average G4D-level 1	Average G4D-level 2	Average G4D-level 3
G4D1F	0.92	G4D2E	0.69	G4D3F	0.90				
G4D1E	1.36	G4D2F	0.82	G4D3E	1.02		1.05	0.67	0.83
G4D1G	0.79	G4D2G	0.56	G4D3G	0.71				
G4D1I	0.65	G4D2H	0.79	G4D3I	0.69				
G4D1H	1.19	G4D2I	0.84	G4D3H	0.73				
G4B1A	0.87	G4B2A	0.69	G4B3A	0.78		Average G4B-level 1	Average G4B-level 2	Average G4B-level 3
G4B1C	0.97	G4B2B	0.67	G4B3C	0.62				
G4B1B	0.83	G4B2C	0.50	G4B3B	0.69		0.88	0.65	0.60
G4B1D	0.90	G4B2D		G4B3D	0.69				
G4B1F	0.83	G4B2E	0.66	G4B3F	0.55				
G4B1E	0.82	G4B2F	0.68	G4B3E	0.63				
G4B1G	0.81	G4B2G	0.61	G4B3G	0.53				
G4B1I	0.92	G4B2H	0.78	G4B3I	0.46				
G4B1H	0.95	G4B2I	0.59	G4B3H	0.44				

G4-IT area

Sites	IT-area micron 2	Sites	IT-area micron 2	Sites	IT-area micron 2		Average area µ2 G4 (IT)-level 1	Average area µ2 G4 (IT)-level 2	Average area µ2 G4 (IT)-level 3
							1948.49	1962.13	1882.51
G4D1A	2167.75	G4D2A	2415.68	G4D3A	2142.62				
G4D1C	1880.13	G4D2B	2342.14	G4D3C	2361.65				
G4D1B	1961.18	G4D2C	2332.22	G4D3B	2190.03				
G4D1D	1740.89	G4D2D	1925.20	G4D3D	2166.21				
G4D1F	2088.17	G4D2E	1958.35	G4D3F	1913.92				
G4D1E	1831.97	G4D2F	2024.22	G4D3E	2095.99				
G4D1G	2057.97	G4D2G	2094.52	G4D3G	1820.63				
G4D1I	2361.36	G4D2H	1865.47	G4D3I	1953.99				
G4D1H	1791.79	G4D2I	2060.98	G4D3H	1878.97				
G4B1A	2067.27	G4B2A	1988.85	G4B3A	1833.37				
G4B1C	1720.41	G4B2B	1856.38	G4B3C	1778.67				
G4B1B	1899.52	G4B2C	1879.28	G4B3B	1714.20				
G4B1D	1666.82	G4B2D	1712.66	G4B3D	1170.04				
G4B1F	1962.03	G4B2E		G4B3F	1805.86				
G4B1E	1910.59	G4B2F	1737.27	G4B3E	1583.47				
G4B1G	1868.55	G4B2G	1803.16	G4B3G	1710.60				
G4B1I	2130.14	G4B2H	1642.89	G4B3I					
G4B1H	1966.23	G4B2I	1716.95	G4B3H					

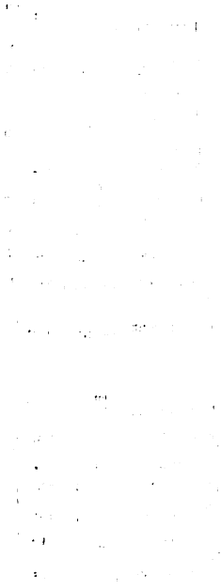

G6-tubule density

Sites	holes per mm 2	Sites	holes per mm 2	Sites	holes per mm 2				
G6D1A	12537.16	G6D2A	15576.47	G6D3A	19755.53		Average	Average	Average
G6D1C	27353.80	G6D2B	25454.23	G6D3C	40650.79		G6D-level 1	G6D-level 2	G6D-level 3
G6D1B	18615.78	G6D2C	33812.34	G6D3B	31532.86		23934.58	26340.70	26467.34
G6D1D	37611.48	G6D2D	33432.43	G6D3D	36091.83				
G6D1F	19755.53	G6D2E	25834.15	G6D3F	21655.10				
G6D1E	25834.15	G6D2F	24314.49	G6D3E	31912.77				
G6D1G	9117.93	G6D2G	23934.58	G6D3G	16336.30				
G6D1I	36091.83	G6D2H	28113.63	G6D3I	20515.35				
G6D1H	28493.55	G6D2I	26593.98	G6D3H	19755.53				
G6B1A	50908.47	G6B2A	37991.39	G6B3A	27353.80		Average	Average	Average
G6B1C	54707.61	G6B2B	28873.46	G6B3C	26593.98		G6B-level 1	G6B-level 2	G6B-level 3
G6B1B	51288.38	G6B2C	33812.34	G6B3B	24694.41		37527.06	26889.47	23385.81
G6B1D	34952.08	G6B2D	34952.08	G6B3D	23934.58				
G6B1F	50148.64	G6B2E	29633.29	G6B3F	29253.37				
G6B1E	45589.67	G6B2F	34572.17	G6B3E	26593.98				
G6B1G	13676.90	G6B2G	15956.39	G6B3G	22794.84				
G6B1I	19755.53	G6B2H	15576.47	G6B3I	14056.82				
G6B1H	16716.21	G6B2I	10637.59	G6B3H	15196.56				

G6-tubule diam.

Sites	Hole Diameter	Sites	Hole Diameter	Sites	Hole Diameter		Average G6-level 1	Average G6-level 2	Average G6-level 3
							1.46	1.89	1.99
G6D1A	0.93	G6D2A	1.92	G6D3A	2.08				
G6D1C	1.68	G6D2B	1.89	G6D3C	1.78				
G6D1B	1.17	G6D2C	1.70	G6D3B	1.85				
G6D1D	1.69	G6D2D	1.62	G6D3D	1.77		Average	Average	Average
G6D1F	1.37	G6D2E	1.86	G6D3F	2.01		G6D-level 1	G6D-level 2	G6D-level 3
G6D1E	1.68	G6D2F	1.91	G6D3E	1.86		1.42	1.82	1.93
G6D1G	0.88	G6D2G	1.88	G6D3G	2.13				
G6D1I	1.73	G6D2H	1.76	G6D3I	1.92				
G6D1H	1.68	G6D2I	1.84	G6D3H	1.99				
G6B1A	1.77	G6B2A	1.93	G6B3A	2.13		Average	Average	Average
G6B1C	1.74	G6B2B	1.84	G6B3C	2.14		G6B-level 1	G6B-level 2	G6B-level 3
G6B1B	1.58	G6B2C	2.20	G6B3B	2.22		1.50	1.96	2.05
G6B1D	1.54	G6B2D	1.93	G6B3D	2.02				
G6B1F	1.67	G6B2E	1.87	G6B3F	2.06				
G6B1E	1.61	G6B2F	2.00	G6B3E	2.00				
G6B1G	0.99	G6B2G	2.13	G6B3G	1.81				
G6B1I	1.38	G6B2H	1.94	G6B3I	2.11				
G6B1H	1.17	G6B2I	1.85	G6B3H	1.93				

G6-PT width

Sites	PT width microns	Sites	PT width microns	Sites	PT width microns		Average G6-level 1	Average G6-level 2	Average G6-level 3
							0.63	0.56	0.54
G6D1A	0.58	G6D2A	0.63	G6D3A	0.46				
G6D1C	0.89	G6D2B	0.44	G6D3C	0.59				
G6D1B	0.81	G6D2C	0.59	G6D3B	0.56				
G6D1D	0.91	G6D2D	0.64	G6D3D	0.62		Average	Average	Average
G6D1F	0.79	G6D2E	0.55	G6D3F	0.61		G6D-level 1	G6D-level 2	G6D-level 3
G6D1E	0.64	G6D2F	0.66	G6D3E	0.48		0.74	0.58	0.54
G6D1G	0.53	G6D2G	0.68	G6D3G	0.46				
G6D1I	0.51	G6D2H	0.56	G6D3I	0.57				
G6D1H	0.95	G6D2I	0.52	G6D3H	0.52				
G6B1A	0.49	G6B2A	0.50	G6B3A	0.60		Average	Average	Average
G6B1C	0.56	G6B2B	0.49	G6B3C	0.61		G6B-level 1	G6B-level 2	G6B-level 3
G6B1B	0.43	G6B2C	0.52	G6B3B	0.50		0.52	0.54	0.54
G6B1D	0.65	G6B2D	0.69	G6B3D	0.51				
G6B1F	0.58	G6B2E	0.40	G6B3F	0.44				
G6B1E	0.46	G6B2F	0.55	G6B3E	0.56				
G6B1G	0.45	G6B2G	0.61	G6B3G	0.48				
G6B1I	0.60	G6B2H	0.61	G6B3I	0.64				
G6B1H	0.49	G6B2I	0.52	G6B3H	0.54				

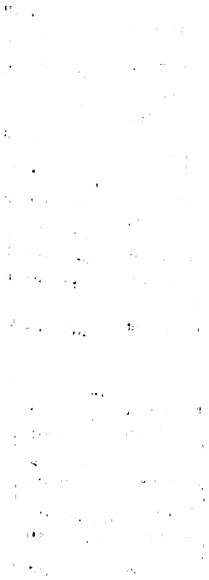

G6-IT area

Sites	IT-area micron 2	Sites	IT-area micron 2	Sites	IT-area micron 2		Average area µ2 G6 (IT)-level 1	Average area µ2 G6 (IT)-level 2	Average area µ2 G6 (IT)-level 3
							2122.63	2131.39	2148.84
G6D1A	2517.66	G6D2A	2305.96	G6D3A	2263.49				
G6D1C	1955.39	G6D2B	2227.59	G6D3C	1899.92				
G6D1B	2331.55	G6D2C	2051.61	G6D3B	2058.15				
G6D1D	1672.79	G6D2D	2055.15	G6D3D	1958.44				
G6D1F	2274.90	G6D2E	2161.47	G6D3F	2163.19				
G6D1E	2161.69	G6D2F	2104.67	G6D3E	2107.65				
G6D1G	2560.93	G6D2G	2114.90	G6D3G	2318.66				
G6D1I	2073.43	G6D2H	2152.96	G6D3I	2236.99				
G6D1H	1882.05	G6D2I	2178.35	G6D3H	2260.40				
G6B1A	1831.68	G6B2A	1956.61	G6B3A	2002.07				
G6B1C	1700.75	G6B2B	2158.92	G6B3C	2013.97				
G6B1B	2002.30	G6B2C	1897.06	G6B3B	2102.68				
G6B1F	1798.99	G6B2F	1945.19	G6B3D	2173.17				
G6B1D	2049.348	G6B2E	2192.56	G6B3F	2109.19				
G6B1E	2030.82	G6B2D	1841.37	G6B3E	2096.02				
G6B1G	2531.05	G6B2G	2261.85	G6B3G	2271.55				
G6B1I	2360.78	G6B2H	2310.84	G6B3I	2299.34				
G6B1H	2471.31	G6B2I	2448.01	G6B3H	2344.15				

G7-tubule density

Holes sites	holes per mm 2	sites	holes per mm 2	sites	holes per mm 2				
G7D1A	14056.82	G7D2A	30013.20	G7D3A	18995.70		Average	Average	Average
G7D1C	18235.87	G7D2B	47489.24	G7D3C	47869.16		G7D-level 1	G7D-level 2	G7D-level 3
G7D1B	17096.13	G7D2C	42550.36	G7D3B	32672.60		16716.21	43732.32	44323.29
G7D1D	15956.39	G7D2D	47869.16	G7D3D	45209.76				
G7D1F	17476.04	G7D2E	45969.59	G7D3F	48249.07				
G7D1E	19755.53	G7D2F	45589.67	G7D3E	55087.52				
G7D1G	15576.47	G7D2G	45589.67	G7D3G	52428.13				
G7D1I	17855.96	G7D2H	33432.43	G7D3I	47489.24				
G7D1H	14436.73	G7D2I	55087.52	G7D3H	50908.47				
G7B1A	18235.87	G7B2A	42930.28	G7B3A	44449.93		Average	Average	Average
G7B1C	13676.90	G7B2B	43690.10	G7B3C	50908.47		G7B-level 1	G7B-level 2	G7B-level 3
G7B1B	13676.90	G7B2C	45209.76	G7B3B	48249.07		19671.10	45758.52	48586.77
G7B1D	27353.80	G7B2D	50528.56	G7B3D	55467.44				
G7B1F	25454.23	G7B2E	43690.10	G7B3F	55087.52				
G7B1E	23554.66	G7B2F	45209.76	G7B3E	53187.95				
G7B1G	21275.18	G7B2G	42170.45	G7B3G	46349.50				
G7B1I	20515.35	G7B2H	44070.02	G7B3I	34572.17				
G7B1H	13296.99	G7B2I	54327.69	G7B3H	49008.90				

G7-tubule diam.

Sites	Hole Diameter	Sites	Hole Diameter	Sites	Hole Diameter		Average G7-level 1	Average G7-level 2	Average G7-level 3
							1.15	1.44	1.77
G7D1A	0.97	G7D2A	1.35	G7D3A	1.39				
G7D1C	1.08	G7D2B	1.59	G7D3C	1.73				
G7D1B	1.09	G7D2C	1.27	G7D3B	1.70				
G7D1D	1.09	G7D2D	1.60	G7D3D	1.87		Average	Average	Average
G7D1F	0.95	G7D2E	1.46	G7D3F	1.74		G7D-level 1	G7D-level 2	G7D-level 3
G7D1E	1.13	G7D2F	1.63	G7D3E	1.75		1.07	1.42	1.71
G7D1G	1.04	G7D2G	1.43	G7D3G	1.81				
G7D1I	1.25	G7D2H	1.11	G7D3I	1.59				
G7D1H	1.06	G7D2I	1.38	G7D3H	1.81				
G7B1A	1.11	G7B2A	1.47	G7B3A	1.66		Average	Average	Average
G7B1C	1.08	G7B2B	1.49	G7B3C	1.79		G7B-level 1	G7B-level 2	G7B-level 3
G7B1B	1.05	G7B2C	1.42	G7B3B	1.62		1.22	1.46	1.82
G7B1D	1.24	G7B2D	1.63	G7B3D	2.01				
G7B1F	1.39	G7B2E	1.46	G7B3F	2.00				
G7B1E	1.24	G7B2F	1.51	G7B3E	1.99				
G7B1G	1.30	G7B2G	1.50	G7B3G	2.07				
G7B1I	1.36	G7B2H	1.46	G7B3I	1.56				
G7B1H	1.25	G7B2I	1.22	G7B3H	1.70				

G7-PT width

Sites	PT width microns	Sites	PT width microns	Sites	PT width microns		Average G7-level 1	Average G7-level 2	Average G7 -level 3
							0.46	0.54	0.49
G7D1A	0.53	G7D2A	0.49	G7D3A	0.31				
G7D1C	0.51	G7D2B	0.46	G7D3C	0.41				
G7D1B	0.57	G7D2C	0.68	G7D3B	0.46				
G7D1D	0.43	G7D2D	0.55	G7D3D	0.69		Average	Average	Average
G7D1F	0.46	G7D2E	0.60	G7D3F	0.37		G7D-level 1	G7D-level 2	G7D-level 3
G7D1E	0.55	G7D2F	0.54	G7D3E	0.45		0.46	0.50	0.44
G7D1G	0.25	G7D2G	0.41	G7D3G	0.50				
G7D1I	0.51	G7D2H	0.47	G7D3I	0.36				
G7D1H	0.34	G7D2I	0.35	G7D3H	0.43				
G7B1A	0.41	G7B2A	0.60	G7B3A	0.45		Average	Average	Average
G7B1C	0.49	G7B2B	0.57	G7B3C	0.49		G7B-level 1	G7B-level 2	G7B-level 3
G7B1B	0.45	G7B2C	0.57	G7B3B	0.66		0.45	0.57	0.54
G7B1D	0.49	G7B2D	0.59	G7B3D	0.75				
G7B1F	0.64	G7B2E	0.66	G7B3F	0.62				
G7B1E	0.62	G7B2F	0.57	G7B3E	0.39				
G7B1G	0.29	G7B2G	0.65	G7B3G	0.41				
G7B1I	0.33	G7B2H	0.46	G7B3I	0.57				
G7B1H	0.33	G7B2I	0.46	G7B3H	0.57				

G7-IT area

Sites	IT-area micron 2	Sites	IT-area micron 2	Sites	IT-area micron 2		Average area µ2 G7 (IT)-level 1	Average area µ2 G7 (IT)-level 2	Average area µ2 G7 (IT)-level 3
							2464.65	2039.65	1944.28
G7D1A	2512.98	G7D2A	2300.10	G7D3A	2472.45				
G7D1C	2467.06	G7D2B	2016.62	G7D3C	1986.19				
G7D1B	2458.14	G7D2C	2020.38	G7D3B	2167.83				
G7D1D	2507.61	G7D2D	1909.84	G7D3D	1650.96				
G7D1F	2506.19	G7D2E	1961.58	G7D3F	2015.15				
G7D1E	2428.89	G7D2F	1936.43	G7D3E	1830.99				
G7D1G	2555.94	G7D2G	2154.68	G7D3G	1809.11				
G7D1I	2442.18	G7D2H	2344.64	G7D3I	2105.33				
G7D1H	2540.63	G7D2I	2140.34	G7D3H	1877.13				
G7B1A	2491.66	G7B2A	1997.39	G7B3A	2035.29				
G7B1C	2511.73	G7B2B	2005.34	G7B3C	1826.34				
G7B1B	2525.88	G7B2C	2021.65	G7B3B	1771.60				
G7B1D	2353.94	G7B2D	1801.75	G7B3D					
G7B1F	2257.15	G7B2E	1937.14	G7B3F					
G7B1E	2335.42	G7B2F	1979.01	G7B3E	1793.09				
G7B1G	2477.75	G7B2G	1946.38	G7B3G	1834.41				
G7B1I	2458.07	G7B2H	2120.14	G7B3I	2111.93				
G7B1H	2532.48	G7B2I	2120.32	G7B3H	1820.71				

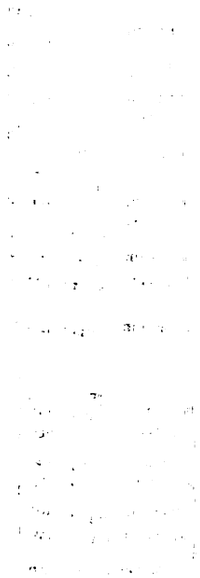

H2-tubule density

Sites	holes per mm 2	Sites	holes per mm 2	Sites	holes per mm 2				
H2D1A	8358.11	H2D2A	20515.35	H2D3A	30393.12		Average	Average	Average
H2D1C	12917.07	H2D2B	22035.01	H2D3C	25454.23		H2D-level 1	H2D-level 2	H2D-level 3
H2D1B	13296.99	H2D2C	22414.92	H2D3B	27733.72		15154.35	26551.76	31026.31
H2D1D	10257.68	H2D2D	28873.46	H2D3D	27733.72				
H2D1F	20895.27	H2D2E	30393.12	H2D3F	36471.74				
H2D1E	17855.96	H2D2F	30013.20	H2D3E	31532.86				
H2D1G	23174.75	H2D2G	30773.03	H2D3G	33812.34				
H2D1I	9117.93	H2D2H	26214.06	H2D3I	31532.86				
H2D1H	20515.35	H2D2I	27733.72	H2D3H	34572.17				
H2B1A	14436.73	H2B2A	14436.73	H2B3A	22414.92		Average	Average	Average
H2B1C	4558.97	H2B2B	11397.42	H2B3C	8358.11		H2B-level 1	H2B-level 2	H2B-level 3
H2B1B	8358.11	H2B2C	6838.45	H2B3B	15196.56		14352.30	19671.10	20979.69
H2B1D	4558.97	H2B2D	18615.78	H2B3D	14816.64				
H2B1F	23174.75	H2B2E	24314.49	H2B3F	35711.91				
H2B1E	13676.90	H2B2F	29253.37	H2B3E	23934.58				
H2B1G	33052.51	H2B2G	43310.19	H2B3G	42550.36				
H2B1I	6838.45	H2B2H	18995.70	H2B3I	6838.45				
H2B1H	20515.35	H2B2I	9877.76	H2B3H	18995.70				

H2-tubule diam.

Sites	Hole Diameter	Sites	Hole Diameter	Sites	Hole Diameter		Average H2-level 1	Average H2-level 2	Average H2-level 3
							1.79	1.99	2.09
H2D1A	1.68	H2D2A	1.66	H2D3A	1.86				
H2D1C	1.68	H2D2B	1.87	H2D3C	2.30				
H2D1B	1.16	H2D2C	1.96	H2D3B	1.99				
H2D1D	1.41	H2D2D	2.09	H2D3D	2.24		Average	Average	Average
H2D1F	1.95	H2D2E	2.14	H2D3F	2.02		H2D-level 1	H2D-level 2	H2D-level 3
H2D1E	1.69	H2D2F	1.92	H2D3E	2.09		1.60	1.99	2.23
H2D1G	1.74	H2D2G	1.96	H2D3G	2.38				
H2D1I	1.19	H2D2H	2.16	H2D3I	2.64				
H2D1H	1.94	H2D2I	2.14	H2D3H	2.51				
H2B1A	1.94	H2B2A	1.95	H2B3A	1.68		Average	Average	Average
H2B1C	1.59	H2B2B	2.09	H2B3C	2.35		H2B-level 1	H2B-level 2	H2B-level 3
H2B1B	2.26	H2B2C	2.19	H2B3B	2.06		1.97	1.98	1.95
H2B1D	1.74	H2B2D	1.86	H2B3D	2.03				
H2B1F	1.77	H2B2E	1.68	H2B3F	1.87				
H2B1E	2.32	H2B2F	1.76	H2B3E	1.77				
H2B1G	2.03	H2B2G	2.00	H2B3G	1.78				
H2B1I	2.27	H2B2H	1.88	H2B3I	2.12				
H2B1H	1.78	H2B2I	2.43	H2B3H	1.88				

H2-PT width

Sites	PT width microns	Sites	PT width microns	Sites	PT width microns		Average H2-level 1	Average H2-level 2	Average H2-level 3
							0.76	0.79	0.73
H2D1A	0.78	H2D2A	1.04	H2D3A	0.76				
H2D1C	0.72	H2D2B	0.82	H2D3B	0.66				
H2D1B	0.65	H2D2C	0.89	H2D3C	0.77				
H2D1D	0.64	H2D2D	0.77	H2D3D	1.10		Average	Average	Average
H2D1F	0.85	H2D2E	0.78	H2D3F	0.74		H2D-level 1	H2D-level 2	H2D-level 3
H2D1E	0.92	H2D2F	0.66	H2D3E	0.66		0.78	0.89	0.75
H2D1G	0.96	H2D2G	1.11	H2D3G	0.71				
H2D1I	0.66	H2D2H	0.98	H2D3I	0.73				
H2D1H	0.86	H2D2I	0.98	H2D3H	0.63				
H2B1A	0.97	H2B2A	0.84	H2B3A	0.75		Average	Average	Average
H2B1C	0.72	H2B2B	0.70	H2B3C	0.82		H2B-level 1	H2B-level 2	H2B-level 3
H2B1B	0.85	H2B2C	0.87	H2B3B	0.76		0.73	0.69	0.71
H2B1D	0.68	H2B2D	0.59	H2B3D	0.64				
H2B1F	0.71	H2B2E	0.64	H2B3F	0.57				
H2B1E	0.80	H2B2F	0.52	H2B3E	0.67				
H2B1G	0.65	H2B2G	0.63	H2B3G	0.54				
H2B1I	0.59	H2B2H	0.58	H2B3I	0.90				
H2B1H	0.66	H2B2I	0.86	H2B3H	0.74				

H2-IT area

Sites	IT-area micron 2	Sites	IT-area micron 2	Sites	IT-area micron 2		Average area µ2 H2 (IT)-level 1	Average area µ2 H2 (IT)-level 2	Average area µ2 H2 (IT)-level 3
							2283.08	2023.78	1961.66
H2D1A	2451.73	H2D2A	2036.43	H2D3A	1912.65				
H2D1C	2371.53	H2D2B	2072.86	H2D3C	1859.08				
H2D1B	2465.49	H2D2C	1983.57	H2D3B	2002.29				
H2D1D	2478.19	H2D2D	1844.53	H2D3D	1497.82				
H2D1F	2054.03	H2D2E	1767.59	H2D3F	1702.91				
H2D1E	2172.25	H2D2F	1979.10	H2D3E	1880.73				
H2D1G	1989.69	H2D2G	1520.84	H2D3G	1616.99				
H2D1I	2513.09	H2D2H	1713.96	H2D3I	1533.11				
H2D1H	2062.50	H2D2I	1664.97	H2D3H	1614.97				
H2B1A	2183.45	H2B2A	2236.18	H2B3A	2162.68				
H2B1C	2545.92	H2B2B	2343.92	H2B3C	2357.29				
H2B1B	2361.50	H2B2C	2414.69	H2B3B	2229.78				
H2B1D	2541.66	H2B2D	2278.49	H2B3D	2297.70				
H2B1F	2145.55	H2B2E	2189.19	H2B3F	1967.04				
H2B1E	2199.16	H2B2F	2155.58	H2B3E	2153.74				
H2B1G	1873.12	H2B2G	1677.49	H2B3G	1915.71				
H2B1I	2464.27	H2B2H	2268.04	H2B3I	2415.27				
H2B1H	2222.30	H2B2I	2280.66	H2B3H	2190.05				

H3-tubule density

Sites	holes per mm 2	Sites	holes per mm 2	Sites	holes per mm 2				
H3D1A	14816.64	H3D2A	23554.66	H3D3A	30013.20		Average	Average	Average
H3D1C	27733.72	H3D2B	23934.58	H3D3C	42170.45		H3D-level 1	H3D-level 2	H3D-level 3
H3D1B	18615.78	H3D2C	31532.86	H3D3B	33052.51		25285.38	30308.69	37780.33
H3D1D	30013.20	H3D2D	32672.60	H3D3D	44829.85				
H3D1F	22794.84	H3D2E	31532.86	H3D3F	31912.77				
H3D1E	28873.46	H3D2F	26214.06	H3D3E	34952.08				
H3D1G	26593.98	H3D2G	31532.86	H3D3G	40650.79				
H3D1I	30393.12	H3D2H	37231.57	H3D3I	41790.53				
H3D1H	27733.72	H3D2I	34572.17	H3D3H	40650.79				
H3B1A	17096.13	H3B2A	17476.04	H3B3A	28873.46		Average	Average	Average
H3B1C	30773.03	H3B2B	24694.41	H3B3C	39131.14		H3B-level 1	H3B-level 2	H3B-level 3
H3B1B	21655.10	H3B2C	36091.83	H3B3B	30393.12		27100.53	30730.82	36682.80
H3B1D	33812.34	H3B2D	39890.96	H3B3D	40270.88				
H3B1F	20515.35	H3B2E	34192.26	H3B3F	37611.48				
H3B1E	32292.69	H3B2F	30013.20	H3B3E	40270.88				
H3B1G	23174.75	H3B2G	29253.37	H3B3G	31912.77				
H3B1I	32672.60	H3B2H	28873.46	H3B3I	42930.28				
H3B1H	31912.77	H3B2I	36091.83	H3B3H	38751.22				

H3-tubule diam.

Holes	Hole Diameter		Hole Diameter		Hole Diameter		Average H3-level 1	Average H3-level 2	Average H3-level 3
							1.56	1.70	1.89
H3D1A	1.60	H3D2A	1.76	H3D3A	1.73				
H3D1C	1.66	H3D2B	1.64	H3D3C	1.96				
H3D1B	1.63	H3D2C	1.78	H3D3B	1.79				
H3D1D	1.27	H3D2D	1.65	H3D3D	2.23		Average	Average	Average
H3D1F	1.68	H3D2E	1.66	H3D3F	1.63		H3D-level 1	H3D-level 2	H3D-level 3
H3D1E	1.57	H3D2F	1.66	H3D3E	1.77		1.55	1.69	1.78
H3D1G	1.53	H3D2G	1.45	H3D3G	1.72				
H3D1I	1.41	H3D2H	1.71	H3D3I	1.76				
H3D1H	1.63	H3D2I	1.87	H3D3H	1.38				
H3B1A	1.69	H3B2A	1.50	H3B3A	1.80		Average	Average	Average
H3B1C	1.54	H3B2B	1.87	H3B3C	2.42		H3B-level 1	H3B-level 2	H3B-level 3
H3B1B	1.82	H3B2C	1.76	H3B3B	1.83		1.56	1.71	2.01
H3B1D	1.40	H3B2D	1.60	H3B3D	2.38				
H3B1F	1.68	H3B2E	1.73	H3B3F	1.68				
H3B1E	1.51	H3B2F	1.68	H3B3E	2.03				
H3B1G	1.51	H3B2G	1.63	H3B3G	1.81				
H3B1I	1.40	H3B2H	1.80	H3B3I	2.28				
H3B1H	1.49	H3B2I	1.81	H3B3H	1.84				

H3-PT width

Sites	PT width microns	Sites	PT width microns	Sites	PT width microns		Average H3-level 1	Average H3-level 2	Average H3-level 3
H3D1A	0.82	H3D2A	0.85	H3D3A	0.80		1.02	0.92	0.70
H3D1C	0.87	H3D2B	0.97	H3D3C	0.79				
H3D1B	0.76	H3D2C	0.91	H3D3B	0.59				
H3D1D	1.08	H3D2D	0.91	H3D3D	0.56		Average	Average	Average
H3D1F	1.07	H3D2E	0.97	H3D3F	0.74		H3D-level 1	H3D-level 2	H3D-level 3
H3D1E	1.11	H3D2F	0.99	H3D3E	0.56		0.98	0.89	0.76
H3D1G	1.10	H3D2G	0.90	H3D3G	0.90				
H3D1I	1.03	H3D2H	0.69	H3D3I	0.88				
H3D1H		H3D2I	0.85	H3D3H	1.00				
H3B1A	0.88	H3B2A	1.17	H3B3A	0.91		Average	Average	Average
H3B1C	1.00	H3B2B	0.88	H3B3C	0.58		H3B-level 1	H3B-level 2	H3B-level 3
H3B1B	1.00	H3B2C	0.92	H3B3B	0.77		1.06	0.94	0.65
H3B1D	1.17	H3B2D		H3B3D	0.55				
H3B1F	0.99	H3B2E	0.98	H3B3F	0.74				
H3B1E	1.08	H3B2F	1.02	H3B3E	0.55				
H3B1G	1.24	H3B2G	0.98	H3B3G	0.81				
H3B1I	1.17	H3B2H	0.81	H3B3I	0.47				
H3B1H	1.02	H3B2I	0.78	H3B3H	0.48				

H3-IT area

Sites	IT-area micron 2	Sites	IT-area micron 2	Sites	IT-area micron 2		Average area µ2 H3 (IT)-level 1	Average area µ2 H3 (IT)-level 2	Average area µ2 H3 (IT)-level 3
H3D1A	2311.60	H3D2A	2049.44	H3D3A	1939.23		1948.44	1862.04	1786.73
H3D1C	1966.23	H3D2B	1995.49	H3D3C	1538.31				
H3D1B	2251.22	H3D2C	1780.69	H3D3B	2028.12				
H3D1D	1899.09	H3D2D	1824.80	H3D3D	1594.32				
H3D1F	1942.62	H3D2E	1788.15	H3D3F	1990.64				
H3D1E	1778.38	H3D2F	1915.28	H3D3E	2029.00				
H3D1G	1864.78	H3D2G	1942.90	H3D3G	1588.18				
H3D1I	1871.39	H3D2H	1900.48	H3D3I	1561.73				
H3D1H	1795.93	H3D2I	1720.29	H3D3H	1673.28				
H3B1A	2213.09	H3B2A	2102.47	H3B3A	1848.82				
H3B1C	1833.03	H3B2B	1961.99	H3B3C	1592.33				
H3B1B	1976.18	H3B2C	1660.03	H3B3B	1917.11				
H3B1D		H3B2D		H3B3D	1618.77				
H3B1F	2062.68	H3B2E	1673.10	H3B3F	1850.31				
H3B1E	1738.67	H3B2F	1772.55	H3B3E	1814.40				
H3B1G	1864.24	H3B2G	1849.66	H3B3G	1855.38				
H3B1I		H3B2H	1935.17	H3B3I	1716.67				
H3B1H	1805.99	H3B2I	1782.17	H3B3H	2004.54				

H4-tubule density

Sites	holes per mm 2	Sites	holes per mm 2	Sites	holes per mm 2				
H4D1A	11397.42	H4D2A	17096.13	H4D3A	24314.49		Average	Average	Average
H4D1C	13296.99	H4D2B	18995.70	H4D3C	28113.63		H4D-level 1	H4D-level 2	H4D-level 3
H4D1B	12537.16	H4D2C	20895.27	H4D3B	22035.01		13465.84	22077.22	31026.31
H4D1D	12917.07	H4D2D	24314.49	H4D3D	36471.74				
H4D1F	14436.73	H4D2E	20515.35	H4D3F	28113.63				
H4D1E	10257.68	H4D2F	19375.61	H4D3E	33432.43				
H4D1G	10637.59	H4D2G	26973.89	H4D3G	33812.34				
H4D1I	20895.27	H4D2H	25454.23	H4D3I	36471.74				
H4D1H	14816.64	H4D2I	25074.32	H4D3H	36471.74				
H4B1A	22414.92	H4B2A	32292.69	H4B3A	33432.43		Average	Average	Average
H4B1C	26973.89	H4B2B	27733.72	H4B3C	24314.49		H4B-level 1	H4B-level 2	H4B-level 3
H4B1B	36471.74	H4B2C	19375.61	H4B3B	26973.89		30435.33	29253.37	31532.86
H4B1D	30773.03	H4B2D	26973.89	H4B3D	28873.46				
H4B1F	26214.06	H4B2E	30013.20	H4B3F	41030.71				
H4B1E	30773.03	H4B2F	36471.74	H4B3E	34952.08				
H4B1G	41030.71	H4B2G	31152.94	H4B3G	35711.91				
H4B1I	27733.72	H4B2H	38371.31	H4B3I	25834.15				
H4B1H	31532.86	H4B2I	20895.27	H4B3H	32672.60				

H4-tubule diam.

Sites	Hole Diameter	Sites	Hole Diameter	Sites	Hole Diameter		Average H4-level 1	Average H4-level 2	Average H4-level 3
H4D1A	0.98	H4D2A	1.65	H4D3A	1.67		1.39	1.80	1.85
H4D1C	1.80	H4D2B	2.04	H4D3C	1.66				
H4D1B	1.30	H4D2C	1.82	H4D3B	1.85				
H4D1D	1.82	H4D2D	1.75	H4D3D	1.96		Average	Average	Average
H4D1F	1.59	H4D2E	1.84	H4D3F	1.80		H4D-level 1	H4D-level 2	H4D-level 3
H4D1E	1.48	H4D2F	2.04	H4D3E	1.78		1.59	1.86	1.80
H4D1G	1.53	H4D2G	1.88	H4D3G	1.72				
H4D1I	1.84	H4D2H	1.78	H4D3I	1.95				
H4D1H	1.97	H4D2I	1.91	H4D3H	1.83				
H4B1A	0.98	H4B2A	1.73	H4B3A	1.89		Average	Average	Average
H4B1C	1.19	H4B2B	1.76	H4B3C	1.92		H4B-level 1	H4B-level 2	H4B-level 3
H4B1B	1.11	H4B2C	1.57	H4B3B	1.91		1.19	1.75	1.89
H4B1D	1.07	H4B2D	1.55	H4B3D	1.86				
H4B1F	1.89	H4B2E	1.74	H4B3F	1.84				
H4B1E	1.26	H4B2F	1.94	H4B3E	1.96				
H4B1G	1.08	H4B2G	1.63	H4B3G	1.76				
H4B1I	1.05	H4B2H	1.74	H4B3I	2.03				
H4B1H	1.06	H4B2I	2.09	H4B3H	1.81				

H4-PT width

Sites	PT width microns	Sites	PT width microns	Sites	PT width microns		Average H4-level 1	Average H4-level 2	Average H4-level 3
							0.97	0.98	0.81
H4D1A	0.79	H4D2A	1.14	H4D3A	0.79				
H4D1C	0.76	H4D2B	0.96	H4D3C	0.88				
H4D1B	0.75	H4D2C	1.00	H4D3B	0.70				
H4D1D	0.73	H4D2D	1.10	H4D3D	0.66		Average	Average	Average
H4D1F	0.65	H4D2E	1.32	H4D3F	0.67		H4D-level 1	H4D-level 2	H4D-level 3
H4D1E	0.81	H4D2F	0.78	H4D3E	0.87		0.76	0.99	0.75
H4D1G	0.63	H4D2G	0.73	H4D3G	0.76				
H4D1I	0.89	H4D2H	0.94	H4D3I	0.73				
H4D1H	0.81	H4D2I	0.99	H4D3H	0.66				
H4B1A	0.96	H4B2A	0.92	H4B3A	0.66		Average	Average	Average
H4B1C	1.48	H4B2B	0.94	H4B3C	0.90		H4B-level 1	H4B-level 2	H4B-level 3
H4B1B	1.31	H4B2C	1.13	H4B3B	0.87		1.17	0.97	0.88
H4B1D	1.19	H4B2D	0.97	H4B3D	0.79				
H4B1F	1.25	H4B2E	0.91	H4B3F	0.82				
H4B1E	1.27	H4B2F	0.85	H4B3E	0.76				
H4B1G	0.94	H4B2G	1.04	H4B3G	1.09				
H4B1I	1.19	H4B2H	0.93	H4B3I	0.99				
H4B1H	0.97	H4B2I	1.08	H4B3H	1.04				

H4-IT area

Sites	IT-area micron 2	Sites	IT-area micron 2	Sites	IT-area micron 2		Average area µ2 H4 (IT)-level 1	Average area µ2 H4 (IT)-level 2	Average area µ2 H4 (IT)-level 3
							2101.11	1887.22	1850.36
H4D1A	2475.22	H4D2A	2090.19	H4D3A	2100.05				
H4D1C	2329.65	H4D2B	2014.20	H4D3C	1945.50				
H4D1B	2428.38	H4D2C	2000.28	H4D3B	2153.26				
H4D1D	2345.60	H4D2D	1846.93	H4D3D	1819.49				
H4D1F	2383.17	H4D2E	1780.85	H4D3F	2059.01				
H4D1E	2428.79	H4D2F	2115.21	H4D3E	1777.21				
H4D1G	2461.01	H4D2G	2013.75	H4D3G	1901.36				
H4D1I	2174.76	H4D2H	1927.90	H4D3I	1755.69				
H4D1H	2237.11	H4D2I	1843.39	H4D3H	1889.71				
H4B1A	2245.83	H4B2A	1787.22	H4B3A	1919.27				
H4B1C	1672.16	H4B2B	1870.04	H4B3C	1940.98				
H4B1B	1654.87	H4B2C	2045.11	H4B3B	1894.19				
H4B1D	1870.32	H4B2D	1950.68	H4B3D	1923.42				
H4B1F	1584.13	H4B2E	1843.42	H4B3F	1602.18				
H4B1E	1713.95	H4B2F	1630.26	H4B3E	1753.90				
H4B1G	1814.54	H4B2G	1747.51	H4B3G	1487.51				
H4B1I	1953.91	H4B2H	1610.26	H4B3I	1776.11				
H4B1H	2046.54	H4B2I	1852.81	H4B3H	1607.58				

APPENDIX B

Statistical analysis

Tubule Density
CUSPIDS and LATERALS only
Using ROWS and COLUMNS for sites

General Linear Models Procedure
Class Level Information

Class	Levels	Values
TOOTH	9	D2 D4 D5 G4 G6 G7 M2 M3 M4
DIR	2	B D
TYPE	2	cuspid lateral
SLICE	3	1 2 3

Dependent Variable: DENSITY

Source	DF	Sum of Squares	Mean Square	F Value	Pr > F
Model	25	38451366253.08960000	1538054650.12358000	14.38	0.0001
Error	454	48551192192.97450000	106941392.91606700		
Corrected Total	479	87002758646.06410000			

R-Square	C.V.	Root MSE	DENSITY Mean
0.441956	30.85363	10341.24716541	33517.11670640

Source	DF	Type III SS	Mean Square	F Value	Pr > F
TOOTH(TYPE)	7	13545204910.99100000	1935029272.99872000	18.09	0.0001
DIR	1	2098477536.70749000	2098477536.70749000	19.62	0.0001
SLICE	2	5575704851.95055000	2787852425.97527000	26.07	0.0001
ROW	1	282761337.48125700	282761337.48125700	2.64	0.1046
COL	1	16149206.35839420	16149206.35839420	0.15	0.6978
ROW*SLICE	2	136976090.71754100	68488045.35877060	0.64	0.5275
COL*SLICE	2	52636571.82653000	26318285.91326500	0.25	0.7819
DIR*SLICE	2	1143530028.51985000	571765014.25992700	5.35	0.0051
TYPE*SLICE	2	210352913.45166100	105176456.72583000	0.98	0.3748
ROW*DIR	1	551655543.56359700	551655543.56359700	5.16	0.0236
COL*DIR	1	653917126.28406100	653917126.28406100	6.11	0.0138
ROW*TYPE	1	1592851084.78951000	1592851084.78951000	14.89	0.0001
COL*TYPE	1	315504291.51748200	315504291.51748200	2.95	0.0865

Tests of Hypotheses using the Type III MS for TOOTH(TYPE) as an error term

Source	DF	Type III SS	Mean Square	F Value	Pr > F
TYPE	1	12971707491.71110000	12971707491.71110000	6.70	0.0160

Tubule Density
CUSPIDS and LATERALS only
Using ROWS and COLUMNS for sites

---------- DIR=B ----------

Source	DF	Type III SS	Mean Square	F Value	Pr > F
TOOTH(TYPE)	7	7356714347.65743000	1050959192.52249000	9.79	0.0001
SLICE	2	832302180.16625400	416151090.08312700	3.88	0.0222
ROW	1	4009.29469493	4009.29469493	0.00	0.9951
COL	1	252477108.76130000	252477108.76130000	2.35	0.1266
ROW*SLICE	2	53592687.66429690	26796343.83214840	0.25	0.7793
COL*SLICE	2	32698684.39379970	16349342.19689990	0.15	0.8588
TYPE*SLICE	2	32901345.56923570	16450672.78461780	0.15	0.8580
ROW*TYPE	1	1582880682.48746000	1582880682.48746000	14.74	0.0002
COL*TYPE	1	294977469.17100300	294977469.17100300	2.75	0.0988

Tests of Hypotheses using the Type III MS for TOOTH(TYPE) as an error term

Source	DF	Type III SS	Mean Square	F Value	Pr > F
TYPE	1	9666664721.21969000	9666664721.21969000	9.20	0.0190

---------- DIR=D ----------

Source	DF	Type III SS	Mean Square	F Value	Pr > F
TOOTH(TYPE)	7	11581417841.80790000	1654774834.54199000	19.62	0.0001
SLICE	2	[illegible]	[illegible]	14.79	0.0001
ROW	1	[illegible]	[illegible]	6.66	0.0105
COL	1	468963806.21055800	468963806.21055800	5.50	0.0199
ROW*SLICE	2	82314666.39877630	41157333.19938810	0.48	0.6175
COL*SLICE	2	37598557.87457110	18799278.93728550	0.22	0.8022
TYPE*SLICE	2	215662958.16164300	107831479.08082100	1.27	0.2841
ROW*TYPE	1	273749002.68619400	273749002.68619400	3.21	0.0744
COL*TYPE	1	64398734.96717650	64398734.96717650	0.76	0.3856

Tests of Hypotheses using the Type III MS for TOOTH(TYPE) as an error term

Source	DF	Type III SS	Mean Square	F Value	Pr > F
TYPE	1	3902440103.02383000	3902440103.02383000	2.36	0.1685

Tubule Density
CUSPIDS and LATERALS only
Using ROWS and COLUMNS for sites

---------- SLICE=1 ----------

Source	DF	Type III SS	Mean Square	F Value	Pr > F
TOOTH(TYPE)	7	105230661368.76110000	15032951955.51758000	17.88	0.0001
DIR	1	20950174466.09073000	20950174466.09073000	24.92	0.0001
ROW	1	173125566.04061790	173125566.04061790	0.21	0.6506
COL	1	154353955.95505130	154353955.95505130	0.18	0.6689
ROW*DIR	1	1461223111.88039600	1461223111.88039600	1.74	0.1895
COL*DIR	1	1265992924.47222900	1265992924.47222900	1.51	0.2218
DIR*TYPE	1	973906323.36967980	973906323.36967980	1.16	0.2836
ROW*TYPE	1	7562753140.03804200	7562753140.03804200	9.00	0.0032
COL*TYPE	1	371435039.95849330	371435039.95849330	0.44	0.5073

Tests of Hypotheses using the Type III MS for TOOTH(TYPE) as an error term

TYPE	1	58613692247.70703000	58613692247.70703000	3.90	0.0889

---------- SLICE=2 ----------

Source	DF	Type III SS	Mean Square	F Value	Pr > F
TOOTH(TYPE)	7	49913711084.48372000	7130530154.49767500	10.94	0.0001
DIR	1	2991097794.04613800	2991097794.04613800	4.59	0.0339
ROW	1	2805864794.92987300	2805864794.92987300	4.30	0.0398
COL	1	399893956.62086120	399893956.62086120	0.61	0.4348
ROW*DIR	1	2064105187.77900200	2064105187.77900200	3.17	0.0771
COL*DIR	1	2747773407.70859500	2747773407.70859500	4.21	0.0419
DIR*TYPE	1	2516884297.00979100	2516884297.00979100	3.86	0.0514
ROW*TYPE	1	3580460537.43589200	3580460537.43589200	5.49	0.0205
COL*TYPE	1	1862249487.65712000	1862249487.65712000	2.86	0.0932

Tests of Hypotheses using the Type III MS for TOOTH(TYPE) as an error term

TYPE	1	42679175207.26419000	42679175207.26419000	5.99	0.0443

---------- SLICE=3 ----------

Source	DF	Type III SS	Mean Square	F Value	Pr > F
TOOTH(TYPE)	7	100401862637.17490000	14344123231.31071000	14.19	0.0001
DIR	1	52176757.57125746	52176757.57125746	0.05	0.8206
ROW	1	675726527.78032430	675726527.78032430	0.67	0.4149
COL	1	124709337.29332760	124709337.29332760	0.12	0.7259
ROW*DIR	1	2022301608.84375600	2022301608.84375600	2.00	0.1594
COL*DIR	1	2513043897.49846400	2513043897.49846400	2.49	0.1171
DIR*TYPE	1	3567104187.28137600	3567104187.28137600	3.53	0.0624
ROW*TYPE	1	5151168557.26753900	5151168557.26753900	5.10	0.0255
COL*TYPE	1	1158607987.51060900	1158607987.51060900	1.15	0.2862

Tests of Hypotheses using the Type III MS for TOOTH(TYPE) as an error term

TYPE	1	30527755737.48281000	30527755737.48281000	2.13	0.1880

Tubule Density
CUSPIDS and LATERALS only
Using ROWS and COLUMNS for sites

---------- TYPE=lateral ----------

Source	DF	Type III SS	Mean Square	F Value	Pr > F
TOOTH	5	108657686616.01800000	21731151721.20161000	15.72	0.0001
SLICE	2	26946958078.55895000	13473479939.27947000	9.75	0.0001
ROW	1	3977373314.06873400	3977373314.06873400	2.88	0.0909
COL	1	3564878022.28847800	3564878022.28847800	2.58	0.1094
DIR	1	27347793087.79579000	27347793087.79579000	19.78	0.0001
ROW*SLICE	2	168388243.06861600	84194121.53430800	0.61	0.5445
COL*SLICE	2	54086232.54231390	27043116.27115690	0.20	0.8224
DIR*SLICE	2	554899750.18048300	277449875.09024100	2.01	0.1362
ROW*DIR	1	817120695.45709500	817120695.45709500	5.91	0.0156
COL*DIR	1	280457471.87307300	280457471.87307300	2.03	0.1554

---------- TYPE=cuspid ----------

Source	DF	Type III SS	Mean Square	F Value	Pr > F
TOOTH	2	27117917921.10689000	13560958960.55344000	32.29	0.0001
SLICE	2	30003547931.99533000	15001773965.99766000	35.70	0.0001
ROW	1	12086700431.79600000	12086700431.79600000	28.76	0.0001
COL	1	713133247.73869250	713133247.73869250	1.70	0.1947
DIR	1	325029066.61459740	325029066.61459740	0.77	0.3806
ROW*SLICE	2	48432279.99147352	24216139.99573676	0.06	0.9440
COL*SLICE	2	281292115.57961800	140646057.78980900	0.33	0.7161
DIR*SLICE	2	6230675604.40567500	3115337802.20283700	7.41	0.0009
ROW*DIR	1	654853.14668184	654853.14668184	0.00	0.9686
COL*DIR	1	4116541327.80178000	4116541327.80178000	9.80	0.0021

Tubule Density
CUSPIDS and LATERALS only
Using ROWS and COLUMNS for sites

---------- TYPE=lateral DIR=B ----------

Source	DF	Type III SS	Mean Square	F Value	Pr > F
TOOTH	5	4477015475.17949000	895403095.03589900	6.58	0.0001
SLICE	2	398621691.02381900	199310845.51190900	1.47	0.2343
ROW*SLICE	2	74030290.11028910	37015145.05514460	0.27	0.7621
COL*SLICE	2	7460374.81412676	3730187.40706338	0.03	0.9729

Parameter	Estimate	T for H0: Parameter=0	Pr > |T|	Std Error of Estimate
Column Slope	113.49266	0.10	0.9204	1133.76977
Row Slope	-3310.17617	-2.95	0.0037	1122.09041

---------- TYPE=lateral DIR=D ----------

Source	DF	Type III SS	Mean Square	F Value	Pr > F
TOOTH	5	10196017260.59710000	2039207452.11947000	17.11	0.0001
SLICE	2	2869135210.91841000	1434567605.45920000	11.82	0.0001
ROW*SLICE	2	94443554.91142740	47221777.45571370	0.39	0.6785
COL*SLICE	2	55308776.00101840	27654388.00050920	0.23	0.7966

Parameter	Estimate	T for H0: Parameter=0	Pr > |T|	Std Error of Estimate
Column Slope	2477.26554	2.31	0.0221	1071.04536
Row Slope	606.47509	0.57	0.5702	1065.69402

Tukey's Studentized Range (HSD) Test for variable: DENSITY

SLICE Comparison			Simultaneous Lower Confidence Limit	Difference Between Means	Simultaneous Upper Confidence Limit	
3	-	2	-321	4724	9769	
3	-	1	5139	10207	15276	***
2	-	1	439	5483	10528	***

Tubule Density
CUSPIDS and LATERALS only
Using ROWS and COLUMNS for sites

---------- TYPE=cuspid DIR=B ----------

Source	DF	Type III SS	Mean Square	F Value	Pr > F
TOOTH	2	2883741339.45303000	1441870669.72651000	27.08	0.0001
SLICE	2	450879935.66539400	225439967.83269700	4.23	0.0184
ROW*SLICE	2	13380352.82854130	6690176.41427065	0.13	0.8821
COL*SLICE	2	85510237.25343430	42755118.62671710	0.80	0.4521

Parameter	Estimate	T for H0: Parameter=0	Pr > |T|	Std Error of Estimate
Column Slope	-2764.92930	-2.78	0.0069	993.027368
Row Slope	3320.72934	3.34	0.0013	993.027368

Tukey's Studentized Range (HSD) Test for variable: DENSITY

SLICE Comparison			Simultaneous Lower Confidence Limit	Difference Between Means	Simultaneous Upper Confidence Limit	
3	-	2	-1576	3180	7936	
3	-	1	1013	5769	10525	***
2	-	1	-2167	2589	7345	

---------- TYPE=cuspid DIR=D ----------

Source	DF	Type III SS	Mean Square	F Value	Pr > F
TOOTH	2	1182585127.03360000	591292563.51680100	42.32	0.0001
SLICE	2	3172542418.73562000	1586271209.36781000	113.51	0.0001
ROW*SLICE	2	8021935.11611682	4011967.55805841	0.29	0.7511
COL*SLICE	2	1115713.18618049	1667866.59309024	0.12	0.8877

Parameter	Estimate	T for H0: Parameter=0	Pr > |T|	Std Error of Estimate
Column Slope	1139.74185	2.24	0.0282	508.671856
Row Slope	3369.97744	6.63	0.0001	508.671856

Tukey's Studentized Range (HSD) Test for variable: DENSITY

SLICE Comparison			Simultaneous Lower Confidence Limit	Difference Between Means	Simultaneous Upper Confidence Limit	
3	-	2	4529	6965	9401	***
3	-	1	12873	15309	17745	***
2	-	1	5908	8344	10780	***

Tubule Density
CUSPIDS and LATERALS only
Averaging across all sites

General Linear Models Procedure
Class Level Information

Class	Levels	Values
TOOTH	9	D2 D4 D5 G4 G6 G7 M2 M3 M4
DIR	2	B D
TYPE	2	cuspid lateral
SLICE	3	1 2 3

Dependent Variable: DENSITY

Source	DF	Sum of Squares	Mean Square	F Value	Pr > F
Model	15	35015324593.63290000	2334354972.90886000	20.83	0.0001
Error	464	51987434052.43000000	112041883.73368500		
Corrected Total	479	87002758646.06300000			

Source	DF	Type III SS	Mean Square	F Value	Pr > F
TOOTH(TYPE)	7	13513044342.52810000	1931292048.93259000	17.24	0.0001
DIR	1	2100318689.43202000	2100318689.43202000	18.75	0.0001
SLICE	2	5554561025.32346000	2777280512.66173000	24.79	0.0001
DIR*SLICE	2	1126107873.90483000	563053936.95241900	5.03	0.0069
TYPE*SLICE	2	214703948.60323300	107351974.30161600	0.96	0.3844

Tests of Hypotheses using the Type III MS for TOOTH(TYPE) as an error term

Source	DF	Type III SS	Mean Square	F Value	Pr > F
TYPE	1	12972152809.27300000	12972152809.27300000	6.71	0.0159

Tubule Density
CUSPIDS and LATERALS only
Averaging across all sites

---------- DIR=B ----------

Source	DF	Type III SS	Mean Square	F Value	Pr > F
TOOTH(TYPE)	7	7358416550.35160000	1051202364.33594000	9.25	0.0001
SLICE	2	834354104.46127600	417177052.23063800	3.67	0.0270
TYPE*SLICE	2	33574005.61304050	16787002.80652020	0.14	0.8666

Tests of Hypotheses using the Type III MS for TOOTH(TYPE) as an error term

Source	DF	Type III SS	Mean Square	F Value	Pr > F
TYPE	1	9669739239.59276000	9669739239.59276000	9.20	0.0190

Tukey's Studentized Range (HSD) Test for variable: DENSITY

	Comparison	Simultaneous Lower Confidence Limit	Difference Between Means	Simultaneous Upper Confidence Limit	
SLICE	3 - 2	-1390	2611	6613	
	3 - 1	331	4308	8285	***
	2 - 1	-2280	1697	5674	
TYPE	lateral - cuspid	2864	13339	23815	***

---------- DIR=D ----------

Source	DF	Type III SS	Mean Square	F Value	Pr > F
TOOTH(TYPE)	7	11[illegible]1078[illegible]6.87660000	16[illegible]729696.69667000	18.49	0.0001
SLICE	2	5892992961.75769000	2946496481.87884000	33.18	0.0001
TYPE*SLICE	2	222737578.17524200	111368789.08762100	1.25	0.2872

Tests of Hypotheses using the Type III MS for TOOTH(TYPE) as an error term

Source	DF	Type III SS	Mean Square	F Value	Pr > F
TYPE	1	3902260128.76611000	3902260128.76611000	2.16	0.1681

Tukey's Studentized Range (HSD) Test for variable: DENSITY

	SLICE Comparison	Simultaneous Lower Confidence Limit	Difference Between Means	Simultaneous Upper Confidence Limit	
	3 - 2	1942	5446	8950	***
	3 - 1	8414	11929	15444	***
	2 - 1	2979	6483	9987	***

Tubule Diameter

General Linear Models Procedure
Class Level Information

Class	Levels	Values
TOOTH	9	D2 D4 D5 G4 G6 G7 H2 H3 H4
DIR	2	B D
TYPE	2	cuspid lateral
SLICE	3	1 2 3

Source	DF	Type III SS	Mean Square	F Value	Pr > F
TOOTH(TYPE)	7	13.40015075	1.91430725	17.60	0.0001
DIR	1	0.55740597	0.55740597	10.95	0.0010
SLICE	2	14.13533182	7.06766591	138.81	0.0001
ROW	1	0.02959867	0.02959867	0.58	0.4462
COL	1	0.81070748	0.81070748	16.32	0.0001
ROW*SLICE	2	0.04378176	0.02189088	0.43	0.6508
COL*SLICE	2	0.11715941	0.05857971	1.15	0.3174
DIR*SLICE	2	0.03286352	0.01643176	0.32	0.7243
TYPE*SLICE	2	0.46756906	0.23378453	4.59	0.0106
ROW*DIR	1	0.19098797	0.19098797	3.75	0.0534
COL*DIR	1	0.06498504	0.06498504	1.28	0.2592
ROW*TYPE	1	0.05698158	0.05698158	1.12	0.2907
COL*TYPE	1	0.00053471	0.00053471	0.01	0.9184

Tests of Hypotheses using the Type III MS for TOOTH(TYPE) as an error term

Source	DF	Type III SS	Mean Square	F Value	Pr > F
TYPE	1	1.65113860	1.65113860	0.86	0.3839

Tubule Diameter

---------- TYPE=lateral ----------

Source	DF	Type III SS	Mean Square	F Value	Pr > F
TOOTH	5	11.04994111	2.20998822	46.81	0.0001
DIR	1	0.91129911	0.91129911	19.02	0.0001
SLICE	2	14.18650016	7.09325008	147.75	0.0001
ROW*SLICE	2	0.09615534	0.04807767	1.00	0.3686
COL*SLICE	2	0.21817958	0.10908979	2.27	0.1049
DIR*SLICE	2	0.04031986	0.02015993	0.42	0.6575
ROW*DIR	1	0.09223883	0.09223883	1.93	0.1668
COL*DIR	1	0.10255080	0.10255080	2.14	0.1449

Parameter	Estimate	T for H0: Parameter=0	Pr > |T|	Std Error of Estimate
Column Slope	0.05278887	3.49	0.0006	0.01513725
Row Slope	-0.00369516	-0.24	0.8073	0.01513362

Tukey's Studentized Range (HSD) Test for variable: DIAM

	Comparison		Simultaneous Lower Confidence Limit	Difference Between Means	Simultaneous Upper Confidence Limit	
DIR	B	- D	0.03803	0.08678	0.13554	***
SLICE	3	- 2	0.16069	0.23244	0.30420	***
	3	- 1	0.42983	0.50107	0.57231	***
	2	- 1	0.19721	0.26863	0.34004	***

---------- TYPE=cuspid ----------

Source	DF	Type III SS	Mean Square	F Value	Pr > F
TOOTH	2	2.37984589	1.18992294	23.22	0.0001
DIR	1	0.00311269	0.00311269	0.06	0.8057
SLICE	2	3.75512713	1.87756357	36.64	0.0001
ROW	1	0.06190548	0.06190548	1.25	0.2659
COL	1	0.33088412	0.33088412	6.46	0.0121
ROW*SLICE	2	0.00645287	0.00122644	0.06	0.9190
COL*SLICE	2	0.67247714	0.11621857	6.26	0.0019
DIR*SLICE	2	0.01259081	0.00629541	0.12	0.8845
ROW*DIR	1	0.10982201	0.10982201	2.14	0.1453
COL*DIR	1	0.00001635	0.00001635	0.00	0.9858

Tubule Diameter

---------- TYPE=cuspid SLICE=1 ----------

Source	DF	Type III SS	Mean Square	F Value	Pr > F
TOOTH	2	1.42495971	0.71247986	8.06	0.0010
DIR	1	0.00111475	0.00111475	0.01	0.9103
ROW*DIR	1	0.08248981	0.08248981	0.93	0.3392
COL*DIR	1	0.03572138	0.03572138	0.40	0.5282

Parameter	Estimate	T for H0: Parameter=0	Pr > |T|	Std Error of Estimate
Column Slope	-0.04191316	-0.85	0.4021	0.04956544
Row Slope	0.02310166	0.47	0.6434	0.04956544

---------- TYPE=cuspid SLICE=2 ----------

Source	DF	Type III SS	Mean Square	F Value	Pr > F
TOOTH	2	0.76269962	0.38134981	15.66	0.0001
DIR	1	0.01227823	0.01227823	0.50	0.4813
ROW*DIR	1	0.00025786	0.00025786	0.01	0.9185
COL*DIR	1	0.00009900	0.00009900	0.00	0.9494

Parameter	Estimate	T for H0: Parameter=0	Pr > |T|	Std Error of Estimate
Column Slope	0.05660481	2.18	0.0347	0.02601175
Row Slope	0.03434450	1.32	0.1933	0.02601175

---------- TYPE=cuspid SLICE=3 ----------

Source	DF	Type III SS	Mean Square	F Value	Pr > F
TOOTH	2	0.58954053	0.29477027	7.63	0.0014
DIR	1	0.00229054	0.00229054	0.06	0.8088
ROW*DIR	1	0.07329208	0.07329208	1.90	0.1752
COL*DIR	1	0.03461658	0.03461658	0.90	0.3489

Parameter	Estimate	T for H0: Parameter=0	Pr > |T|	Std Error of Estimate
Column Slope	0.15136158	4.62	0.0001	0.03276905
Row Slope	0.01552957	0.47	0.6378	0.03276905

Tubule Diameter

Averaging across all sites

Source	DF	Type III SS	Mean Square	F Value	Pr > F
TOOTH(TYPE)	7	11.12670189	1.58981484	16.02	0.0001
DIR	1	0.55704863	0.55704863	10.56	0.0011
SLICE	2	14.08434242	7.04217121	133.25	0.0001
DIR*SLICE	2	0.03228637	0.01614319	0.31	0.7369
TYPE*SLICE	2	0.45686645	0.22842323	4.32	0.0138

Tests of Hypotheses using the Type III MS for TOOTH(TYPE) as an error term

TYPE	1	1.66273990	1.66273990	0.87	0.3811

---------- TYPE=lateral ----------

Source	DF	Type III SS	Mean Square	F Value	Pr > F
TOOTH	5	11.01739080	2.20347816	43.85	0.0001
DIR	1	0.92121714	0.92121714	18.30	0.0001
SLICE	2	14.14252155	7.07126078	140.46	0.0001
DIR*SLICE	2	0.03826298	0.01913149	0.38	0.6842

Tukey's Studentized Range (HSD) Test for variable: DIAM

DIR Comparison	Simultaneous Lower Confidence Limit	Difference Between Means	Simultaneous Upper Confidence Limit	
B - D	0.01606	0.08678	0.13670	***
3 - 2	0.15898	0.23246	0.30591	***
3 - 1	0.42813	0.50107	0.57401	***
2 - 1	0.19551	0.26861	0.34175	***

---------- TYPE=cuspid ----------

Source	DF	Type III SS	Mean Square	F Value	Pr > F
TOOTH	2	2.37984589	1.18992294	21.15	0.0001
DIR	1	0.00311269	0.00311269	0.06	0.8144
SLICE	2	3.75512713	1.87756357	33.37	0.0001
DIR*SLICE	2	0.01259081	0.00629541	0.11	0.8942

Tukey's Studentized Range (HSD) Test for variable: DIAM

SLICE Comparison	Simultaneous Lower Confidence Limit	Difference Between Means	Simultaneous Upper Confidence Limit	
3 - 2	0.00446	0.11249	0.22051	***
3 - 1	0.25614	0.36417	0.47221	***
2 - 1	0.14364	0.25168	0.35971	***

Peritubular width

General Linear Models Procedure
Class Level Information

Class	Levels	Values
TOOTH	9	D2 D4 D5 G4 G6 G7 M2 M1 M4
DIR	2	B D
TYPE	2	cuspid lateral
SLICE	3	1 2 3

Source	DF	Type III SS	Mean Square	F Value	Pr > F
TOOTH(TYPE)	7	1.68068404	0.24009772	5.54	0.0001
DIR	1	0.00885817	0.00885817	0.20	0.6514
SLICE	2	0.58592527	0.29296263	6.76	0.0013
ROW	1	0.00212654	0.00212654	0.05	0.8248
COL	1	0.48272295	0.48272295	11.14	0.0009
ROW*SLICE	2	0.00232456	0.00116228	0.03	0.9735
COL*SLICE	2	0.01170844	0.00585422	0.14	0.8736
DIR*SLICE	2	0.00485853	0.00242927	0.06	0.9455
TYPE*SLICE	2	0.12329821	0.06164910	1.42	0.2421
ROW*DIR	1	0.02333941	0.02333941	0.54	0.4634
COL*DIR	1	0.01151653	0.01151653	0.27	0.6064
ROW*TYPE	1	0.00035158	0.00035158	0.01	0.9283
COL*TYPE	1	0.31644754	0.31644754	7.30	0.0071

Tests of Hypotheses using the Type III MS for TOOTH(TYPE) as an error term

Source	DF	Type III SS	Mean Square	F Value	Pr > F
TYPE	1	3.37260369	3.37260369	14.05	0.0072

Peritubular width

---------- TYPE=lateral ----------

Source	DF	Type III SS	Mean Square	F Value	Pr > F
TOOTH	5	1.21054252	0.24210850	4.66	0.0004
DIR	1	0.04872985	0.04872985	0.92	0.3373
SLICE	2	0.19016512	0.09508256	1.80	0.1668
ROW*SLICE	2	0.00082020	0.00041410	0.01	0.9922
COL*SLICE	2	0.00368178	0.00184089	0.03	0.9657
DIR*SLICE	2	0.13313784	0.06656892	1.26	0.2847
ROW*DIR	1	0.00190442	0.00190442	0.04	0.8495
COL*DIR	1	0.00635052	0.00635052	0.12	0.7289

Parameter	Estimate	T for H0: Parameter=0	Pr > |T|	Std Error of Estimate
Column Slope	-0.07399975	-6.70	0.0001	0.01574848
Row Slope	-0.00166258	-0.10	0.9166	0.01587240

---------- TYPE=cuspid ----------

Source	DF	Type III SS	Mean Square	F Value	Pr > F
TOOTH	2	0.44788812	0.22394406	9.34	0.0002
DIR	1	0.02441574	0.02441574	1.02	0.3147
SLICE	2	0.43485200	0.21742600	9.06	0.0002
ROW	1	0.00204471	0.00204471	0.09	0.7707
COL	1	0.00659123	0.00659123	0.27	0.6009
ROW*SLICE	2	0.00660547	0.00330273	0.14	0.8715
COL*SLICE	2	0.02498725	0.01249363	0.52	0.5951
DIR*SLICE	2	0.15654086	0.07827043	3.26	0.0411
ROW*DIR	1	0.03657010	0.03657010	1.52	0.2189
COL*DIR	1	0.00499584	0.00499584	0.21	0.6488

Peritubular width

---------- TYPE=cuspid DIR=B ----------

Source	DF	Type III SS	Mean Square	F Value	Pr > F
TOOTH	2	0.61794859	0.10897429	11.97	0.0001
SLICE	2	0.40092059	0.20046029	7.77	0.0009
ROW*SLICE	2	0.01242382	0.00621191	0.24	0.7867
COL*SLICE	2	0.01823032	0.00911516	0.35	0.7037

Parameter	Estimate	T for H0: Parameter=0	Pr > |T|	Std Error of Estimate
Column Slope	-0.00101086	-0.05	0.9613	0.02186109
Row Slope	-0.02286760	-1.05	0.2991	0.02186109

Tukey's Studentized Range (HSD) Test for variable: WIDTH

SLICE Comparison	Simultaneous Lower Confidence Limit	Difference Between Means	Simultaneous Upper Confidence Limit	
1 - 2	-0.00636	0.09833	0.20303	
1 - 3	0.06701	0.17173	0.27642	***
2 - 3	-0.01130	0.07339	0.17809	

---------- TYPE=cuspid DIR=D ----------

Source	DF	Type III SS	Mean Square	F Value	Pr > F
TOOTH	2	0.05961698	0.02980849	1.46	0.2383
SLICE	2	0.19541353	0.09770676	4.80	0.0112
ROW*SLICE	2	0.01931386	0.00965693	0.47	0.6242
COL*SLICE	2	0.02069560	0.01034780	0.51	0.6037

Parameter	Estimate	T for H0: Parameter=0	Pr > |T|	Std Error of Estimate
Column Slope	-0.01461347	-0.75	0.4542	0.01941359
Row Slope	0.01500392	0.76	0.4470	0.01961617

Tukey's Studentized Range (HSD) Test for variable: WIDTH

SLICE Comparison	Simultaneous Lower Confidence Limit	Difference Between Means	Simultaneous Upper Confidence Limit	
2 - 1	-0.04170	0.05219	0.14609	
2 - 3	0.02673	0.11974	0.21274	***
3 - 1	-0.16144	-0.06754	0.02635	

Peritubular width

---------- TYPE=cuspid SLICE=1 ----------

Source	DF	Type III SS	Mean Square	F Value	Pr > F
TOOTH	2	0.36108911	0.18054466	7.46	0.0016
DIR	1	0.14871115	0.14871115	6.15	0.0170
ROW*DIR	1	0.06014554	0.06014554	2.49	0.1218
COL*DIR	1	0.01853993	0.01853993	0.77	0.3860

Parameter	Estimate	T for H0: Parameter=0	Pr > |T|	Std Error of Estimate
Column Slope	-0.01216761	-0.48	0.6356	0.02592222
Row Slope	-0.00016853	-0.01	0.9949	0.02633262

Tukey's Studentized Range (HSD) Test for variable: WIDTH

DIR Comparison	Simultaneous Lower Confidence Limit	Difference Between Means	Simultaneous Upper Confidence Limit	
B - D	0.02376	0.10983	0.19591	***

---------- TYPE=cuspid SLICE=2 ----------

Source	DF	Type III SS	Mean Square	F Value	Pr > F
TOOTH	2	0.17981619	0.08990809	5.27	0.0087
DIR	1	0.02235603	0.02235603	1.31	0.2583
ROW*DIR	1	0.00205553	0.00205553	0.12	0.7301
COL*DIR	1	0.00002897	0.00002897	0.00	0.9673

Parameter	Estimate	T for H0: Parameter=0	Pr > |T|	Std Error of Estimate
Column Slope	0.01267218	0.58	0.5634	0.02177339
Row Slope	-0.01481044	-0.68	0.4998	0.02177339

---------- TYPE=cuspid SLICE=3 ----------

Source	DF	Type III SS	Mean Square	F Value	Pr > F
TOOTH	2	0.08749326	0.04374663	1.45	0.2447
DIR	1	0.00043084	0.00043084	0.01	0.9053
ROW*DIR	1	0.00264396	0.00264396	0.09	0.7684
COL*DIR	1	0.00036560	0.00036560	0.01	0.9128

Parameter	Estimate	T for H0: Parameter=0	Pr > |T|	Std Error of Estimate
Column Slope	-0.02174107	-0.82	0.4161	0.02893317
Row Slope	0.00402386	0.14	0.8900	0.02893317

Peritubular width

Averaging across all sites

Source	DF	Type III SS	Mean Square	F Value	Pr > F
TOOTH(TYPE)	7	1.67635587	0.23947941	5.32	0.0001
DIR	1	0.00788734	0.00788734	0.18	0.6758
SLICE	2	0.58416708	0.29208354	6.48	0.0017
DIR*SLICE	2	0.00644412	0.00322206	0.07	0.9310
TYPE*SLICE	2	0.12368536	0.06184268	1.37	0.2544

Tests of Hypotheses using the Type III MS for TOOTH(TYPE) as an error term

Source	DF	Type III SS	Mean Square	F Value	Pr > F
TYPE	1	3.33833107	3.33833107	11.94	0.0071

Tukey's Studentized Range (HSD) Test for variable: WIDTH

	Comparison		Simultaneous Lower Confidence Limit	Difference Between Means	Simultaneous Upper Confidence Limit	
SLICE	1	- 2	-0.02344	0.03253	0.08850	
	1	- 3	0.02162	0.07750	0.13338	***
	2	- 3	-0.01109	0.04497	0.10103	
TYPE	cuspid	- lateral	0.06420	0.17623	0.28827	***

Tubule Density
CUSPIDS and LATERALS only
Averaging across all sites

General Linear Models Procedure
Class Level Information

Class	Levels	Values
TOOTH	9	D2 D4 D5 G4 G6 G7 M2 M3 M4
DIR	2	B D
TYPE	2	cuspid lateral
SLICE	3	1 2 3

Dependent Variable: DENSITY

Source	DF	Sum of Squares	Mean Square	F Value	Pr > F
Model	16	35676776881.82780000	2229798555.23923000	20.11	0.0001
Error	463	51325981762.23630000	110855253.18625500		
Corrected Total	479	87002758644.06410000			

R-Square	C.V.	Root MSE	DENSITY Mean
0.410065	31.61315	10528.78208666	33317.11670640

Source	DF	Type III SS	Mean Square	F Value	Pr > F
TOOTH(TYPE)	7	13556194054.35840000	1936599150.62263000	17.47	0.0001
DIR	1	1224872811.58657000	1224872811.58657000	11.05	0.0010
SLICE	2	5565601093.28704000	2782801546.64352000	25.10	0.0001
DIR*SLICE	2	1119720964.58165000	559860482.29082800	5.05	0.0068
TYPE*SLICE	2	212392836.34679000	106196417.17339509	0.96	0.3844
DIR*TYPE	1	661452390.19490400	661452390.19490400	5.97	0.0150

Tests of Hypotheses using the Type III MS for TOOTH(TYPE) as an error term

Source	DF	Type III SS	Mean Square	F Value	Pr > F
TYPE	1	12986479744.68580000	12986479744.68580000	6.71	0.0160

Tubule Diameter
CUSPIDS and LATERALS only
Averaging across all sites

Dependent Variable: DIAM

SLICE=1

Source	DF	Sum of Squares	Mean Square	F Value	Pr > F
Model	10	9.10792362	0.91079236	15.96	0.0001
Error	149	8.50323145	0.05706867		
Corrected Total	159	17.61115507			

R-Square	C.V.	Root MSE	DIAM Mean
0.517168	16.39731	0.23889049	1.45688809

Source	DF	Type III SS	Mean Square	F Value	Pr > F
TOOTH(TYPE)	7	7.48995813	1.06999405	18.75	0.0001
DIR	1	0.15775966	0.15775966	2.76	0.0985
DIR*TYPE	1	0.20430837	0.20430837	3.58	0.0604

Tests of Hypotheses using the Type III MS for TOOTH(TYPE) as an error term

Source	DF	Type III SS	Mean Square	F Value	Pr > F
TYPE	1	1.28658677	1.28658677	1.20	0.3091

SLICE=2

Source	DF	Sum of Squares	Mean Square	F Value	Pr > F
Model	10	6.20398551	0.62089855	22.35	0.0001
Error	146	3.93269773	0.02693629		
Corrected Total	156	10.22168325			

R-Square	C.V.	Root MSE	DIAM Mean
0.615259	9.537268	0.16412378	1.72085743

Source	DF	Type III SS	Mean Square	F Value	Pr > F
TOOTH(TYPE)	7	5.20269663	0.74324338	27.59	0.0001
DIR	1	0.04121530	0.04121530	1.53	0.2181
DIR*TYPE	1	0.14587203	0.14587203	5.42	0.0213

Tests of Hypotheses using the Type III MS for TOOTH(TYPE) as an error term

Source	DF	Type III SS	Mean Square	F Value	Pr > F
TYPE	1	0.76006340	0.76006340	1.02	0.3656

Tubule Diameter
CUSPIDS and LATERALS only
Averaging across all sites

Dependent Variable: DIAM

---------- SLICE=3 ----------

Source	DF	Sum of Squares	Mean Square	F Value	Pr > F
Model	10	3.81155179	0.38115518	6.51	0.0001
Error	147	8.60880057	0.05856327		
Corrected Total	157	12.42035237			

Source	DF	Type III SS	Mean Square	F Value	Pr > F
TOOTH(TYPE)	7	3.54819743	0.50688535	8.66	0.0001
DIR	1	0.10117136	0.10117136	1.73	0.1908
DIR*TYPE	1	0.05781760	0.05781760	0.99	0.3220

Tests of Hypotheses using the Type III MS for TOOTH(TYPE) as an error term

Source	DF	Type III SS	Mean Square	F Value	Pr > F
TYPE	1	0.04568113	0.04568113	0.09	0.7727

Testing whether SLOPES are different

Parameter	Test	Subgroup	Z	p-value
Tubule Density	Direction within tooth type	Laterals	1.24	0.215
		Cuspids	2.98	0.003
	Tooth type within direction	Buccal	0.32	0.749
		Distal	1.15	0.250
Tubule Diameter	Direction	Laterals	0.80	0.424
	Tooth type	(none)	-2.26	0.024
Peritubular Width	Tooth type	(none)	-1.04	0.298

Robust SE Estimates

Parameter	Tooth type	Direction	Depth	N	SE	SD
Tubular Density	Laterals	Buccal	Slice 1	54	3795.160	27629
			Slice 2	52	2960.355	21141
			Slice 3	52	3836.252	27396
		Distal	Slice 1	53	4420.215	31875
			Slice 2	54	3115.576	22682
			Slice 3	53	5020.099	36200
	Cuspids	Buccal	Slice 1	27	4001.397	20403
			Slice 2	27	2830.523	14433
			Slice 3	27	3773.587	19242
		Distal	Slice 1	27	3013.492	15366
			Slice 2	27	1942.632	9906
			Slice 3	27	1838.213	9373
Tubular Diameter	Laterals	Buccal	Slice 1	54	0.097	0.706
			Slice 2	49	0.090	0.624
			Slice 3	51	0.072	0.509
		Distal	Slice 1	52	0.108	0.771
			Slice 2	54	0.091	0.662
			Slice 3	53	0.086	0.620
		Overall	Slice 1	106	0.075	0.768
			Slice 2	103	0.065	0.656
			Slice 3	104	0.058	0.589
	Cuspids	Overall	Slice 1	54	0.094	0.684
			Slice 2	54	0.069	0.507
			Slice 3	54	0.060	0.437
Peritubular Width	Laterals	Overall	Slice 1	107	0.049	0.504
			Slice 2	104	0.016	0.162
			Slice 3	105	0.022	0.224
	Cuspids	Overall	Slice 1	53	0.048	0.346
			Slice 2	54	0.033	0.240
			Slice 3	54	0.023	0.167